

## REVIEW

[View Article Online](#)  
[View Journal](#) | [View Issue](#)Cite this: *J. Mater. Chem. B*, 2023, **11**, 2334Surface modification of TiO<sub>2</sub> nanoparticles with organic molecules and their biological applicationsFarid Hajareh Haghighi,<sup>a</sup> Martina Mercurio,<sup>a</sup> Sara Cerra,<sup>a</sup> Tommaso Alberto Salamone,<sup>a</sup> Roya Bianymotlagh,<sup>a</sup> Cleofe Palocci,<sup>ab</sup> Vincenzo Romano Spica<sup>c</sup> and Ilaria Fratoddi<sup>a</sup>

In recent years, titanium(IV) dioxide nanoparticles (TiO<sub>2</sub>NPs) have shown promising potential in various biological applications such as antimicrobials, drug delivery, photodynamic therapy, biosensors, and tissue engineering. For employing TiO<sub>2</sub>NPs in these fields, their nanosurface must be coated or conjugated with organic and/or inorganic agents. This modification can improve their stability, photochemical properties, biocompatibility, and even surface area for further conjugation with other molecules such as drugs, targeting molecules, polymers, etc. This review describes the organic-based modification of TiO<sub>2</sub>NPs and their potential applications in the mentioned biological fields. In the first part of this review, around 75 recent publications (2017–2022) are mentioned on the common TiO<sub>2</sub>NP modifiers including organosilanes, polymers, small molecules, and hydrogels, which improve the photochemical features of TiO<sub>2</sub>NPs. In the second part of this review, we presented 149 recent papers (2020–2022) about the use of modified TiO<sub>2</sub>NPs in biological applications, in which specific bioactive modifiers are introduced in this part with their advantages. In this review, the following information is presented: (1) the common organic modifiers for TiO<sub>2</sub>NPs, (2) biologically important modifiers and their benefits, and (3) recent publications on biological studies on the modified TiO<sub>2</sub>NPs with their achievements. This review shows the paramount significance of the organic-based modification of TiO<sub>2</sub>NPs to enhance their biological effectiveness, paving the way toward the development of advanced TiO<sub>2</sub>-based nanomaterials in nanomedicine.

Received 25th November 2022,  
Accepted 24th January 2023

DOI: 10.1039/d2tb02576k

[rsc.li/materials-b](https://rsc.li/materials-b)

## 1. Introduction

With the advent of nanotechnology, numerous nanomaterials have been synthesized and applied for various applications and among them, titanium dioxide nanoparticles (TiO<sub>2</sub>NPs) are commonly used in the fields of biomedicine,<sup>1</sup> food industry,<sup>2</sup> wastewater purification,<sup>3</sup> and cosmetics<sup>4</sup> owing to their unique physicochemical properties such as high chemical stability and photodynamic effects. Regarding their industrial importance, the global market size of TiO<sub>2</sub>NPs was estimated to be \$1.1 billion in 2021, and forecasted to have a compound annual growth rate of 6.5% until 2026, with annual production

predicted to reach 2.5 million tons by 2025.<sup>5,6</sup> In the biomedical fields, TiO<sub>2</sub>NPs are frequently studied for photodynamic therapy,<sup>1,7</sup> drug delivery,<sup>8</sup> antimicrobial applications,<sup>3,9–12</sup> biosensors,<sup>13</sup> and tissue engineering.<sup>14</sup> For these applications, an appropriate surface modification of TiO<sub>2</sub>NPs is required to improve their physicochemical properties and biological effectiveness and, more importantly, decrease their potential toxicity in mammalian cells.<sup>5</sup> The surface modification not only prevents the agglomeration of TiO<sub>2</sub>NPs but also provides the possibility for further functionalization/conjugation. The modification of TiO<sub>2</sub>NPs can be achieved using two different approaches: non-covalent and covalent conjugation of organic (or inorganic) species with TiO<sub>2</sub>NPs. The non-covalent strategy is based on physical interactions (electrostatic, hydrogen bond, van der Waals, and hydrophobic interactions), having benefits of being relatively simple and not changing the structure of the modifiers. However, this type of modification can be easily influenced by different external stimuli, such as temperature, pH, and ionic strength.<sup>15</sup> On the other side, the covalent modification (or chemical modification) occurs *via* covalent

<sup>a</sup> Department of Chemistry, Sapienza University of Rome, Piazzale Aldo Moro 5, 00185, Rome, Italy. E-mail: [ilaria.fratoddi@uniroma1.it](mailto:ilaria.fratoddi@uniroma1.it), [farid.hajarehaghghi@uniroma1.it](mailto:farid.hajarehaghghi@uniroma1.it); Tel: 0039-06 4991 3182

<sup>b</sup> Research Center for Applied Sciences to the Safeguard of Environment and Cultural Heritage (CIABC), Sapienza University of Rome, Piazzale Aldo Moro 5, 00185 Rome, Italy

<sup>c</sup> Department of Movement, Health and Human Sciences, University of Rome Foro Italico, Piazza Lauro De Bosis, 15, 00135 Rome, Italy

bonding of modifiers to the  $\text{TiO}_2\text{NP}$  surface which can be performed using various coupling agents such as polymers, organophosphorus molecules, carboxylic acids, and organosilanes, and among them, silane compounds are more common for the surface modification of  $\text{TiO}_2\text{NPs}$ .<sup>16</sup> In recent years, there has been increasing interest for these two types of modification strategies and this review presents recent publications of organic-based  $\text{TiO}_2\text{NP}$  modification, followed by the presentation of those organic modifiers which were used for the biomedical applications with their advantages.

## 2. Surface chemistry of $\text{TiO}_2\text{NPs}$

Like other types of nanoparticles,  $\text{TiO}_2\text{NPs}$  have two distinct atoms: (1) internal and (2) surface atoms. The internal part of  $\text{TiO}_2\text{NPs}$  is chemically inert (each Ti atom has four chemical bonds with four neighboring oxygens) and so, the remaining surface atoms are mainly responsible for the interaction of nanoparticles with the environment. The surface atoms are not chemically saturated (they are only attached to the internal atoms), so they should complete their coordination number to gain a stable electronic configuration. Ti and O are considered as hard atoms based on the HSAB concept (hard and soft (Lewis) acids and bases)<sup>8</sup> and they tend to interact with the hard atoms. Due to the adsorption of water molecules from the environment, the surface of  $\text{TiO}_2\text{NPs}$  has two main OH groups: (1) Ti-OH and (2) Ti-O<sub>br</sub>H-Ti (br: bridging) (Fig. 1).<sup>17–21</sup> The interaction of  $\text{TiO}_2\text{NPs}$  with the surroundings occurs through these two types of OH groups.

## 3. Surface modification of $\text{TiO}_2\text{NPs}$

Organic stabilizers can bind to the  $\text{TiO}_2\text{NP}$  surface by either physical or chemical interactions. The chemical stabilization (or covalent stabilization) is much stronger than the physical one and, in most cases, it results in long-term stability for the modified  $\text{TiO}_2\text{NPs}$ .<sup>22</sup> In the following sections, the common surface stabilizers of  $\text{TiO}_2\text{NPs}$  will be presented into two groups of (1) organofunctional silanes and (2) polymers, small molecules, and hydrogels. In the structure of silane modifiers, there are active functional groups (for example hydrolysable alkoxy groups) which are suitable for the chemical interaction with  $\text{TiO}_2\text{NPs}$ .<sup>23</sup> On the other hand, physical modification can be

carried out by using these organic molecules which are adsorbed on the  $\text{TiO}_2\text{NP}$  surface by electrostatic, hydrogen bond, van der Waals, and hydrophobic interactions.<sup>24</sup>

### 3.1. Organofunctional silanes

**3.1.1. Tetraethoxysilane (TEOS).** Silica coating is a common chemical method for the surface modification of  $\text{TiO}_2\text{NPs}$ , providing several benefits such as long-term stability, biocompatibility, and hydrophilicity of silane-modified  $\text{TiO}_2\text{NPs}$  ( $\text{TiO}_2\text{NPs}@SiO_2$ ). There are standard procedures to control the thickness of the silica layer and four main approaches are commonly used to prepare  $\text{TiO}_2\text{NPs}@SiO_2$  (Table 1).<sup>25</sup>

The Stöber method is the most employed method for the silica modification of bare  $\text{TiO}_2\text{NPs}$ . In the standard Stöber approach,  $\text{TiO}_2\text{NPs}$  are uniformly dispersed in an ethanol solution, followed by the addition of tetraethoxysilane (TEOS) and aqueous ammonia solution ( $\text{NH}_3(\text{aq})$ ), respectively.<sup>26</sup> Ammonia acts as a basic catalyst to control TEOS hydrolysis and silica thickness to form particles with a regular morphology (see Fig. 2). In this hydrolysis reaction, the  $-\text{Si}-\text{OC}_2\text{H}_5$  groups of TEOS convert to silanol groups ( $-\text{Si}-\text{OH}$ ), and then, the condensation reaction occurs between these  $-\text{Si}-\text{OH}$  groups and the surface  $-\text{OH}$  groups of  $\text{TiO}_2\text{NPs}$  to form chemical Ti-O-Si bonds. This sol-gel reaction results in a 3D silica network around the  $\text{TiO}_2\text{NP}$  core. Chen *et al.* applied the Stöber process to have varying thicknesses of  $\text{SiO}_2$  onto the surface of anatase and rutile  $\text{TiO}_2\text{NPs}$ .<sup>27,28</sup> They reported an enhancement of the photocatalytic activity of the modified  $\text{TiO}_2\text{NPs}$  when the  $\text{SiO}_2$  loading weight was lower than 3.25 wt%, while with higher loading percentages, lower photocatalytic activity was observed. Regarding the rutile phase, the complete coverage of  $\text{TiO}_2\text{NPs}$  with  $\text{SiO}_2$  resulted in an enhancement of the photocatalytic activity.

The second approach of silica modification is the micro-emulsion method, having two different types: (1) water-in-oil (W/O, normal micelles) and (2) oil-in-water (O/W, reverse micelles). Using this method, Xie *et al.* prepared monodisperse  $\text{TiO}_2\text{NPs}@SiO_2$  core-shell particles and showed that the contents of the anatase and rutile crystalline phases of these  $\text{TiO}_2\text{NPs}$  were decreased and increased, respectively, when the temperature was increased from 550 °C to 650 °C. In the temperature range of 600–800 °C, the  $\text{TiO}_2\text{NPs}@SiO_2$  particles were mainly anatase.<sup>29</sup>

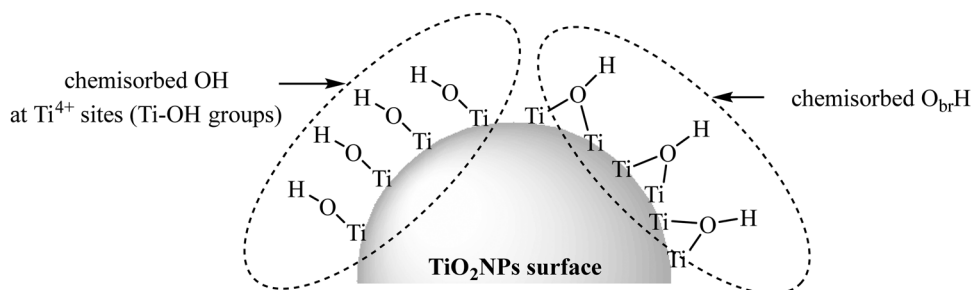
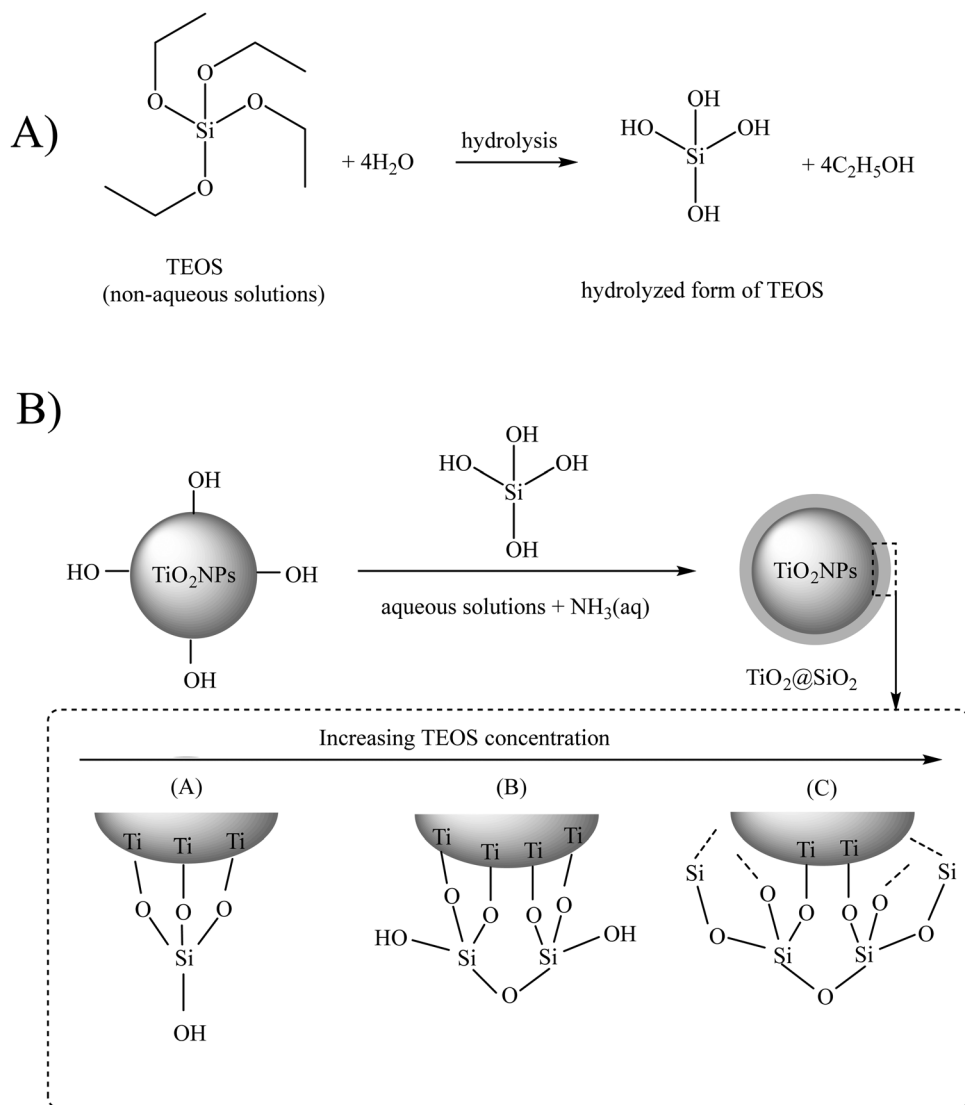


Fig. 1 Two different OH groups of the  $\text{TiO}_2\text{NP}$  surface. Adapted with permission from ref. 20. Copyright 2014 American Chemical Society.



**Table 1** Four main methods for the silica coating of TiO<sub>2</sub>NPs.<sup>25</sup>

Synthesis methods	Advantages	Disadvantages
Stöber method	Controllable silica shell and TiO <sub>2</sub> monodispersity	Lack of understanding of its kinetics and mechanism
Microemulsion	Control of the TiO <sub>2</sub> NP size and high homogeneity	Poor yield, time consuming and large amounts of solvent required
Aerosol pyrolysis	Highly productive and suitable for large-scale production	Complex experimental conditions
Methods based on sodium silicate solution	Control of the crystallinity and surface area	Depends on the preparation method

**Fig. 2** (A) Hydrolysis and (B) condensation reactions of tetraethoxysilane (TEOS). Adapted with permission from ref. 22. Royal Society of Chemistry.

The third strategy to synthesize TiO<sub>2</sub>NPs@SiO<sub>2</sub> particles is aerosol pyrolysis, considered as an innovative and productive approach, which is usually carried out in a flame environment and can be used for the large-scale production of modified TiO<sub>2</sub>NP powders. In 2021, Temerov *et al.* synthesized TiO<sub>2</sub>NPs@SiO<sub>2</sub> (50–70 nm) using a liquid flame spray (LFS) deposition method in a single flame environment.<sup>30</sup> They

studied the photocatalytic activity of deposited TiO<sub>2</sub>NPs@SiO<sub>2</sub> for oxidation of acetylene into carbon dioxide and they investigated the effect of the silica shell on the photocatalytic activity of these modified TiO<sub>2</sub>NPs. They reported that the catalytic activity was significantly suppressed when the SiO<sub>2</sub> content was increased to 0.5%, 1.0%, 3.0% and 5.0% (33%, 44%, 70% and 100% of suppression, respectively). They mentioned that this



suppression might be due to the thick passivating silica layer around the  $\text{TiO}_2\text{NP}$  core. Maskrot *et al.* synthesized a core-shell  $\text{TiO}_2\text{NPs}@SiO_2$  composite with different Ti/Si ratios, by the laser pyrolysis of a gas-spray mixture of TEOS and titanium tetra-isopropoxide.<sup>31</sup> By increasing the Ti/Si ratio, the color of these modified  $\text{TiO}_2\text{NPs}@SiO_2$  composite changes from dark to light blue. Their results showed the correlation between the chemical composition and the size of these  $\text{TiO}_2\text{NPs}@SiO_2$  nanoparticles as a function of the Ti/Si ratio.

The fourth route is based on sodium silicate solution as a cheap silica precursor. For instance, Shao *et al.* used sodium silicate to prepare the  $\text{TiO}_2\text{-SiO}_2$  composites using controllable and reproducible approaches to improve the textural properties of the nanostructures.<sup>32</sup> The practical photocatalytic application of these  $\text{TiO}_2\text{-SiO}_2$  composites was successfully tested for decolorization of methylene blue, as a model pollutant in textile industries.

**3.1.2. Bifunctional silane coupling agents (trialkoxysilanes).** In the previous section, it was mentioned that the TEOS silica coating provides modified  $\text{TiO}_2\text{NPs}@SiO_2$  having -OH

groups on the outer part of the nanosurface (see Fig. 2), which come from the silica shell. However, for some specific biological applications, it is necessary to introduce new functional groups on the surface of modified  $\text{TiO}_2\text{NPs}$  for retaining the benefits of the silica coating as well. For this goal, trialkoxysilanes are one of the most important surface modifiers which can provide both biocompatibility and long-term colloidal stability for the particles. More importantly, these bifunctional silanes supply suitable functional groups on the surface of silane-modified  $\text{TiO}_2\text{NPs}$  for the further attachment of other species to the nanoparticles. The commercially available trialkoxysilanes,  $(\text{RO})_3\text{Si}-(\text{CH}_2)_n\text{-X}$  ( $\text{X} = -\text{NH}_2, -\text{SH}, -\text{C}\equiv\text{C}, \text{epoxy}, \text{etc.}$ ;  $n = \text{typically } 3$ ), are considered as effective bifunctional silane linkers having two different functional groups in their structures including: (1) -OR moiety (attached to the -Si) and (2) -SH/or - $\text{NH}_2$  (or other functional groups) attached to the end of a carbon chain.<sup>22</sup> In the general formulation of  $(\text{RO})_3\text{Si}-(\text{CH}_2)_n\text{-X}$ , R can be an alkyl, aryl or generally organofunctional group. As shown in Fig. 3, for the surface modification of  $\text{TiO}_2\text{NPs}$ , the

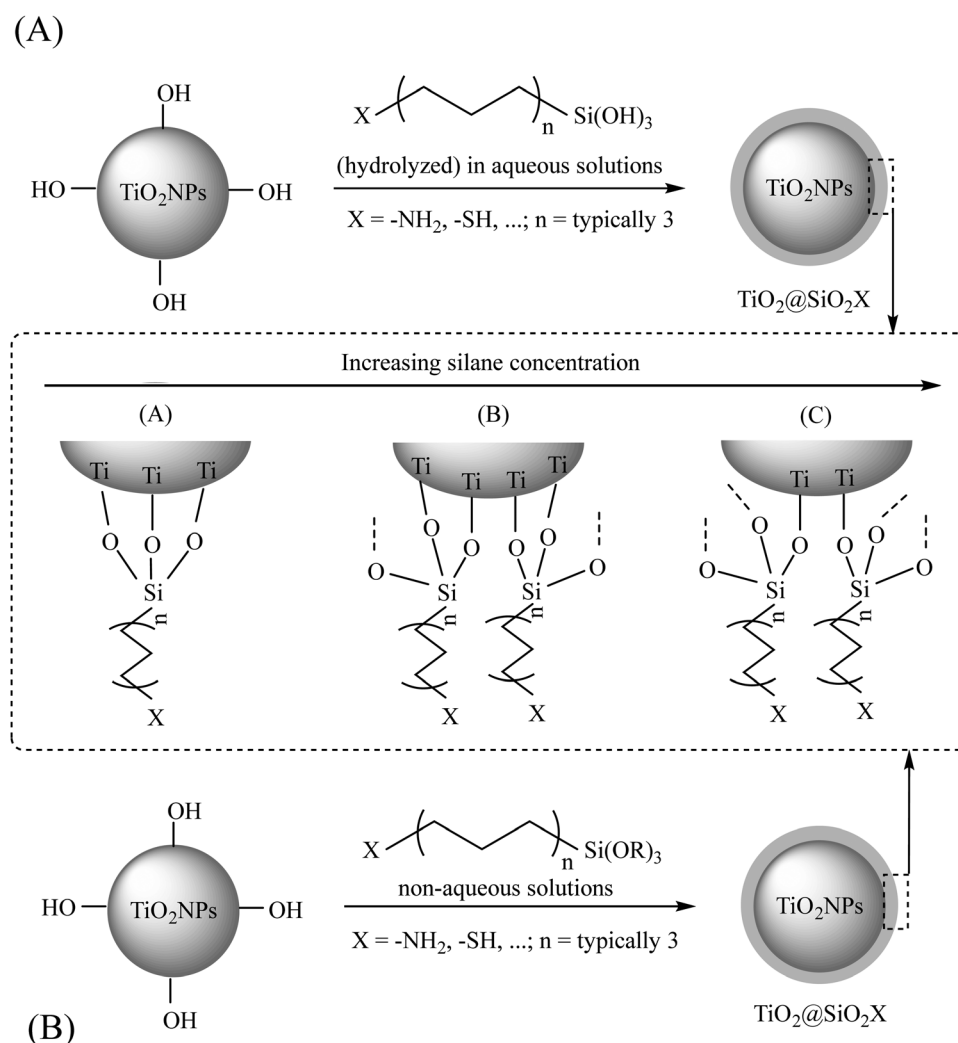


Fig. 3 The interaction between a general silane coupling agent and  $\text{TiO}_2\text{NPs}$  in aqueous (A) and non-aqueous (B) solutions. Adapted with permission from ref. 22. Royal Society of Chemistry.



–OR groups should be hydrolyzed to form silanol groups (–SiOH), followed by the condensation of these silanols with the –OH groups of the bare TiO<sub>2</sub> nanosurface, resulting in the formation of a silica network around the TiO<sub>2</sub>NP core and providing the suitable X functional groups onto the surface. As common organosilane coupling agents, 3-methacryloxypropyltrimethoxysilane (MPS),<sup>33</sup> 3-aminopropyltriethoxysilane (APTES),<sup>34–38</sup> 3-glycidioxypropyltrimethoxysilane (GPS),<sup>39</sup> and *n*-propyltriethoxysilane<sup>22</sup> are used for different applications. The other recommendations for this type of modification are shown in Table 2.

Because of the importance of such bifunctional silane linkers, recent publications on some of these triorganosilanes will be presented as follows:

**3.1.3. (3-Aminopropyl)triethoxysilane (APTES).** As one of the most important trialkoxysilanes, APTES can provide –NH<sub>2</sub> groups onto the outer surface of modified TiO<sub>2</sub>NPs. In 2022, Mokhtari Aghdami *et al.* functionalized TiO<sub>2</sub>NPs with APTES to improve the thermal, mechanical, and antibacterial properties of poly(lactic acid)/silicone rubber (PLA/SR) blends, reinforced with APTES-functionalized TiO<sub>2</sub>NPs.<sup>53</sup> In another recent study, Massoumi *et al.* immobilized *S*-nitroso-*N*-acetylpenicillamine (SNAP) on TiO<sub>2</sub>NPs to form a NO-releasing TiO<sub>2</sub>NP/SNAP system, for antibacterial applications. For this goal, TiO<sub>2</sub>NPs were first silanized with APTES, and then *N*-acetyl-*D*-penicillamine was grafted to them *via* an amide bond.<sup>54</sup> TiO<sub>2</sub>NPs@APTES-SNAP showed antimicrobial properties (5 mg mL<sup>–1</sup>) on both Gram-positive *Staphylococcus aureus* (*S. aureus*) and Gram-negative *Escherichia coli* (*E. coli*) bacteria and the biocompatibility on 3T3 mouse fibroblast cells, at all tested concentrations. Dymerska *et al.* proposed a nanocomposite made from ultrasmall TiO<sub>2</sub>NPs embedded in a silica/carbon matrix.<sup>55</sup> This composite was fabricated first by the surface modification of TiO<sub>2</sub>NPs with APTES, followed by the encapsulation of the TiO<sub>2</sub>NPs@APTES in a carbon sphere-like structure formed with biocompatible glucose as the carbon precursor. The resultant system exhibited high photocatalytic activity for degradation of methylene blue as a model hazardous organic dye. Yoo *et al.* synthesized highly pure TiO<sub>2</sub>NPs through thermal plasma and deposited them directly on an interdigitated electrode.<sup>56</sup> The nanosurface of the TiO<sub>2</sub>-deposited electrode was modified with APTES, followed by attaching a single-stranded probe deoxyribonucleic acid (DNA) to construct a DNA biosensor for the selective detection of *E. coli* O157:H7, as a well-known pernicious pathogenic bacterial species. Zhang *et al.* developed a novel electrode material for supercapacitors, in which they used APTES to link polyaniline (PANI) to TiO<sub>2</sub> nanowires (TNWs).<sup>57</sup> Compared to PANI–TNW, the better capacitive properties of PANI–APTES–TNW were observed due to the anchoring effect of APTES, which was highly interactive and showed compact structures between the TNW nanoparticles and PANI, resulting in a stable structure during the rapid charge–discharge process. Wanag *et al.* reported TiO<sub>2</sub>NP modification with APTES utilizing a solvothermal method, with different concentrations of APTES (10–3000 mM).<sup>58</sup> The photocatalytic activity of these TiO<sub>2</sub>NPs@APTES was successfully tested for methylene blue decomposition under UV light irradiation.

Their results showed that the photocatalytic properties enhanced with the increase of the APTES concentration. Mallakpour and Barati reported the APTES modification of TiO<sub>2</sub>NPs and showed the improvement of the heat resistance of these modified TiO<sub>2</sub>NPs.<sup>59</sup> Shakeri *et al.* synthesized a stable TiO<sub>2</sub>NPs@APTES nanohybrid for the photocatalytic degradation of a pink food dye used as an organic pollutant.<sup>60</sup> Klaysri *et al.* reported a one-step synthesis method of APTES-functionalized TiO<sub>2</sub>NPs for the photocatalytic decolonization of methylene blue.<sup>61</sup>

**3.1.4. (3-Mercaptopropyl)trimethoxysilane (MPTMS).** MPTMS is another interesting silane coupling agent that can provide free –SH groups on the surface of modified TiO<sub>2</sub>NPs. This trimethoxysilane is specifically suitable for the chemical attachment of nanoparticles such as Au- and AgNPs to TiO<sub>2</sub>NPs. For instance, Meng *et al.* employed MPTMS to functionalize commercial TiO<sub>2</sub>NPs with the silica layer and, more importantly, provide the surface –SH groups to decorate AgNPs on the modified TiO<sub>2</sub>NPs.<sup>47</sup> They synthesized TiO<sub>2</sub>NPs@MPTMS-AgNPs for the catalytic reduction of 4-nitrophenol, as a chemical pollutant. Lee *et al.* reported the surface modification of the photocatalyst TiO<sub>2</sub> using MPTMS, on a nylon fabric surface.<sup>62</sup> They showed that the antimicrobial and photodegradation properties of this nylon fabric were improved for the treatment of *S. aureus* and *E. coli* strains on the treated nylon containing the modified TiO<sub>2</sub>@MPTMS.

**3.1.5. Vinyltriethoxysilanes (VTES) and other non-silane coupling agents.** In some applications it is necessary to introduce –C=C on the TiO<sub>2</sub>NP surface, and vinyltriethoxysilane (VTES) can be an excellent recommendation in this regard. Aqeel Ashraf *et al.* successfully used VTES and TEOS to modify TiO<sub>2</sub>NPs (*via* a hybrid sol–gel coating) to protect the commercial AZ91 magnesium alloy against corrosion in a 0.05 M NaCl solution.<sup>63</sup> Tangchantra *et al.* modified TiO<sub>2</sub>NPs with three different silane coupling agents, such as VTES, hexadecyltrimethoxysilane (HTMS), and aminopropyltrimethoxysilane (APTMS).<sup>64</sup> Their results demonstrated that the VETS modification could improve the dispersibility and mechanical properties of the TiO<sub>2</sub>NPs. Yang *et al.* reported the VTES silanization of TiO<sub>2</sub> particles (*via* a sol–gel method) and their results exhibited the improvement of colloidal stability in tetrachloroethylene solvent.<sup>65</sup>

Regarding the other types of silanes and non-silane coupling agents, there are several worthwhile publications which are briefly mentioned here. For example, Caris *et al.* utilized conventional emulsion polymerization to encapsulate TiO<sub>2</sub> in poly(methyl methacrylate) (PMMA).<sup>66</sup> Weng and Wei studied the radical polymerization of styrene and methyl methacrylate (MMA), initiated at the surface of TiO<sub>2</sub> particles by adsorbed hydroperoxide macroinitiators.<sup>67</sup> Erdem *et al.* modified TiO<sub>2</sub>NPs by the miniemulsion polymerization of styrene and polybutene–succinimide pentamine being used as the stabilizer at the oil/water interface.<sup>68</sup> Rong *et al.* reported the modification of TiO<sub>2</sub>NPs by (3-trimethoxysilyl)propylmethacrylate, followed by the free-radical copolymerization of styrene with the methacrylate group of 3-methacryloxypropyltrimethoxysilane (MPS).<sup>69</sup>



**Table 2** Some trialkoxysilane agents and other organic functionalizing molecules containing the active functional groups

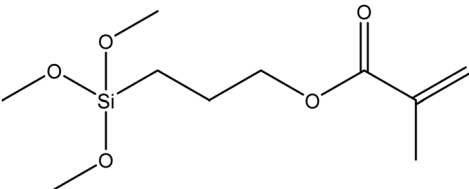
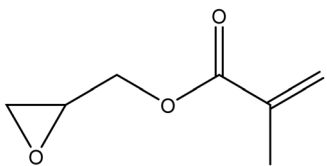
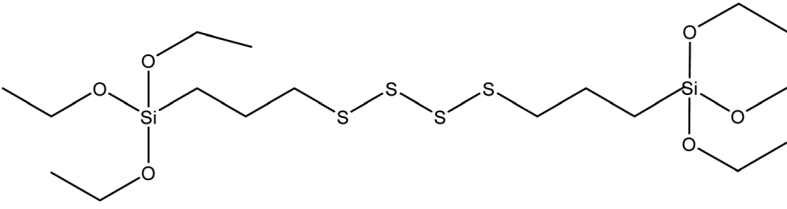
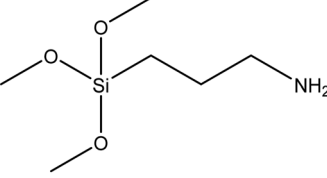
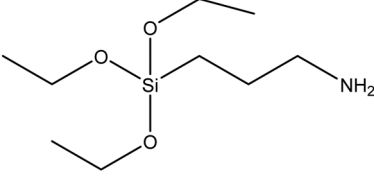
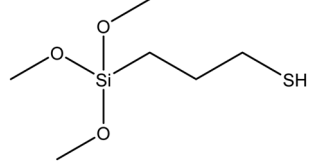
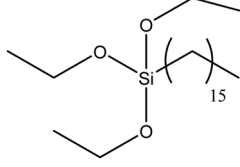
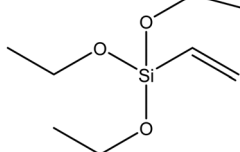
Modifying agent	Structure	Ref.
(3-Trimethoxysilyl)propyl methacrylate, KH-570		40
Fluorosilane	$\text{H}_3\text{Si-F}$	41
Glycidyl methacrylate		42
Bis-(3-triethoxysilylpropyl)tetrasulfide (TESPT)		43
(3-Aminopropyl)trimethoxysilane		44 and 45
(3-Aminopropyl)triethoxysilane (APTES)		46
(3-Mercaptopropyl)triethoxysilane (MPTES)		47
Hexadecyltrimethoxysilane		48
Vinyltrimethoxysilane (VTMS)		49





Table 2 (continued)

Modifying agent	Structure	Ref.
Ascorbic acid 6-palmitate		50
(3-Methacryloxypropyl)trimethoxysilane		51
3-Isocyanato propyl trimethoxysilane		52

Yang and Dan used a similar approach to attach poly(methyl methacrylate) on the modified surface of  $\text{TiO}_2\text{NPs}$ .<sup>70</sup> Milanese *et al.* employed a mixture of isomeric octyltriethoxysilanes (OTESs) to form a hydrophobic layer around  $\text{TiO}_2\text{NPs}$ .<sup>71</sup> They reported the formation of cross-linked and chemical bonded  $\text{Ti}-\text{O}-\text{Si}$  onto the modified  $\text{TiO}_2\text{NPs}$ . Xiang *et al.* used MPS to modify the  $\text{TiO}_2\text{NP}$  surface and enhance their compatibility with the poly(butyl acrylate) (PBA) matrix.<sup>72</sup> In another study, Qi *et al.* synthesized hydrophobic  $\text{TiO}_2\text{NPs}$  using the acrylonitrile-styrene-acrylate (ASA) terpolymer for cool materials.<sup>51</sup> Wang *et al.* functionalized commercial  $\text{TiO}_2\text{NPs}$  with MPS *via* ultrasonic treatment at room temperature.<sup>73</sup> Godnjavec *et al.* coated  $\text{TiO}_2\text{NPs}$  by 3-glycidyloxypropyltrimethoxysilane (GLYMO) as an additive in a clear polyacrylic coating and reported that the modified  $\text{TiO}_2\text{NPs}$  improved dispersion, transparency, and UV protection of the clear acrylic coating.<sup>74</sup> Dalod *et al.* modified  $\text{TiO}_2\text{NPs}$  with APTES, 3-(2-aminoethylamino)propyldimethoxymethylsilane (AEAPS), and *n*-decyltriethoxysilane (DTES) using a hydrothermal method and reported that the shape and structure of these nanoparticles depend on the type of silane coupling groups.<sup>75</sup>

### 3.2. Polymers, small molecules, and hydrogels

**3.2.1. Polymers.** In recent years, the polymeric modification of  $\text{TiO}_2\text{NPs}$  has attracted growing attention owing to their widespread application in various nanomedicinal fields. *In situ* coating and post (*ex situ*) surface coating are two common methods for the polymeric modification of  $\text{TiO}_2\text{NPs}$ . For *in situ* coating, the polymer is used simultaneously with the  $\text{TiO}_2$  precursor during the synthesis of  $\text{TiO}_2\text{NPs}$ , and both synthesis and modification occur simultaneously in a single step. However, for the post (*ex situ*) modification of  $\text{TiO}_2\text{NPs}$ , the polymers are added to pre-synthesized  $\text{TiO}_2\text{NPs}$ , which is a separate step (next step) from the synthesis. To date, polyethylene glycol

(PEG), dextran, chitosan, alginate, polyvinyl alcohol (PVA), polydopamine (PDA), polysaccharides, polyethyleneimine (PEI), polyvinylpyrrolidone (PVP), polyetherimide, and polyamidoamine (PAMAM) have been applied for the surface modification of  $\text{TiO}_2\text{NPs}$  (Table 3).

PEG is a commonly used water-soluble polymer for the surface modification of  $\text{TiO}_2\text{NPs}$ , which can enhance the biocompatibility and hydrophilicity of the nanoparticles for biological applications. Recently, several excellent research studies have been reported on the PEG-coated  $\text{TiO}_2\text{NPs}$ ; for example, in 2022, Connolly *et al.* compared the bioaccumulation, biodistribution and depuration profile of uncoated  $\text{TiO}_2\text{NPs}$  and PEG-modified  $\text{TiO}_2\text{NPs}$  in rainbow trout, after 10 days dietary exposure and a 42 day depuration phase.<sup>76</sup> Their results showed that PEG modification had an influence on levels of uptake and distributions of the modified  $\text{TiO}_2\text{NPs}$ , and a higher uptake of PEG-coated  $\text{TiO}_2\text{NPs}$  was observed, compared to the fish exposed to the uncoated  $\text{TiO}_2\text{NPs}$ . Tsotetsi *et al.* synthesized  $\text{TiO}_2\text{NPs}$  and then modified their surface with PEG, polyvinylpyrrolidone (PVP), and Pluronic F127 as pore forming agents, to investigate the effects of surface modification on the pore size, morphology, specific surface area, and optical properties of the  $\text{TiO}_2\text{NPs}$ .<sup>77</sup> All these three modified samples showed porous morphologies with spherical shapes and specific surface areas of  $\sim 69.82$ ,  $37.80$  and  $57.08 \text{ m}^2 \text{ g}^{-1}$  for  $\text{TiO}_2\text{-F127}$ ,  $\text{TiO}_2\text{-PVP}$  and  $\text{TiO}_2\text{-PEG}$ , respectively (after calcination at  $550^\circ\text{C}$ ). The pore sizes were estimated to be  $\sim 13.01$ ,  $10.10$  and  $8.53 \text{ nm}$  for  $\text{TiO}_2\text{-F127}$ ,  $\text{TiO}_2\text{-PVP}$  and  $\text{TiO}_2\text{-PEG}$ , respectively. Their results indicated that the surface modification of bare  $\text{TiO}_2\text{NPs}$  can improve their photophysical properties to act as an efficient electron transporting layer in solar cell applications. Koushali *et al.* studied the effects of synthesized  $\text{TiO}_2\text{-PEG}$  on the morphological, thermal, and mechanical properties of unsaturated polyester (UPE) nanocomposites.<sup>78</sup>



Table 3 Main polymers used for TiO<sub>2</sub>NP modification

Polymers	Source/production/preparation <sup>25</sup>	Ref.
Polyethylene glycol (PEG)	Produced by the interaction of ethylene oxide with water, ethylene glycol, or ethylene glycol oligomers	76–85
Polyvinylpyrrolidone (PVP)	Made from the monomer <i>N</i> -vinylpyrrolidone	86
Polyethyleneimine (PEI)	Branched PEI: by the ring opening polymerization of aziridine Linear PEI: by the post-modification of other polymers like poly(2-oxazolines) or <i>N</i> -substituted polyaziridines	87
Polyacrylic acids (PAA)	Polymerization of acrylic acid	88 and 89
Polyvinyl alcohol (PVA)	Polymerization of vinyl acetate and then the saponification of polyvinyl acetate	90 and 91
Polydopamine (PDA)	Formed from dopamine at slightly basic pH	92
Dextran	Produced by lactic acid bacteria	93
Chitosan	Extracted from shellfish or the fungal cell wall	94–97
Starch	Produced by green plants	98 and 99
Alginate	Extracted from brown algae	100 and 101
Polyphenol	Found in some common plant foods like cocoa, beans, tea, and vegetables	102
Amino acids	In nature	103
Flavonoids	Found in some common plant foods like fruits, vegetables, beans, and tea	104 and 105

The UPE/PEG/TiO<sub>2</sub> nanocomposites were prepared by direct mechanical mixing of these three components at different weight ratios of both TiO<sub>2</sub>NPs and PEG. Their results showed an improvement in the mechanical and thermal characteristics of the nanocomposites containing 0.5 wt% of synthesized TiO<sub>2</sub>NPs and 10 wt% of PEG, compared to the pristine polyester. Abasifard Dehkordi *et al.* studied the addition of TiO<sub>2</sub>/ZnO nanoparticles and PEG (with different molar ratios) to Portland cement to improve the photocatalytic and antibacterial activities of the cement.<sup>79</sup> They evaluated the potential ability of this composite for decolorization of an azo dye (as an organic pollutant) and inactivation of *E. coli* and *S. aureus* mutants. Their results showed a concentration-dependence antibacterial effect of the modified cement and effective photocatalytic degradation of the dye, which showed promising potential of this modified cement to be used as a self-cleaning and antibacterial coating for urban constructions. Iqbal *et al.* deposited gold nanoparticles onto TiO<sub>2</sub>NPs, followed by the PEG modification of the TiO<sub>2</sub>-Au nanohybrid.<sup>106</sup> The authors used this nanohybrid as a novel photosensitizing agent after biodistribution toward the targeted site (cancerous cell injury in the MCF-7 cell line), and showed that the different morphologies of PEG-modified Au-doped TiO<sub>2</sub>NPs provided various therapeutic effects. Landolsi *et al.* synthesized TiO<sub>2</sub>NPs and then modified them with PEG, followed by decoration of Fe<sub>2</sub>O<sub>3</sub>NPs onto the surface of modified TiO<sub>2</sub>NPs.<sup>81</sup> The photocatalytic activity of the TiO<sub>2</sub>NPs-PEG-Fe<sub>2</sub>O<sub>3</sub>NPs was studied for the degradation of methylene blue and the significant degradability performance was observed under visible light irradiation (up to 70% after 150 min of irradiation). Bai *et al.* synthesized ultrasmall iron-doped TiO<sub>2</sub> nanodots (Fe-TiO<sub>2</sub> NDs) as a type of sonosensitizers to study their potential applications in sonodynamic therapy.<sup>82</sup> After PEG modification, Fe-TiO<sub>2</sub>-PEG NDs showed improved physiological stability and biocompatibility, with efficient tumor retention. Compared to commercial TiO<sub>2</sub>NPs, this modified TiO<sub>2</sub> nanostructure demonstrated higher *in vivo* therapeutic performance with no long-term toxicity to the treated mice

after one month. Birinci *et al.* used PEG-modified TiO<sub>2</sub>NPs in the formulation of a novel nano-antioxidant that utilized quercetin-conjugated TiO<sub>2</sub>NPs (QTiO<sub>2</sub>, quercetin is a potent antioxidant) for fortifying skin defense against oxidative toxicity.<sup>83</sup> The PEG-modified TiO<sub>2</sub>NPs exhibited better colloidal stability and biocompatibility (compared to the unmodified TiO<sub>2</sub>NPs), which causes an easy adhesion of these nanosurfaces onto living cells. This nano-antioxidant QTiO<sub>2</sub> showed an efficient delivery of Q molecules into mouse fibroblast cells and improved the cellular antioxidant defense system against oxidative toxicity. Wang *et al.* synthesized TiO<sub>2</sub>NPs and studied their surface modification with single and mixed stabilizers, such as PEG, cetyltrimethylammonium bromide (CTAB) and carboxamide.<sup>107</sup> Their results showed that the surfactants strongly affect the morphology of these TiO<sub>2</sub>NPs and, for the PEG, they obtained ellipse modified TiO<sub>2</sub>NPs having an improved photocatalytic activity for the degradation of methyl orange under UV irradiation. Wang *et al.* synthesized ultrafine titanium monoxide nanorods (TiO<sub>1+x</sub> NRs) and then modified them with PEG.<sup>84</sup> TiO<sub>1+x</sub> NRs-PEG was used as a new sonodynamic agent and showed much more efficiency for the ultrasound-induced generation of reactive oxygen species (ROS), compared to the conventional sonosensitizer. Interestingly, TiO<sub>1+x</sub> NRs-PEG could also generate hydroxyl radicals (OH<sup>•</sup>) from endogenous H<sub>2</sub>O<sub>2</sub> in the tumor to enable chemodynamic therapy (CDT). For the treated mice, TiO<sub>1+x</sub> NRs-PEG showed efficient passive retention in tumors post-intravenous injection, with no significant long-term toxicity, indicating the potential ability of this modified TiO<sub>2</sub> nanostructure to be used as a sonosensitizer and a CDT agent.

Chitosan (CS) is another frequent hydrophilic polymer for the surface modification of TiO<sub>2</sub>NPs, which has low toxicity, good biocompatibility and biodegradability.<sup>94</sup> Chitosan-modified TiO<sub>2</sub>NPs (TiO<sub>2</sub>NPs-CS) have potential applications in various technologies such as photocatalytic nanostructures,<sup>108</sup> antibacterial package materials,<sup>109</sup> wound healing materials,<sup>110,111</sup> wastewater treatment,<sup>112</sup> and sensors.<sup>113</sup>





From a structural point of view, CS has reactive amino and hydroxyl side groups which can interact with  $\text{TiO}_2\text{NPs}$  by hydrogen bonding and form stable nanoco-hybrids.<sup>94</sup> For instance, in 2022, Moulahou *et al.* synthesized  $\text{TiO}_2$ -chitosan nanocomposites ( $\text{TiO}_2\text{NPs-CS}$ ) and combined them with various metal ions (silver, zinc, copper, and iron) to prepare novel chitosan-based films and improve the physicochemical and biological activities of the individual components.<sup>95</sup> The antimicrobial properties of these films were studied against three pathogens (*P. aeruginosa*, *C. albicans*, and *S. aureus*) under different light conditions. Among these nanocomposites,  $\text{TiO}_2\text{NPs-CS-Ag}$  showed the best antibacterial activity. Besides, the nanocomposites were tested for the photocatalytic degradation of methylene blue (MB), and the best data were observed for  $\text{TiO}_2\text{NPs-CS-Cu}$  with a higher specificity towards MB than the other two tested dyes (methyl orange and bromophenol blue). These results showed that the  $\text{TiO}_2\text{NPs-CS-metal ions}$  have great potential as ambient light packaging materials, coating materials, and photocatalysts. In another recent study, Castillo *et al.* used  $\text{TiO}_2\text{NPs-chitosan}$  for the electroanalytical detection of imidacloprid, (a neonicotinoid) that is a systemic insecticide and can accumulate in agricultural products and negatively affect human health.<sup>94</sup> The authors showed that the  $\text{TiO}_2\text{NPs-chitosan}$ , with a high surface area, served as molecular recognition sites for the imidacloprid detection, with an optimum concentration of 40 wt% of  $\text{TiO}_2\text{NPs}$ . Elmeahbad *et al.* prepared two new chitosan derivatives by incorporating salicylhydrazide into a chitosan Schiff base (SCsSB) and chitosan (SCs) to make two nanohybrids, SCs/ $\text{TiO}_2$ -1% and SCs/ $\text{TiO}_2$ -3%.<sup>96</sup> The anti-biofilm and antimicrobial activities of these nanostructures were ranked as SCs/ $\text{TiO}_2$ -3% > SCs/ $\text{TiO}_2$ -1% > SCs > SCsSB. Their results showed that the modification of  $\text{TiO}_2\text{NPs}$  with the chitosan polymer enhanced the antibacterial performance of the components. SCs/ $\text{TiO}_2$ -3% was biocompatible with normal human cells, indicating the potential ability of this nanocomposite for antimicrobial agents. Majnis *et al.* integrated chitosan (CS) and  $\text{ZrO}_2$  into  $\text{TiO}_2\text{NPs}$  through a sol-gel fabrication method, to make the CS- $\text{ZrO}_2/\text{TiO}_2$  photocatalyst having a smaller band gap, compared to the unmodified  $\text{TiO}_2\text{NPs}$ .<sup>97</sup> The photodegradation efficiency of CS- $\text{ZrO}_2/\text{TiO}_2$  was tested (under solar irradiation) using a model dye, malachite green (MG), and the results showed an increase efficiency from 11.87% (for  $\text{TiO}_2\text{NPs}$  alone) to 30.72% (with  $\text{ZrO}_2$  and CS addition in  $\text{TiO}_2\text{NPs}$ ).

Also, other polymers such as polydopamine (PDA), polysaccharide, polylactic acid (PLA), polyacrylic acid (PAA), alginate (Al), polyvinylidene fluoride, PEI, PVP, and PAMAM (polyamidoamine)<sup>114,115</sup> are used for the surface modification of  $\text{TiO}_2\text{NPs}$  (see Table 4). For example, Dong *et al.* used polydopamine (PDA) with excellent hydrophilicity for the surface modification of  $\text{TiO}_2\text{NPs}$ .<sup>92</sup> Then, these PDA-modified  $\text{TiO}_2\text{NPs}$  were combined with hydrophobic graphene (Gr) *via* the  $\pi$ - $\pi$  non-covalent interaction to enhance the water dispersion stability of Gr. Regarding practical applications, this nanocomposite was tested for its fire resistance ability inside the intumescent waterborne epoxy coating. The results showed

that introducing PDA and  $\text{TiO}_2\text{NPs}$  effectively improved the oxidation resistance and stability of the composite. Zhang *et al.* prepared  $\text{TiO}_2\text{NP-PDA}$  hybrid nanoparticles to reduce oxygen vacancies in  $\text{TiO}_2\text{NPs}$  and provide better stability for the polymer matrix.  $\text{TiO}_2\text{NP-PDA}$  was composited with polylactic acid (PLA) to prepare PLA/ $\text{TiO}_2\text{NP-PDA}$  nanocomposites.<sup>116</sup> These nanocomposite films showed excellent UV-shielding performance without sacrificing transparency (the transmittance at 550 nm was 85.7%). PLA is very sensitive to UV light; however, due to the shielding effect of  $\text{TiO}_2\text{NPs-PDA}$  in this film, the performance of PLA was improved, and it can broaden its application for environmental materials having a wider range of uses with a longer service life.

$\text{TiO}_2\text{NPs}$  are also used as food whitening in candies, chocolates, and cakes with a high carbohydrate content. However, there is a little knowledge about the potential interaction between the food carbohydrate and food grade- $\text{TiO}_2\text{NPs}$ . In the case of polysaccharides, Qiaorun *et al.* studied the interaction between  $\text{TiO}_2\text{NPs}$  and seven common carbohydrates (including monosaccharides, disaccharides, and polysaccharides).<sup>117</sup> Their results showed that the  $\text{TiO}_2\text{NPs}$  can interact with all these tested carbohydrates and enter the body as a food additive, and interact with the food matrix for a series of reactions. The food polysaccharides showed stronger adsorption onto the  $\text{TiO}_2\text{NPs}$  than monosaccharides and disaccharides.

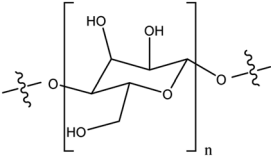
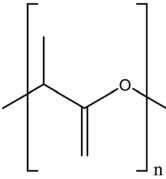
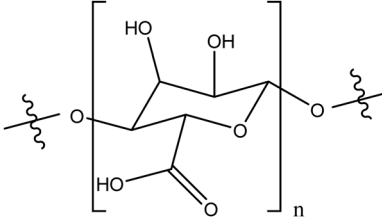
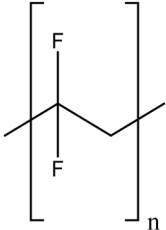
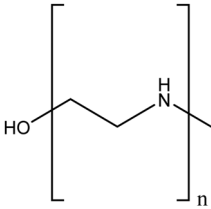
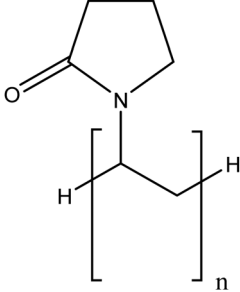
Regarding polylactic acid (PLA), Tajdari *et al.* prepared ZnO-PLA,  $\text{TiO}_2$ -PLA and ZnO/ $\text{TiO}_2$ -PLA nanocomposites with different percentages of nanoparticles and two different types of ZnO morphologies.<sup>118</sup> Their results showed the enhanced mechanical and optical properties of PLA when it was combined with the nanoparticles. Also, the antibacterial activity of PLA was improved against Gram-positive *L. monocytogenes* and Gram-negative bacteria *E. coli* by incorporating nanoparticles.

Dextran (Dex) is a polysaccharide with excellent biocompatibility and good water solubility, so the modification of  $\text{TiO}_2\text{NPs}$  with dextran can improve the physicochemical properties of the nanoparticle. Naghibi *et al.* compared the *in situ* and *ex situ* surface modifications of  $\text{TiO}_2\text{NPs}$  using dextran (Dex) and Dex/poly ethylene glycol (PEG), by comparing the colloidal stability of the modified  $\text{TiO}_2\text{NPs}$  prepared by these two methods.<sup>93</sup> Their results showed that the *in situ* additions of Dex and PEG, during the synthesis of  $\text{TiO}_2\text{NPs}$  (hydrothermal synthesis), resulted in a highly stable colloidal solution (more than 60 days), whereas the *ex situ* additions of Dex and PEG (after the  $\text{TiO}_2\text{NP}$  synthesis) did not significantly impact on the colloidal stability of  $\text{TiO}_2\text{NPs}$ .

**3.2.2. Small molecules.** Another important group of stabilizing agents are small molecules which can provide either lipophilic or hydrophilic character for the modified  $\text{TiO}_2\text{NPs}$ . The lipophilic small molecules such as oleic acid are considered as “fat-loving” or “fat-liking” and have great importance for the preparation of lipophilic  $\text{TiO}_2\text{NPs}$  with good dispersity in non-aqueous solutions. More importantly, oleic acid can form a dense protective monolayer around the  $\text{TiO}_2\text{NPs}$  and can strongly attach to the nanosurface.<sup>25</sup> The chemical structure of oleic acid and two recent publications on oleic acid-modified  $\text{TiO}_2\text{NPs}$  are summarized in Table 5.



Table 4 Some characteristics of polymers used for the surface modification of TiO<sub>2</sub>NPs

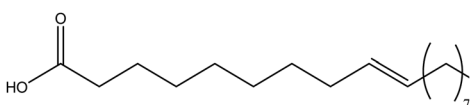
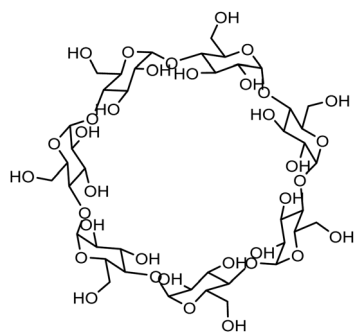
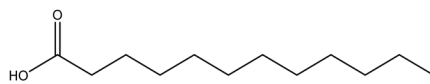
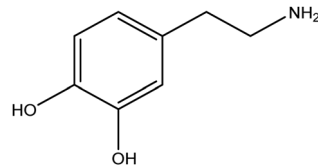
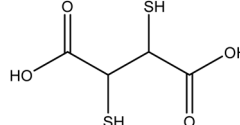
Name	Structure	Stability	Modification mechanism (covalent/non-covalent)	Applications	Ref.
Polysaccharide		Strongly modified the TiO <sub>2</sub> NP stability by inducing their partial and rapid disagglomeration, by steric effects and electrostatic interactions	N/A	Water purification	119
Poly lactic acid		Highly dispersible by steric effects	Hydrogen bonding interactions	Antimicrobial against <i>S. aureus</i> , <i>Salmonella</i> and <i>E. coli</i>	90, 120 and 121
Alginate acid		Enhanced stability in water, compared to unmodified TiO <sub>2</sub> NPs through combination of electrostatic repulsion and steric effects	Electrostatic interactions	Environmental applications	100 and 101
Polyvinylidene fluoride		Excellent stability of modified TiO <sub>2</sub> NPs by steric effects	N/A	Increased anti-fouling properties	122 and 123
Polyethyleneimine (PEI)		Enhanced stability in water, compared to unmodified TiO <sub>2</sub> NPs by electrostatic repulsion	Physical interactions	Photodegradation of methylene blue	87
Polyvinylpyrrolidone (PVP)		Considerable improvement in terms of stability compared to unmodified TiO <sub>2</sub> NPs via steric hindrance	N/A	Enhancing the TiO <sub>2</sub> NP dispersion in blood and urine	86

However, in some biomedical applications, the use of lipophilic-modified TiO<sub>2</sub>NPs is greatly limited due to low dispersity of the nanoparticles in biological aqueous solutions. For the medical applications of modified TiO<sub>2</sub>NPs, the research is more focused on the synthesis of hydrophilic or water dispersible TiO<sub>2</sub>NPs. In this regard, several small organic molecules such as amino acids, citric acid, cyclodextrin, dopamine, lauric

acid, and dimercaptosuccinic acid (DMSA) are often used for the surface modification of TiO<sub>2</sub>NPs to enhance the hydrophilicity of modified nanoparticles for the biological applications. In the case of citrate (or citric acid), Connolly *et al.* studied the bioaccumulation of uncoated TiO<sub>2</sub>NPs and TiO<sub>2</sub>NPs–citrate in fish to investigate the relationship between surface coating and uptake (biokinetics) *in vivo*.<sup>76</sup> Rainbow trout (*Oncorhynchus mykiss*) were



Table 5 Small organic molecules for the surface modification of TiO<sub>2</sub>NPs

Name	Structure	Stability	Modification mechanism	Applications	Ref.
Oleic acid		Steric hindrance	Chemically bonded with the surface titanium ion (by bidentate linkages)	Healing excision wounds were studied in the rat animal model	126–128
Cyclodextrin		Improvement of the colloidal stability, steric hindrance	N/A	Degradation of wastewater pollutants, antibacterials	129
Lauric acid		The functionalized TiO <sub>2</sub> NPs exhibited significantly reduced agglomeration, both in dry and in dispersed states (in oily media)	Chemical interaction with silane-functionalized TiO <sub>2</sub> NPs	UV filtering ability	130
Dopamine		Steric stabilization of TiO <sub>2</sub> NPs when it is polymerized to polydopamine	Probable chemical interactions (determined by computational chemistry)	Drug discovery, diagnostics, environmental applications, and food safety	131
Dimercaptosuccinic acid (DMSA)		Improve dispersity of TiO <sub>2</sub> NPs in solutions and increase electrostatic repulsion between nanoparticles	N/A	Cytotoxicity on human aortic and endothelial cells	132 and 133

fed diets spiked with the uncoated and citrate-coated TiO<sub>2</sub>NPs (100 mg NPs per kg feed) for 10 days and thereafter, fish were allowed to depurate for 42 days. Their results showed that the surface modification affected the uptake and, in some cases, caused slower depuration and distinct distributions. In another research, Liu *et al.* synthesized citrate-coated Gd-doped TiO<sub>2</sub> ellipsoidal nanoparticles (GdTl-SC NPs) to improve the efficiency of gadolinium-based T1 contrast agents (CAs) for magnetic resonance imaging (MRI).<sup>124</sup> The *in vivo* MRI tests on rats demonstrated that the modified TiO<sub>2</sub>NPs have a high potential ability as high-performance T1 contrast agents for the sensitive imaging of blood vessels and the accurate diagnosis of vascular lesions. Peper *et al.* studied redox reactions of aqueous colloidal solutions of both citrate capped- and uncapped-TiO<sub>2</sub>NPs (c-TiO<sub>2</sub> and uc-TiO<sub>2</sub>) and reported the different redox behaviors of these two systems.<sup>125</sup>

**3.2.3. Hydrogels.** Hydrogels are gel-like materials processing a three-dimensional (3D) network composed of hydrophilic polymer building blocks. The polymers link to each other forming an insoluble 3D matrix which can absorb and trap a significant amount of water. The hydrogels have excellent biocompatibility, reversible swelling/deswelling behavior, and high potential adsorption capacity, making them suitable

materials for biological applications including tissue engineering, drug delivery, cosmetics, personal hygiene, and diapers.<sup>134,135</sup> They have suitable functional groups for the interaction with the TiO<sub>2</sub>NPs and therefore, they can be used for the modification/stabilization and encapsulation of TiO<sub>2</sub>NPs.<sup>136</sup> In all these systems, the hydrogel matrix provides a protecting and modifying environment for the TiO<sub>2</sub>NPs and stabilize them in a gel-like media, preventing their agglomeration. Moreover, hybridization of TiO<sub>2</sub>NPs with hydrogels can have a significant positive effect on the structural, mechanical, and thermal properties of the hydrogels. For example, in 2022, Makhado *et al.* prepared a ghatti gum/poly(acrylic acid)/TiO<sub>2</sub>NPs (GG/poly(AA)/TiO<sub>2</sub>) hydrogel nanocomposite and studied the structure, morphology, and thermomechanical characteristics of the synthesized hydrogel nanocomposite.<sup>137</sup> The incorporation of TiO<sub>2</sub>NPs with the hydrogel matrix improved the hydrogel thermal stability and mechanical strength. Zhao *et al.* synthesized highly dispersible TiO<sub>2</sub>NPs modified with a 3D graphene hydrogel composite (TiO<sub>2</sub>NPs-rGH) using a hydrothermal method.<sup>138</sup> The combination of 2D graphene sheets with hybrid TiO<sub>2</sub>NPs enhanced the specific surface area of the TiO<sub>2</sub>NPs-rGH 3D composite. Their results showed that the TiO<sub>2</sub>NPs-rGH composites have higher photocatalytic



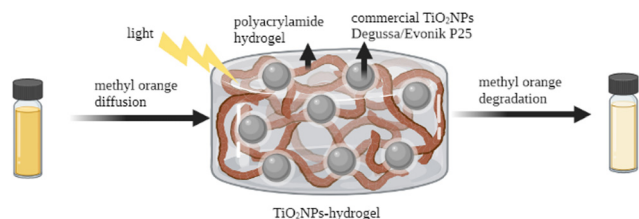


Fig. 4  $\text{TiO}_2\text{NP}$ -hydrogel system for the photocatalytic degradation of methyl orange. Adapted with permission from ref. 139. Copyright 2022 Elsevier.

performance than unmodified  $\text{TiO}_2\text{NPs}$ . Mansurov *et al.* reported the improvement of the photocatalytic degradation of commercial  $\text{TiO}_2\text{NPs}$  Degussa/Evonik P25 after modification with the composite polyacrylamide hydrogel (Fig. 4).<sup>139</sup>

Ulu *et al.* reported the preparation and characterization of chitosan/PEG/ $\text{TiO}_2\text{NP}$  (CH/PEG/ $\text{TiO}_2\text{NP}$ ) composite hydrogels for antibacterial applications.<sup>140</sup> Their results showed that the CH/PEG/ $\text{TiO}_2\text{NPs}$  improved the mechanical and thermal properties of the hydrogel due to the presence of  $\text{TiO}_2\text{NPs}$ . More importantly, this  $\text{TiO}_2$  nanocomposite showed potential antimicrobial activity. Yue *et al.* prepared a novel photocatalytic hydrogel by loading  $\text{TiO}_2\text{NPs}$  onto the surface of 2,2,6,6-tetramethylpiperidine-1-oxyl (TEMPO)-oxidized chitin nanofibers (TOCNs), which were further incorporated into the polyacrylamide (PAM) matrix.<sup>141</sup> The presence of  $\text{TiO}_2\text{NPs}$  enhanced the compressive strength of this hydrogel with excellent stretchability and photocatalytic activity.

In the first part of this review, it can be concluded that the organic-based surface modification of  $\text{TiO}_2\text{NPs}$  can result in a significant improvement of their physicochemical properties for preparing much more effective  $\text{TiO}_2\text{NP}$ -based nanostructures and decreasing the potential toxicity of  $\text{TiO}_2\text{NPs}$  as well. For the following part of this review, the recent biological applications of  $\text{TiO}_2$ -based nanomaterials will be presented. The main aim of this section is to present some specific organic modifiers and polymers for  $\text{TiO}_2\text{NPs}$  which have been recently used (2020–2022) in eight main fields of drug delivery, photodynamic therapy, antibacterial, biosensors, antiviral, antifungal, cancer therapy, and tissue engineering. Also, the advantages of these organic modifiers will be discussed.

## 4. Biological applications of modified $\text{TiO}_2\text{NPs}$

### 4.1. Photo-, thermo-, and sonodynamic effects of modified $\text{TiO}_2\text{NPs}$ on cancer cells

According to the World Health Organization, there is an increase in annual cancer cases from 14 to 22 million in 2012–2030 period.<sup>142</sup> During recent years, modified  $\text{TiO}_2\text{NPs}$  have been studied as promising alternatives for the cancer therapy *via* different methodologies including photodynamic, photothermal, and sonodynamic therapies.<sup>1,7,143–145</sup>

In the photodynamic therapy, they are regarded as inorganic photosensitizers for anti-cancerous photodynamic therapy

(PDT) owing to their unique phototoxic effect upon UV light irradiation. The UV light absorption can excite valence electrons of  $\text{TiO}_2\text{NPs}$  to generate electrons and holes on the nanosurface, and consequently, a series of redox reactions are initiated which produce anti-cancerous reactive oxygen species (ROS) such as hydroxyl radicals ( $\text{HO}^\bullet$ ), superoxide anions ( $\text{O}_2^{\bullet-}$ ), hydrogen peroxide ( $\text{H}_2\text{O}_2$ ), *etc.*<sup>1,7</sup> In spite of their advantages, UV irradiation is not always suitable for PDT due to its limited penetration depth, a lower light content and, more importantly, its harmful side effects for the patients exposed to UV light.<sup>146</sup> On this basis, much research has been dedicated to extending the photoresponse of  $\text{TiO}_2\text{NPs}$  to the visible light region. In this field, the surface modification of  $\text{TiO}_2\text{NPs}$  is focused on the use of biologically active species on the surface of  $\text{TiO}_2\text{NPs}$  to enhance the selectivity and therapeutic efficiency of  $\text{TiO}_2\text{NPs}$ . Besides, this type of surface modification can reduce the potential toxicity of unmodified  $\text{TiO}_2\text{NPs}$ , which is reported in recent publications.<sup>5</sup> In the following, some recent publications will be presented in which the  $\text{TiO}_2\text{NPs}$  have been modified with such types of organic modifiers to prepare the efficient therapeutic  $\text{TiO}_2\text{NPs}$ .

The surface modification of  $\text{TiO}_2\text{NPs}$  with organic dyes, especially porphyrins, has attracted growing interest as it can broaden the absorption range of  $\text{TiO}_2\text{NPs}$  from the UV region to the visible region.<sup>147</sup> Chlorin e6 (Ce6) is a porphyrin-based photosensitizer (PS) with a high sensitizing efficiency,<sup>148</sup> which can be conjugated with the  $\text{TiO}_2\text{NP}$  surface either by non-covalent or covalent modalities.<sup>146</sup> In general, the physical conjugation of PS might suffer from desorption which limit the nanosystem efficiency. Conversely, the covalent attachment of the PS to  $\text{TiO}_2\text{NPs}$  can guarantee the stability of the nanosystem, especially when the silane linkers are used which hold a high affinity towards the hydroxyl groups of  $\text{TiO}_2\text{NPs}$ . For example, Youssef *et al.* studied the attachment of Ce6 to  $\text{TiO}_2\text{NPs}$  by two approaches: (1)  $\text{TiO}_2\text{NPs}$  were encapsulated with silanes (APTES and TEOS) and Ce6 (as PS), followed by polyethylene glycol (PEG) grafting on this shell to obtain  $\text{TiO}_2\text{NPs}@4\text{Si-Ce6-PEG}$  and (2) for the second approach, the  $\text{TiO}_2\text{NPs}$  were first modified only by APTES (as the silane linker) and then Ce6 was covalently attached onto the modified  $\text{TiO}_2\text{NPs}@APTES$  *via* an amide bond to construct  $\text{TiO}_2\text{NPs}@APTES\text{-Ce6}$ .<sup>146</sup> *In vitro* tests on glioblastoma U87 cells were performed to study the cellular uptake, phototoxicity, and dark cytotoxicity of the modified and unmodified  $\text{TiO}_2\text{NPs}$ . In contrast to the PEGylated  $\text{TiO}_2\text{NPs}$ , the APTES-modified ones showed more PDT efficiency, in which a %89 decrease of U87 viability was observed for  $200\text{ }\mu\text{g mL}^{-1}$  of  $\text{TiO}_2\text{NPs}@APTES\text{-Ce6}$ , which corresponds to  $0.22\text{ }\mu\text{M}$  of Ce6. This surface modification resulted in a change of the absorption profile of the hybridized  $\text{TiO}_2\text{NPs}$  from the UV region (for unmodified  $\text{TiO}_2\text{NPs}$ ) to the visible region. Also, it can enhance the biocompatibility of  $\text{TiO}_2\text{NPs}$  and their stability, due to the presence of silane coupling agents on the surface of  $\text{TiO}_2\text{NPs}$ .

The modification of  $\text{TiO}_2\text{NPs}$  with targeting molecules (such as folic acid (FA)) significantly enhances the selectivity of  $\text{TiO}_2\text{NPs}$  to some types of cancer, which is an alternative way





to improve the therapeutic efficiency of PDT. The folic acid-modified TiO<sub>2</sub>NPs can be accumulated in the target sites by increasing the affinity of folic acid-modified NPs to the pathological tissue. Also, this modification can improve cell membrane penetration through folate receptors, which are overexpressed on the surface of some types of cancer cells. For example, Liang *et al.* synthesized a novel TiO<sub>2</sub>NPs–folic acid–Al(III) phthalocyanine chloride tetrasulfonic acid (TiO<sub>2</sub>NPs–FA–Pc) targeting nanosystem for therapy of the folate receptor-positive cancer cells.<sup>149</sup> In this system, folic acid (FA) was conjugated with the TiO<sub>2</sub>NPs as a tumor-targeting agent which enhanced the selectivity of TiO<sub>2</sub>NPs toward the cancer cells. It should be mentioned that the conventional photosensitizer (Pc) exhibited low selectivity for tumor targeting and low two-photon absorption. The modification of TiO<sub>2</sub>NPs using this photosensitizer enhanced its two-photon absorption of TiO<sub>2</sub>NPs–FA–Pc. The *in vitro* studies of these modified TiO<sub>2</sub>NPs showed a high PDT efficiency and biocompatibility. Also, it exhibited tumor growth suppression in mice bearing HeLa xenograft tumors with minimal side effects, using low dose of this nanocomposite under low light irradiation.

In another study, Salama *et al.* investigated the attachment of the epidermal growth factor receptor (EGFR) on PEG-modified TiO<sub>2</sub>NPs for increasing the PDT effect for epithelial cell carcinoma (A431 cell line).<sup>150</sup> The EGFR is vital for cell proliferation and it is highly expressed on many cancer cells, so for this reason, the modification of TiO<sub>2</sub>NPs with EGF could increase the efficiency and selectivity of TiO<sub>2</sub>-based PDT. Their results showed that the EGF modification of TiO<sub>2</sub>NPs–PEG diminished the cell viability of the cancer cells *via* interrupting DNA synthesis. Also, the PEG modification of the TiO<sub>2</sub> core could enhance the stability and bioavailability of this nanosystem.

In spite of the advantage of PDT, the *in vivo* production of toxic ROS and high photosensitivity of treated patients could limit the PDT technique.<sup>7</sup> The development of modified TiO<sub>2</sub>NPs with a high photothermal conversion efficiency has recently gained much attention, as an efficient and non-invasive method, to destroy target tumor tissues.<sup>151</sup> The heat generated by the vibrational relaxation of stimulated TiO<sub>2</sub>NPs (> 42 °C) could trigger several photothermal effects in tumors such as causes necrosis, apoptosis, and necroptosis. The limitation of PTT (photothermal therapy) is the low NIR absorption of cancer cells located far from the tissue surface which can be overcome by modifying TiO<sub>2</sub>NPs with the organic molecules absorbing long-wavelength visible light or NIR. Behnam *et al.* used PEG-modified TiO<sub>2</sub>NPs as PTT agents to increase the water dispersibility and biocompatibility of TiO<sub>2</sub>NPs.<sup>152</sup> Besides, these PEGylated TiO<sub>2</sub>NPs could escape the reticuloendothelial system (RES) and reach to their target tumors. The *in vivo* results showed a relatively high PTT efficacy of these TiO<sub>2</sub>NP–PEG nanosystems on reducing the melanoma tumor size without any symptom of cancer cells in treated cases. Therefore, TiO<sub>2</sub>NPs–PEG can be utilized as a potent agent with low toxicity in the hyperthermia cancer therapy.

As another advanced technique, combined PDT/PTT approaches have much stronger effects than expected; for

instance, Gao *et al.* synthesized polydopamine-modified TiO<sub>2</sub>NPs (TiO<sub>2</sub>-b-P25@PDA NPs) forming a high core-shell structure, as an improved PTT nanosystem.<sup>153</sup> They then prepared synergistic nanoprobes (TiO<sub>2</sub>-b-P25@PDA-Ce6 (Mn)) by combining chlorine e6 (Ce6) and chelating Mn<sup>2+</sup> for use in combined PDT/PTT. These modified-TiO<sub>2</sub>NPs showed high ROS generation and high photothermal conversion efficiency (32.12%). Their *in vivo* tests on a 4T1 tumor-bearing nude mouse model illustrated a synergistic significant antitumor effect of the nanosystem (under the combination of PDT/PTT with a low-dose laser), compared to the partial tumor inhibition by single PDT and single PTT. So, the co-modification of TiO<sub>2</sub>NPs with the PTT and PDT agents can dramatically enhance the therapeutic efficacy of modified TiO<sub>2</sub>NPs, compared to the unmodified structures.

In 2022, Dai *et al.* modified TiO<sub>2</sub>NPs with hyaluronan and porphine for the simultaneous PTT/PDT therapies.<sup>154</sup> They used these two surface modifiers (hyaluronan and porphine) to mildly reduce the lipid level of RAW 264.7 cells without triggering the harsh cell apoptosis, which is an important strategy for the treatment of chronic cardiovascular diseases. For both PTT alone and PTT + PDT therapies, their result demonstrated a considerable decrease of intracellular lipid load without triggering apoptotic cell death or necrosis, below the 45 °C. Conversely, the PDT modality showed a small decrease in lipid levels and a significant apoptosis or necrosis. These results indicated that the surface modification of TiO<sub>2</sub>NPs could increase the PTT efficiency and enhance the local temperature to relatively moderate levels (44 °C) after NIR irradiation, which prevented excessive cell apoptosis or necrosis, while PDT resulted in harsh cell death.

Regarding the sonodynamic effect of TiO<sub>2</sub>NPs, there have been an admirable effort for developing sonodynamic TiO<sub>2</sub>NPs, as a non-invasive method, having high tissue penetration and spatiotemporal selectivity. In SDT (sonodynamic therapy), the ROS generation is triggered under ultrasound (US) stimulation, resulting in selective tumor targeting with minimal damage to nearby healthy cells.<sup>155</sup>

Pancreatic cancer is considered as the third-leading cause of death in 2022 because of its increasing cases and mortality rates.<sup>156</sup> In the advanced-stage of this cancer, surgical resection is the primary method but only 20–15% of patients can survive and the other types of therapeutic modalities, such as chemotherapy and immunotherapy, show poor response to the majority of clinical treatments.<sup>157</sup> Sonodynamic therapy (SDT) has shown to be a promising alternative in this case. However, pancreatic tumors are surrounded by the interstitial fluid pressure (IFP) and hypoxia tumor microenvironment (TME) which decreases the sonosensitizer penetration into the tumor, resulting in low SDT efficiency.<sup>158,159</sup> Collagen is the most abundant protein in the ECM (extracellular matrix) of pancreatic cancer<sup>160</sup> and so, the modification of the TiO<sub>2</sub>NP sonosensitizer with collagenase is a promising strategy to improve the SDT efficiency in pancreatic cancer. Recently, Luo *et al.* synthesized collagenase-modified hollow TiO<sub>2</sub>NPs (H-TiO<sub>2</sub>NPs-Co) capable of degrading stromal barriers and producing sufficient





ROS.<sup>161</sup> The *in vivo* tests in a patient-derived xenograft (PDX) model showed an enhanced penetration and retention of the TiO<sub>2</sub>NPs within tumor tissues, due to the presence of Co on the TiO<sub>2</sub>NP surface. The ultrasonic irradiation caused the controlled release of collagenase which degraded tumor matrix fibers. The attached collagenase (Co) resulted in accumulation of modified TiO<sub>2</sub>NPs within the tumor which generate abundant ROS under the ultrasound (US) irradiation and dramatically increase the selectivity and therapeutic efficiency of SDT.

In 2021, Wei *et al.* synthesized newly modified TiO<sub>2</sub>NPs, functionalized with a malignant melanoma cell membrane (B16F10M) and a targeting aPD-L1 antibody for enhanced sonodynamic tumor therapy.<sup>162</sup> Under ultrasound irradiation, these modified TiO<sub>2</sub>NPs showed a high efficiency to generate ROS (<sup>1</sup>O<sub>2</sub>) along with precise targeting effects, high tumor uptake, and intracellular sonocatalytic killing of the B16F10 cells. In this study, the modification of TiO<sub>2</sub>NPs with the mentioned biomolecules resulted in a dramatic enhancement of biocompatibility, selectivity and therapeutic yield of the modified TiO<sub>2</sub>NPs.

Lin *et al.* reported the synthesis of a multifunctional modified TiO<sub>2</sub>NP sonosensitizer (TiO<sub>2</sub>NPs-Ce6-CpG, CpG: a targeting oligonucleotide) for highly efficient cancer immunotherapy.<sup>163</sup> To improve the biocompatibility and sonotherapeutic ability of these TiO<sub>2</sub>NPs, they were modified with chlorin e6 (Ce6) and a CpG oligonucleotide (CpG ODN) to enhance the immune response. Ce6 is a hydrophilic porphyrin-type sonosensitizer, which accumulates effectively in tumors, and can generate ROS under the ultrasound activation to induce apoptosis and necrosis of the tumor cells. The CpG ODN oligonucleotide is an immunological adjuvant that can trigger cellular immune responses to enhance the anticancer properties of a variety of cancer treatments. The injected TiO<sub>2</sub>NPs-Ce6-CpG could induce the release of tumor-associated antigens and demonstrated vaccine-like functions together with the CpG adjuvant, which activated dendritic cells (DCs) and enhanced tumor-infiltrating CD8<sup>+</sup> T cells to the tumor tissues, inducing a robust antitumor immunological response.

Lee *et al.* studied the potential application of SDT against glioblastoma cells using TiO<sub>2</sub>NPs modified with a targeting molecule, anti-EGFR antibody.<sup>164</sup> Their results showed a dramatic enhancement of the selectivity and internalization of modified TiO<sub>2</sub>NPs toward the target cells, due to the presence of the anti-EGFR antibody on the TiO<sub>2</sub>NP surface. Under the ultrasound irradiation of modified TiO<sub>2</sub>NPs, cell viabilities were reduced because of the ROS generation with minimal effects on apoptosis.

In 2021, Yousefi, *et al.* used porphyrin-loaded TiO<sub>2</sub>NPs and studied their sonotoxicity on MDA-MB-231 cells.<sup>165</sup> To increase the biocompatibility and ultrasound absorption efficiency, the surface of TiO<sub>2</sub>NPs was modified first with the polyvinyl alcohol (PVA) polymer and then with porphyrin. The *in vitro* results indicated that these modified TiO<sub>2</sub>NPs are non-toxic and under the ultrasound radiation they could damage the breast cancer cells.

Pariante *et al.* synthesized sono-responsive TiO<sub>2</sub>NPs modified with poly(ethylene oxide)-poly(propylene oxide) (PEO-PPO) copolymers for their potential in sonodynamic applications.<sup>166</sup> Their results showed an enhanced biocompatibility of these modified TiO<sub>2</sub>NPs, due to the modifying copolymer. Upon irradiation with the therapeutic ultrasound, the nanoparticles generated ROS and induced the apoptosis of Rh30 cells. The compatibility and cellular uptake of these modified TiO<sub>2</sub>NPs were confirmed on the Rh30 cell line, as a model of rhabdomyosarcoma without any significant hemolysis over 24 h treatment.

The other recent publications on the therapeutic effect of TiO<sub>2</sub>NP-based nanostructures are summarized in Table 6.

#### 4.2. Drug delivery

Chemotherapy is limited by the uncontrolled distribution of chemodrugs towards both cancerous and healthy cells which results in adverse side effects for the treated patients. TiO<sub>2</sub>NP-based drug delivery systems have attracted much more interest in recent years to enhance the target specificity of chemotherapy and reduce the systemic side effects. These advanced drug delivery systems benefit various controlled-release mechanisms including pH- and thermo-sensitive, photo-induced, and enzyme-responsive techniques which result in an enhanced specificity of the drugs toward the cancer cells and subsequently, the drug dosage can be significantly minimized while still maintaining the pharmacological effects. Recently, the modified TiO<sub>2</sub>NPs have been used for the delivery of various anticancer drugs, such as temozolomide, cisplatin, doxorubicin, and daunorubicin.<sup>8,182</sup> For instance, Han *et al.* reported the synthesis of poly(acrylic acid)-calcium phosphate modified TiO<sub>2</sub>NPs (TiO<sub>2</sub>NPs@PAA-CaP) for the efficient drug delivery of doxorubicin (DOX).<sup>183</sup> This surface modification of TiO<sub>2</sub>NPs resulted in a significant enhancement of DOX loading and encapsulation up to eight times, compared to that of unmodified TiO<sub>2</sub>NPs. Due to the pH-responsive surface properties of the PAA-CaP modifying layer, DOX-loaded TiO<sub>2</sub>NPs@PAA-CaP exhibited much faster cumulative DOX release at acidic pH = 5.2 than at neutral pH = 7.4. TiO<sub>2</sub>NPs@PAA-CaP(DOX) illustrated an enhanced cellular uptake and a higher cytotoxicity towards MCF-7 tumor cells, compared to that of free DOX. More importantly, this modified nanosystem demonstrated synergistic chemo- and photodynamic therapeutic effects on the target cells.

Neuroblastoma is considered as one of the leading causes of cancer-related deaths in children worldwide<sup>184</sup> and temozolomide (TMZ) has been widely used to treat neuroblastoma.<sup>185,186</sup> The synthesis of TiO<sub>2</sub>NP-TMZ was studied previously for its potential to treat neuroblastoma;<sup>187</sup> however, the clinical application of TiO<sub>2</sub>NPs is strictly limited by its serious cytotoxicity, inflammation, and brain damage.<sup>188</sup> For this reason, alginate was used as a TiO<sub>2</sub>NP modifier due to the biological advantages of alginate such as biocompatibility, anti-inflammatory effects, antioxidant properties, and easy degradation with little toxicity.<sup>189</sup> Zhao *et al.* reported the modification of TiO<sub>2</sub>NPs-temozolomide (TiO<sub>2</sub>NPs-TMZ) with alginate and studied their anti-oxidant, anti-inflammatory, and anti-tumor effects on



Table 6 Other recent publications (2021–2022) on the therapeutic effect of TiO<sub>2</sub>NP-based nanostructures

Nanosystem	Applications	Ref.
Fe <sub>2</sub> O <sub>3</sub> -TiO <sub>2</sub> nanocomposites, using polyvinylpyrrolidone-polyethylene glycol (PVP-PEG)	Showed remarkable PDT activity in HeLa cell lines <i>via</i> the generation of intracellular ROS	167
New nanocomposite, TiO <sub>2</sub> NPs@Ru@siRNA	Remarkable PDT activity on patient-derived xenograft (PDX) and rat oral experimental carcinogenesis models	168
Folic acid-functionalized TiO <sub>2</sub> NPs	Modeling of active targeting of tumor cells	169
Chelate-free gadolinium loaded TiO <sub>2</sub> NPs coated with transferrin (Tf)	Coating of this TiO <sub>2</sub> -Gd NPs with Tf stabilized the nanoconstruct and minimized aggregation, showing a dramatic selectivity for the photodynamic targeting of studied cancer cells	170
TiO <sub>2</sub> NP-Ag nanohybrid modified with the Pluronic® F-127 polymer, which is permitted by the Food and Drug Administration (FDA)	This polymer improved the biocompatibility of TiO <sub>2</sub> NP-Ag, tested in 4T1 breast cancer cells and the nanohybrid showed endocytosed by cancer cells produced high intracellular ROS under UV conditions (5.6 mW cm <sup>-2</sup> ), resulting in cancer cell apoptosis	171
TiO <sub>2</sub> /Cur@ZIF-8 nano-composite (Cur: chemotherapeutic agent curcumin)	Synergistic photodynamic-chemotherapy and pH-/and NIR-stimulated drug release	172
N-doped graphene quantum dots (QDs)/titanium dioxide nanocomposites (N-GQDs/TiO <sub>2</sub> NPs) modified with citric acid	Upon the photo-activation of N-GQDs/TiO <sub>2</sub> NPs with near-infrared (NIR) light, the nanocomposites generated reactive oxygen species (ROS), mainly singlet oxygen ( <sup>1</sup> O <sub>2</sub> ), which caused more significant cell death in MDA-MB-231 (an epithelial, human breast cancer cells) than in HS27 (human foreskin fibroblast)	173
Tc-99m-labeled lupulone-conjugated Fe <sub>3</sub> O <sub>4</sub> @TiO <sub>2</sub> nanocomposite	Lupulone-conjugated Fe <sub>3</sub> O <sub>4</sub> @TiO <sub>2</sub> nanocomposites showed suitable dispersion and the photodynamic effect on prostate cancer without visible aggregation	174
Doped TiO <sub>2</sub> rhombic nanocomposites modified with Pluronic® F-68	Mn-TiO <sub>2</sub> -PF-68 RNCs demonstrated negligible toxicity with physiological stability. Mn <sup>3+</sup> doped with photosensitizers (TiO <sub>2</sub> ) also exhibited a great synergistic effect of photo-killing <i>in vitro</i> by developing hydroxyl radicals	175
Titanium-oxo nanoclusters modified with dopamine and PEG	The introduced dopamine (DA) ligands not only facilitated the water solubility and the photocatalytic properties of the NPs but also involved the tumor-targeting behavior through the binding affinity with DA receptors on cancer cells. Under Cerenkov irradiation, these nanocomposites enable efficient hydroxyl radical generation	176
C-doped TiO <sub>2</sub> NPs	They were prepared and tested as a photosensitizer for visible-light-driven photodynamic therapy against cervical cancer cells (HeLa)	177
Tablet-like TiO <sub>2</sub> /c nanocomposite with a metal-organic-framework (MOF)-derived carbon structure	This nanocomposite continued to generate ROS in response to repeated ultrasound irradiation and was able to induce tumor cell apoptosis <i>via</i> SDT-induced DNA damage <i>in vitro</i> and <i>in vivo</i> . This TiO <sub>2</sub> /C nanocomposite also exhibited good biocompatibility and did not induce any apparent toxicity <i>in vitro</i> and <i>in vivo</i> .	178
Hypoxia-tolerant MOF@TiO <sub>2</sub> (MOF, metal-organic framework)	Hypoxia-tolerant type I photodynamic therapy against hypoxic cancer	179
MnCO@TPP@C-TiO <sub>2</sub> NPs	MnCO@TPP@C-TiO <sub>2</sub> NPs selectively localized in the mitochondria of HeLa cells where the overexpressed-H <sub>2</sub> O <sub>2</sub> triggered CO released, resulting in mitochondrial damage	180
Semiconductor quantum dots (CdX, X = S, Te, Se)-TiO <sub>2</sub> NPs modified with folic acid	Prepared FA-CdX-TiO <sub>2</sub> NPs (X = S, Se) exhibited excellent cancer-targeting ability during PDT treatment. The optimum PDT efficiency of FA-CdSe-TiO <sub>2</sub> NPs indicated that the photocatalytic and targeting abilities were much higher than those of the pure TiO <sub>2</sub> NPs and CdSe-TiO <sub>2</sub> NPs	181

neuroblastoma.<sup>190</sup> Their *in vivo* results showed that the alginate modification enhanced the cytotoxicity toward neuroblastoma cells and decreased inhibitory activity toward normal neuronal cells. This modification increased the antioxidant, anti-inflammatory, and antitumor activities of TiO<sub>2</sub>NPs-TMZ and prolonged the survival time of the neuroblastoma model ( $P < 0.05$ ). The results showed that the alginate modification controlled the TMZ release from the TiO<sub>2</sub>NPs-TMZ-alginate nanoparticles.

In 2020, Keli *et al.* reported a novel drug delivery vehicle of TiO<sub>2</sub>NPs, encapsulated by bilayer shells that allow the reversible incorporation of hydrophobic drugs.<sup>191</sup> In these systems, TiO<sub>2</sub>NPs were chemically encapsulated by the covalent binding of hydrophobic phosphonic acid, followed by the second surface modification by amphiphilic sodium dodecylbenzenesulfonate *via* hydrophobic interactions between the

dodecylbenzene moiety and the hydrophobic first shell. This two-layer modification makes the hydrophobic surface suitable for the loading of hydrophobic drugs. These modified TiO<sub>2</sub>NPs were loaded with hydrophobic anticancer drugs 7-amino-4-methylcoumarin and quercetin. The results showed a sustained release of these anticancer drugs into the cytoplasm due to the presence of these modifying layers around the TiO<sub>2</sub>NP core and induce apoptosis in MCF-7 cancer cells.

Zheng *et al.* synthesized a novel TiO<sub>x</sub> (TiO<sub>x</sub>: oxidized TiO<sub>2</sub>) nanocomposite modified with PEG, targeting peptide YSA, and an anticancer drug cantharidin (CTD).<sup>192</sup> In this nanosystem, PEG could enhance the stability of the nanoplateform and blood circulation time, which increased the tumor accumulation after systemic administration. The YSA peptide, with the YSAYPDSVPMMSK sequence, has been proven to be a targeting motif that mediates drug delivery to tumor cells expressing



EphA2. The anticancer drug cantharidin (CTD), as one of the active components of mylabris, was loaded into TiO<sub>2</sub> for the combination of chemotherapy and PDT. The results showed that this nanosystem could significantly increase ROS production under X-ray exposure and provided a new drug delivery nanocarrier for CTD in combination with PDT to achieve more effective treatment.

In 2020, Kim *et al.* synthesized modified TiO<sub>2</sub>NPs using a tumor targeting polymer phenylboronic acid (pPBA) to encapsulate the anticancer drug doxorubicin (DOX) as a sonodynamic chemotherapeutic agent.<sup>193</sup> In this system, the self-assembled TiO<sub>2</sub>NP-DOX was encapsulated into polymeric phenylboronic acid (pPBA) *via* the formation of phenylboronic esters bonds, which are cleavable by ROS. Also, in this modified TiO<sub>2</sub>NP nanocomposite, the phenylboronic acid (PBA) moiety acts as a tumor-targeting moiety because of its high affinity toward sialylated epitopes overexpressed on the membrane of various cancers. This polymeric modification also provided an enhanced loading of DOX by the interaction of PBA with 1,3-*cis* diol of DOX, and it was reported that DOX can bind on the surface of TiO<sub>2</sub>NPs *via* the coordination of hydroquinone and the quinone moiety of the DOX structure. The loaded DOX was readily released by the sonodynamic ROS generation of TiO<sub>2</sub>NPs due to the ROS-cleavable characteristics of the phenylboronic ester bond. Their results confirmed the tumor targeting by the PBA moiety, intracellular ultrasound-generated ROS, and high tumor accumulation of this nanosystem and its efficient anti-tumor effect on tumor-bearing mice.

Yu *et al.* modified Au@TiO<sub>2</sub>NPs with poly(lactic-co-glycolic acid) (PLGA) followed by loading of the CPT-11 (irinotecan) drug as the targeting moiety.<sup>194</sup> The PLGA modification showed that these Au@TiO<sub>2</sub>NPs-CPT-11-PLGA have an enhanced anti-metastatic activity and reduced cell invasion effects in B-CPAP and FTC-133 thyroid cancer cell lines, with and without NIR irradiation. In this nanosystem, the Au moiety could enhance the NIR absorption of Au@TiO<sub>2</sub>NPs-CPT-11-PLGA, increasing the anticancer effect.

In 2021, Chen *et al.* prepared nanocomposites based on polypyrrole-coated mesoporous TiO<sub>2</sub>NPs with a suitable size distribution for the co-delivery of doxorubicin (DOX) and aspirin prodrugs, with a superior drug loading capacity, due to the presence of the modifier, polypyrrole.<sup>195</sup> Also, these modified TiO<sub>2</sub>NPs showed sonodynamic therapeutic properties and an excellent photothermal conversion efficiency (over 50.8%), with a simultaneous prodrug activation and sustained drug release, under near-infrared (NIR) and ultrasound (US) irradiation. The results showed an enhanced synergistic effect of chemotherapy and photo/sonodynamic effect to suppress the tumor.

As another biologically active polymeric modifier, polypyrrole (PPY) is an ideal photothermal conversion polymer with high photostability which has been successfully used in PTT. He *et al.* modified TiO<sub>2</sub>NPs with polypyrrole (PPY), (mTiO<sub>2</sub>NPs@PPY) to have the synergistic effect of TiO<sub>2</sub>NPs and this polymer enhanced the photothermal effect of TiO<sub>2</sub>NPs.<sup>196</sup> They used this modified mTiO<sub>2</sub>NPs@PPY as a drug

carrier, a photothermal agent and a sonosensitizer, in a single nanoplatform. They loaded honokiol (HNK), as the model antitumor drug, which demonstrated antitumor efficacy in several cancer types such as breast cancer, pancreatic cancer, prostate cancer, lung cancer, hepatoma, and bladder cancer. The modified mTiO<sub>2</sub>NPs@PPY showed the suitable size distribution and good biosafety, due to the presence of PPY on the surface of TiO<sub>2</sub>NPs. The *in vitro* and *in vivo* animal experiments demonstrated that mTiO<sub>2</sub>NPs@PPY-HNK could simultaneously have chemotherapeutic, photothermal, and sonodynamic effects under the laser and ultrasound irradiation. Other recent publications on the drug delivery application of TiO<sub>2</sub>NPs are summarized in Table 7.

#### 4.3. Antibacterials

The widespread overuse of traditional antibiotics has resulted in the emergence of multidrug-resistant bacterial strains and causes serious concerns in different aspects of life such as food safety and human health. In recent years, the research on new antimicrobial substances has focused on metal oxide nanoparticles. Specifically, TiO<sub>2</sub> nanostructures are one of the most attractive antimicrobial compounds, mainly due to their photocatalytic effect and chemical stability, low toxicity, and cost-effectiveness.<sup>9</sup> Different research studies have shown that modified TiO<sub>2</sub>NPs can demonstrate excellent antibacterial properties against a broad range of both Gram-positive and Gram-negative bacteria.<sup>10,204</sup> This section presents the latest advancements and publications in the antibacterial activity of the modified TiO<sub>2</sub>NPs. It is worth mentioning that the antibacterial effect of TiO<sub>2</sub>NPs is due to their ability to absorb light (UV-Vis) to generate reactive oxygen species (ROS) which can be used to damage the chemical structure of microbes. Recently, Diana and Mathew reported the surface modification of TiO<sub>2</sub>NPs with the alpha-lipoic acid (ALA) functionalized bovine serum albumin (BSA) conjugate, as a biocompatible antibacterial (and anticancer) system. The antibacterial ability of this nanosystem was studied against *S. aureus*, *E. coli*, *Streptococcus pneumoniae* (*S. pneumoniae*), *Candida albicans* (*C. albicans*), and *Aspergillus niger* (*A. niger*). The results proved the antimicrobial properties of the developed system and the *in vitro* cytotoxicity of these modified TiO<sub>2</sub>NPs showed that the cytotoxicity was selective for cancer cells and negligible for normal cells.<sup>205</sup> In another recent study, Maheswari *et al.* studied the antibacterial and anticancer properties of six TiO<sub>2</sub>NP systems modified with three plant extracts including: *Withania somnifera* (Ashwagandha), *Eclipta prostrata* (Karisalankanni) and *Glycyrrhiza glabra* (Athimathuram), known as medicinal plants with pharmacological applications.<sup>206</sup> The antibacterial features of these six samples were studied against three Gram-negative bacterial strains (*E. coli*, *Klebsiella pneumoniae* (*K. pneumoniae*), and *Pseudomonas aeruginosa* (*P. aeruginosa*)) and two Gram-positive bacterial strains (*S. aureus* and *Streptococcus mutans* (*S. mutans*)). Among the modified and unmodified TiO<sub>2</sub>NP samples, *Withania somnifera*-*Eclipta prostrata* modified TiO<sub>2</sub>NPs showed the good antibacterial nature against the studied bacteria. Also, these modified TiO<sub>2</sub>NPs exhibited excellent



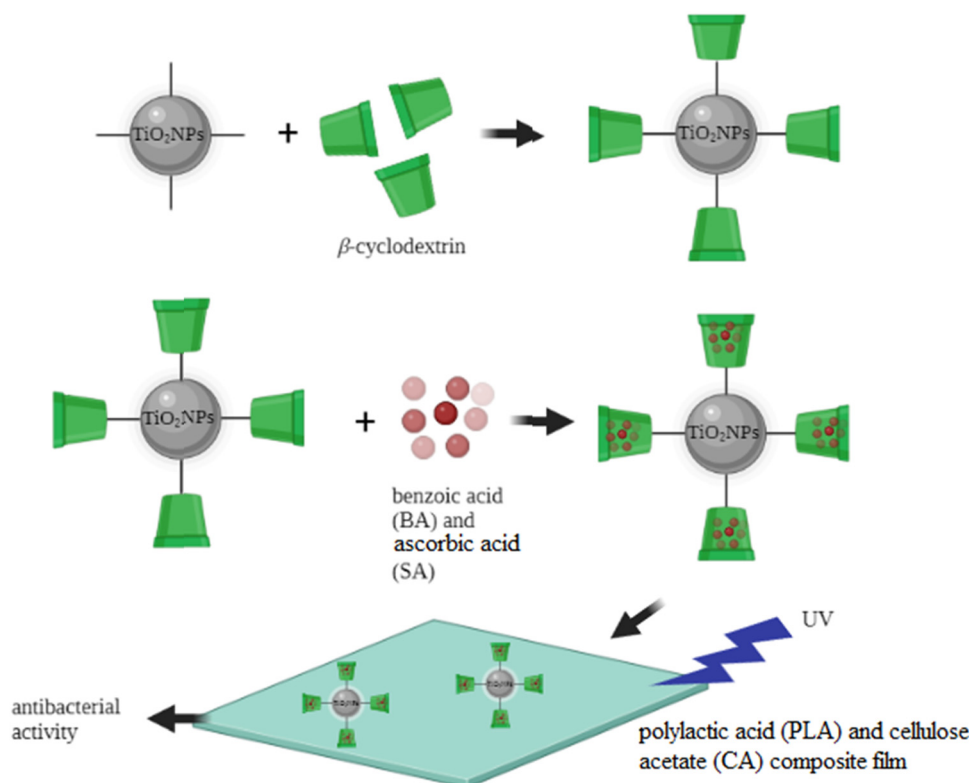
**Table 7** Other research published in 2022 on the drug delivery application of TiO<sub>2</sub>NP-based nanostructures

Nanosystem	Applications	Ref.
Iron-supplement coated anatase TiO <sub>2</sub> NPs modified with folic acid	Fe@TiO <sub>2</sub> NPs showed a controlled pH-sensitive delivery of the loaded imatinib molecules	197
PLGA-TiO <sub>2</sub> NPs (PLGA: poly(lactic-co-glycolic acid))	Controlled release of a natural extract (international patent No. PCT/IB2020/061916)	198
Caffeic acid-mediated synthesis of TiO <sub>2</sub> NPs (CA-TiO <sub>2</sub> NPs)	The results indicated that CA-TiO <sub>2</sub> NPs, as a promising compound with excellent biocompatibility, can be used in healthcare products and clinical and medicinal applications	199
GO-FA-PEG-TiO <sub>2</sub> -Avi/Bio	Enhanced water solubility and potential anti-tumor activity and targeted co-delivery of anticancer drug, SN-38	200
TiO <sub>2</sub> NPs-polydopamine	Delivery of loaded icariin (Ica) for the improvement of the osseointegration process	201
TiO <sub>2</sub> and mSiO <sub>2</sub> drug delivery systems modified with folic acid	<i>In vitro</i> drug release of DOX experiments, hemolysis experiments, and cytotoxicity experiments on HeLa cell lines confirmed that the drug delivery system has good biocompatibility and GSH concentration-dependent drug release behavior	202
pH-Sensitive mesoporous bisphosphonate-based TiO <sub>2</sub> NPs (modified with alendronate sodium trihydrate (AST))	They were used as nanocarriers for dexamethasone (DEX) drug delivery. The pH-sensitive behavior of the NPs can be attributed to the presence of AST's amine groups in the hybrid nanoparticles	203

anticancer activities against KB oral cancer cells, among the other bio modified and unmodified TiO<sub>2</sub>NP samples. These results indicated the improved biological activities of TiO<sub>2</sub>NPs after surface modification. In 2022, PV *et al.* synthesized a TiO<sub>2</sub>/ZnO nanostructure by decorating ZnO nanoparticles over a commercial TiO<sub>2</sub> nanosurface.<sup>207</sup> The ZnO formed over the anatase TiO<sub>2</sub> layer showed excellent antibacterial activity against both *S. aureus* and *E. coli* and was found to be non-toxic towards MG-63 osteosarcoma cells. In 2022, Goñi-Ciauriz and Vélaz prepared polylactic acid (PLA) and cellulose acetate

(CA) composite films with  $\beta$ -cyclodextrin-modified TiO<sub>2</sub>NPs (Fig. 5).<sup>129</sup>

Benzoic acid (BA) and ascorbic acid (SA) were incorporated into  $\beta$ -cyclodextrin-modified TiO<sub>2</sub>NPs, and the antibacterial activities of the PLA and CA composite films were successfully tested against *E. coli* and *S. aureus*. The highest antibacterial activity was observed with the film containing 5% modified TiO<sub>2</sub>NPs achieving 71% inhibition of *E. coli* and 88% inhibition of *S. aureus*. The modification of the TiO<sub>2</sub>NP surface with  $\beta$ -cyclodextrin provided an efficient carrier nanosystem and

**Fig. 5**  $\beta$ -Cyclodextrin-modified TiO<sub>2</sub>NPs for antibacterial applications. Adapted with permission from ref. 129. Copyright 2022 Elsevier.



enhanced the therapeutic ability of the TiO<sub>2</sub>NP core. Previously, these modified TiO<sub>2</sub>NPs were successfully tested to load and release different food preservatives from the  $\beta$ -cyclodextrin grafted TiO<sub>2</sub>NPs. The controlled release of therapeutic molecules from the cavity of  $\beta$ -cyclodextrin may extend the antimicrobial effect of the TiO<sub>2</sub>NPs. Also, it can enhance the thermal stability of the film against volatilization or thermal conversion, when high temperature is applied in the food packing applications. Benzoic acid (BA) and sorbic acid (SA) are known as antimicrobial preservatives in food industry, due to their stable antimicrobial effectiveness against a broad range of microorganisms, including some bacteria, yeasts, and fungi. The authors used the polylactic acid (PLA)/cellulose acetate (CA) film, as a biodegradable polymer matrix, for fixation and stabilization of the modified TiO<sub>2</sub>NPs, as potential active food packaging. The controlled release of benzoic acid (BA) and sorbic acid (SA) from the  $\beta$ -cyclodextrin-modified TiO<sub>2</sub>NPs could dramatically improve the antimicrobial characters of the TiO<sub>2</sub>NPs. These results indicated the great potential of this TiO<sub>2</sub>NP-based nanocomposite to be used as antimicrobial food packaging.

Sathiyaseelan *et al.* synthesized modified TiO<sub>2</sub>NPs using an aqueous extract of the endophytic fungus *Paraconiothyrium brasiliense* (Pb) to improve the antibacterial activity of common standard antibiotics at a minimum concentration.<sup>208</sup> The modification of TiO<sub>2</sub>NPs with the Pb fungus significantly enhanced the antimicrobial and antioxidant properties, biocompatibility, and stability of the TiO<sub>2</sub>NPs. The authors used these modified TiO<sub>2</sub>NPs with standard antibiotics (erythromycin, ampicillin, gentamicin, vancomycin, and tetracycline) to improve the antibacterial properties of these antibiotics without significant adverse effects. Antibacterial studies showed low activity of modified TiO<sub>2</sub>NPs-Pb at a concentration of 20  $\mu\text{g mL}^{-1}$ . However, a combination of tetracycline hydrochloride (TCH) with TiO<sub>2</sub>NPs-Pb significantly enhanced the inhibition of the *E. coli* biofilm. The authors reported the moderate toxicity of TiO<sub>2</sub>NPs-Pb (100  $\mu\text{g mL}^{-1}$ ) on the cell line NIH3T3, red blood cells (RBC), and egg embryos. This research revealed that the antibiotics could be mixed with the modified TiO<sub>2</sub>NPs-Pb to improve the antibacterial efficiency and minimize antimicrobial resistance and environmental toxicity.

Özdemir *et al.* prepared modified TiO<sub>2</sub>NPs using cotton fabric by hydrolysis of the TiCl<sub>4</sub> precursor solution over cotton fabric.<sup>209</sup> The modified TiO<sub>2</sub>NPs enhanced the photodegradation of rhodamine B, compared to the cotton fabric alone. The antibacterial activity of this modified TiO<sub>2</sub>NP was successfully tested against *S. aureus* (ATCC 6538) and *E. coli* (ATCC 25922) as representative strains of Gram-positive and Gram-negative bacteria, respectively. In this modified TiO<sub>2</sub>NP system, the presence of cotton fabric acted as a template to provide active sites for the adsorption of pollutant molecules and microorganisms and more importantly, this template facilitated the transfer of produced ROS to the target molecules for their degradations which resulted in a significant increase of the photocatalytic effect of the TiO<sub>2</sub>NPs.

Metanawin and Metanawin used the mini-emulsion polymerization of the TiO<sub>2</sub>NP-polystyrene (TiO<sub>2</sub>NP-PS) hybrid

antibacterial material.<sup>210</sup> Triethylene glycol dimethacrylate (TEGDMA) was employed, as a crosslinking agent, to improve the stability/modification efficiency of TiO<sub>2</sub>NPs and photocatalytic activity. Their results showed an excellent antibacterial effect of these TiO<sub>2</sub>NPs-PS against both Gram-positive (*S. aureus*) and Gram-negative (*K. pneumoniae*) bacteria. Also, the photocatalytic efficiency of TiO<sub>2</sub>NPs-PS was tested for the photodegradation of methylene blue under UV irradiation. The photocatalytic effect of TiO<sub>2</sub>NPs-PS was increased in the presence of the crosslinking agent TEGDMA due to the self-organized structure of this hybrid system. These surface modifiers could enhance the surface area of TiO<sub>2</sub>NPs which has paramount importance to enhance photocatalytic activity during photocatalysis.

Elbarbary *et al.* synthesized biodegradable poly(PVA/PLA/TiO<sub>2</sub>NPs) nanocomposite films by combining polyvinyl alcohol (PVA) and polylactic acid (PLA) doped with TiO<sub>2</sub>NPs.<sup>90</sup> The addition of 0.8 wt% of TiO<sub>2</sub>NPs showed significant enhancement of the thermal stability of the films and the water resistance properties were obtained using a 2 : 1 PVA : PLA ratio. This poly(PVA/PLA/TiO<sub>2</sub>NPs) nanocomposite displayed an improved antibacterial activity against *S. aureus* and *E. coli* strains. The biodegradation tests were performed in soil burial and the results showed a rapid increase of the degradation of the film in the initial 12 weeks with a significant change of morphology. These results suggested the potential application of this biodegradable poly(PVA/PLA/TiO<sub>2</sub>NP) nanocomposite for developing packaging materials with low environmental impact. The authors used polylactic acid (PLA) because of its thermoplasticity and biodegradability with a wide range of potential industrial applications, such as packaging materials for fresh fruit and vegetables. However, due to the ester group in PLA, it has low mechanical/thermal stability, high rigidity, and poor hydrophilicity. To use PLA in the antibacterial films, it could be combined with synthetic polymers such as polyvinyl alcohol (PVA) to improve the properties of PLA. PVA is considered as a hydrophilic, biodegradable, biocompatible and cost-effective polymer, which is commonly studied in different biological applications such as drug delivery and food packaging. This PLA/PVA film was applied as a template for fixing TiO<sub>2</sub>NPs, enhance their stability and antibacterial effectiveness.

Singh *et al.* conducted the green and cost-effective synthesis of TiO<sub>2</sub>NPs using waste leaves of water hyacinth (WH) (*Eichhornia crassipes*), an aquatic weed, under ambient conditions.<sup>211</sup> The antibacterial efficiency of these modified TiO<sub>2</sub>NPs was tested on a commonly known toilet bacteria, *Serratia marcescens*. They reported a  $\sim 3.0$  cm diameter of the inhibition zone at a 150  $\mu\text{g mL}^{-1}$  concentration of the nanocomposite which is superior to commercial TiO<sub>2</sub>NPs and the WH leaf extract. This research showed great potential of the modified TiO<sub>2</sub>NPs in healthcare industries. In this study, the authors used water hyacinth (WH) as a natural antimicrobial reagent for the TiO<sub>2</sub>NP modification to improve the stability, biocompatibility, and antimicrobial effect of the TiO<sub>2</sub>NPs.





Table 8 Other publications on the antibacterial applications of TiO<sub>2</sub>NP-based nanostructures

Nanosystem	Applications	Ref.
TiO <sub>2</sub> NPs modified with bio agents: <i>Syzygium aromaticum</i> , <i>Eleteria cardamomum</i> , and <i>Cinnamomum verum</i>	Antibacterial and anticancer (KB oral cancer cell line)	215
Pure TiO <sub>2</sub> nanoparticles and turmeric-, ginger-, garlic-modified TiO <sub>2</sub> NPs	Antibacterial against five bacterial strains, anticancer activity against the KB oral cancer cell line	216
Pure TiO <sub>2</sub> NPs, Aqua Rosa-modified TiO <sub>2</sub> NPs and protein powder-modified TiO <sub>2</sub> NPs	Antibacterial against five bacterial strains, anticancer activity against the KB oral cancer cell line	217
TiO <sub>2</sub> NP incorporation into the heparin-polyvinyl alcohol nanocomposite	Enhanced <i>in vitro</i> antibacterial activity and care of <i>in vivo</i> burn injury	218
Poly(lactic acid)/halloysite nanotubes-TiO <sub>2</sub> NPs	High efficiency to both Gram-positive and Gram-negative bacteria	219
Nano-natural antimicrobial agent@polymeric microgels-TiO <sub>2</sub> hybrid films	Antibacterial on the touch screen panel	220
Bio-nanocomposite film (polyvinyl alcohol)/TiO <sub>2</sub> /chitosan/chlorophyll	Inhibits the growth of both <i>S. aureus</i> and <i>E. coli</i> bacteria under LED light irradiation	221
<i>In situ</i> coating of the TiO <sub>2</sub> surface by plant-inspired tannic acid for the fabrication of thin film nano-composite nano-filtration membranes	Enhanced antibacterial performance	222
Functionalization of a polyvinylidene fluoride membrane by the biocidal oxine/TiO <sub>2</sub> nanocomposite	Anti-biofouling properties	223
Cellulose acetate/TiO <sub>2</sub> nanoparticles	Exhibited good antibacterial activity against <i>E. coli</i> with 55.6% sterilization in 12 h	224
Preparation of <i>monsonia burkeana</i> plant extracts	The material was found to be selective against <i>E. coli</i> . In real water samples, this material demonstrated remarkable activity	225
Poly(lactic acid) (PLA)/TiO <sub>2</sub> nanocomposite	Antibacterial activities with optimal inhibition zones against <i>S. aureus</i> followed by <i>E. coli</i>	120

Mallakpour and Mohammadi prepared sodium alginate-pectin composite (ALG-PEC CS) and nanocomposite (NC) films, containing different concentrations of TiO<sub>2</sub>NPs (0.5, 1, and 2 wt%).<sup>212</sup> They used CaCl<sub>2</sub> and glutaraldehyde (Glu) as cross-linkers, which produce rigid scaffolds for hydroxyapatite (HA) sedimentation. The film containing 2 wt% TiO<sub>2</sub>NPs exhibited the best bioactivity and biocompatibility on the MG-63 cell line, as well as the best antibacterial effect against *S. aureus*. The authors modified TiO<sub>2</sub>NPs with the polymeric matrix to enhance the bioactivity and mechanical properties of implants. Generally, the Ti-OH surface groups facilitated the formation of HA on the composite solid surface. To facilitate the interaction between the implant and surrounding bone tissues, TiO<sub>2</sub>NPs should be modified/incorporated with a polymeric substrate.

Youssef *et al.* synthesized TiO<sub>2</sub>NPs and incorporated them into pure low-density polyethylene (TiO<sub>2</sub>NPs-LDPE) at different concentrations (0.5, 1, and 2% weight of the polymer) for potential applications in the packaging materials industry.<sup>213</sup> Their antibacterial tests revealed the high ability of TiO<sub>2</sub>NPs to generate the reactive radical species (ROS) which induced the antibacterial activity of LDPE against Gram-negative and Gram-positive bacteria. Among synthetic polymers, low-density polyethylene (LDPE) is commonly used in food packaging due to its thermal stability and flexibility, cost-effectiveness, transparency, ease of processability, and biocompatibility. Most of the antimicrobial food packaging studies have focused on LDPE polymers and for these reasons this polymer can be a good candidate for the surface modification of TiO<sub>2</sub>NPs, as a biologically active agent to enhance the effectiveness of TiO<sub>2</sub>NPs and their biocompatibility in the food packing industry.

Makableh *et al.* investigated the addition of TiO<sub>2</sub>NPs and ciprofloxacin (CIPRO) to polydimethylsiloxane (PDMS) to

enhance the antibacterial activity and hydrophobicity.<sup>214</sup> The nanocomposite of PDMS was prepared by combining the TiO<sub>2</sub>NPs and/or CIPRO with PDMS before the crosslinking step. Various loading concentrations of TiO<sub>2</sub>NPs (1–5 wt%) were used while the CIPRO concentration was fixed at 0.5 wt%. The antibacterial results revealed the synergistic effect of both TiO<sub>2</sub>NPs and ciprofloxacin which led to an enhanced antibacterial activity against *S. aureus* and *E. coli*. The PDMS polymer has self-healing properties, biocompatibility, cost-effectiveness, high flexibility, and antimicrobial activity. Ciprofloxacin (CIPRO) is also known as a fluoroquinolone drug and considered as one of the most bactericidal agents used widely. So, the modification of TiO<sub>2</sub>NPs with the PDMS polymer and CIPRO could be a promising strategy to enhance the biological effectiveness of TiO<sub>2</sub>NPs and decrease their potential toxicity.

Other recent studies on the antibacterial applications of TiO<sub>2</sub>NP-based nanostructures are summarized in Table 8.

#### 4.4. Biosensors

In recent years, there has been an admirable effort to develop TiO<sub>2</sub>NP-based biosensors,<sup>226</sup> specifically for the development of novel biomolecule-TiO<sub>2</sub>NP systems leading to a dramatic success in the fabrication of bio-nanohybrid devices, such as biomolecule-sensitized solar cells (BSSCs) and photoelectrochemical cells (PECs).<sup>227</sup> The high sensitivity of such biosensors can provide opportunities to improve clinical methods in monitoring the patient's response to medical or surgical therapy. A biosensor should have several essential characteristics for the practical applications, including biocompatibility, cost-effectiveness, user-friendliness, low sensitive detection limit/high accuracy, rapid response, and easy manufacturing for the large-scale production.<sup>228</sup> In this regard, TiO<sub>2</sub>-based nanostructures can fulfill the mentioned properties to be used in



biosensing applications and there has been an extensive scientific work in this area due to their unique electron-transfer properties.<sup>229,230</sup> For instance, in 2022, Feng *et al.* introduced a new fluorescence method to detect the tyrosine phosphatase 1B protein (PTP1B) using modified TiO<sub>2</sub>NPs/single-wall carbon nanohorns (TiO<sub>2</sub>NPs-SWCNHs) (Fig. 6).<sup>13</sup> Single-walled carbon nanohorns (SWCNHs) are a new type of carbon nanomaterials which have a large specific surface area, internal space, and fluorescence-quenching ability to construct optical systems, such as SWCNH-based detection systems for biological molecules. In this study, the TiO<sub>2</sub>NPs were decorated with SCWNHs (TiO<sub>2</sub>-SWCNHs) for providing the on/off quencher moiety on the TiO<sub>2</sub>NP surface which enhanced the discrimination difference in SWCNHs between the phosphorylated and nonphosphorylated peptides. This work was reported as the first TiO<sub>2</sub>NPs-SWCNHs.

The resultant TiO<sub>2</sub>-SWCNH nanocomposite could effectively quench the fluorescence of the phosphorylated-peptide substrate labeled by the fluorophore with a low fluorescence background. In the presence of the target PTP1B protein, dephosphorylation of the attached peptide occurred (due to the PTP1B/peptide reaction), resulting in a detachment of the dye-labeled peptide from the TiO<sub>2</sub>-SWCNH surface and fluorescence enhancement was observed in the system. This demonstrated a simple and fast approach to detect PTP1B activity, having an ultra-low detection limit of 0.01 ng mL<sup>-1</sup> with a linear range of 0–10 ng mL<sup>-1</sup>. The biosensor can be used in the serum medium using the standard addition method and showed the possibility for screening PTP1B inhibitors.

Tao *et al.* prepared TiO<sub>2</sub>NPs modified with graphitized carbon nanofibers (TiO<sub>2</sub>NPs/GNFs) for the sensitive detection

of organophosphorus pesticide residues (OPs).<sup>231</sup> The modification of TiO<sub>2</sub>NPs with GNF resulted in enhanced biocompatibility, catalytic properties, and conductivity, and provided a hydrophilic surface for the effective immobilization of acetylcholinesterase (AChE), as the recognizing moiety. In more detail, the Ti atoms of this nanosurface coordinated with AChE to enhance its stability, and TiO<sub>2</sub> has a high tendency for adsorption on OPs. The AChE/TiO<sub>2</sub>/GNFs/GCE biosensor exhibited a high affinity to acetylthiocholine chloride (ATCh) and demonstrated a low detection limit (3.3 fM) with a wide detection linear range ( $1.0 \times 10^{-13}$ – $1.0 \times 10^{-8}$  M), for paraoxon detection (a model of OPs). It was successfully tested for the determination of OPs in lake water, showing high anti-interference, long-term stability, and acceptable reproducibility, with great potential for the analysis of OPs in ecological environments.

Hong *et al.* developed a label-free electrochemical immunosensor for the ultra-sensitive determination of  $\beta$ -lactoglobulin ( $\beta$ -LG), in which they used TiO<sub>2</sub>NPs, carbon nanochips, and AuNPs on chitosan (as a conducting polymer).<sup>232</sup> This biosensor demonstrated a linear relationship between the log  $\beta$ -LG concentration and the square wave voltammetry (SWV) response, with a detection limit of 0.01 pg mL<sup>-1</sup>. Due to its high stability, reproducibility, and sensitivity, this approach can be applied for the detection of  $\beta$ -LG in real food samples. In this study, TiO<sub>2</sub>NPs incorporated with chitosan (CS), as a biopolymer having high adhesion ability, biocompatibility and mechanical strength and improve the stability of the electrode surface for the biosensing applications. Due to the low conductivity of CS, they used carbon nanochips and AuNPs to facilitate electron transfer and increase the conductivity of this TiO<sub>2</sub>NP-based nanosensor.

Shi *et al.* proposed a novel biosensor for a highly sensitive detection of H9N2 AIV. In fact, the H9N2 subtype avian

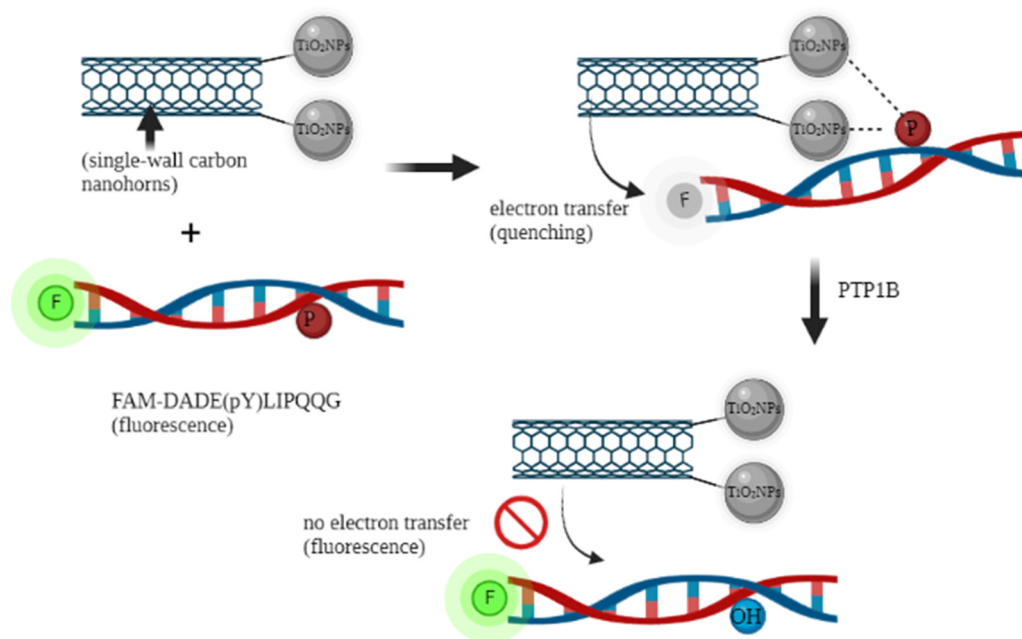


Fig. 6 Modified TiO<sub>2</sub>NP single-wall carbon nanohorns (TiO<sub>2</sub>-SWCNHs) for detecting the tyrosine phosphatase 1B protein (PTP1B). Adapted with permission from ref. 13. Copyright 2022 Elsevier.



Table 9 Recent publications on modified TiO<sub>2</sub>NPs applied as biosensors

Nanosystem	Applications	Ref.
TiO <sub>2</sub> NRs and graphene oxide	For detecting dichlorvos (DDVP)	237
TiO <sub>2</sub> nanotubes and AgNPs	Heat shock protein 70 (HSP70) as a potential tumor marker with high diagnostic sensitivity	238
Gallic acid–TiO <sub>2</sub> nano-composites	Detection of DNA	239
TiO <sub>2</sub> nanotube (NT) arrays	Tumor cell detection	240
11-Mercaptoundecanoic acid self-assembly and the amidated nano-TiO <sub>2</sub> film	For the selective and ultrafast detection of phosphoproteins in food	241
Nanocomposite graphene/TiO <sub>2</sub>	Glucose biosensor	242
TiO <sub>2</sub> -graphene composite modified carbon paste electrode	Determination of sufentanil in human plasma and urine	243

influenza virus (AIV) is a low-pathogenicity AIV that seriously threatens the healthy development of the poultry industry and public health systems.<sup>233</sup> The sensor was constructed by employing a dual-resonance long-period fiber grating (DR-LPFG) modified with TiO<sub>2</sub>NPs, followed by the chemical attachment of the anti-H9N2 monoclonal antibody (anti-H9N2 MAbs) to the TiO<sub>2</sub>NPs on the surface of DR-LPFG. The detection limit of this biosensor was estimated to be  $\sim 2.7 \text{ ng mL}^{-1}$  with a high specificity and rapid detection of 96.1%, which is higher than that of a DR-LPFG-based biosensor modified with the Eudragit L100 copolymer. In this system, DR-LPFG provided a stabilizing medium for the TiO<sub>2</sub>NPs which increased biocompatibility under biological conditions. The attachment of the monoclonal antibody (anti-H9N2 MAbs) to the TiO<sub>2</sub>NPs resulted in high selectivity of this biosensor to detect H9N2 AIV.

Rajeshwari *et al.* combined poly(*p*-phenylenediamine) with TiO<sub>2</sub> and a multiwalled carbon nanotube to make a biosensor nanocomposite for the *in vivo* detection of dopamine, as a biomarker of many mental illnesses.<sup>234</sup> The biosensor demonstrated a considerable sensitivity with a linear range of  $3.81 \times 10^{-11}$ – $4.76 \times 10^{-6} \text{ M}$  with a low detection limit of  $9.45 \times 10^{-12} \text{ M}$ . The incorporation of TiO<sub>2</sub>NPs with poly(*p*-phenylenediamine) and carbon nanotubes significantly enhanced the conductivity of the TiO<sub>2</sub>NPs, along with its stability and biocompatibility.

Zheng *et al.* used HKUST-1 MOFs (molecular organic frameworks) and its derivative, HKUST-CuO, for incorporation with TiO<sub>2</sub>NPs to form two resultant composites of HKUST-1/TiO<sub>2</sub> and HKUST-CuO/TiO<sub>2</sub> to modify the electronic properties of TiO<sub>2</sub>NPs and make a well-suitable band gap energies ( $E_g$ ).<sup>235</sup> Compared with mono-component HKUST-1 or HKUST-CuO, both TiO<sub>2</sub>-based composites showed a synergistic photoelectrochemical (PEC) response due to their heterogeneous structure. The HKUST-CuO/TiO<sub>2</sub>-modified electrode showed a higher photocurrent response which may be due to its hollow structure, greatly enhancing visible light harvesting. Then the authors successfully attached the targeting moiety to this nano-hybrid and fabricated the S1 (probe DNA)/HKUST-CuO/TiO<sub>2</sub>/ITO PEC platform for colitoxin DNA detection without using ascorbic acid (AA) as an electron donor. Compared with S1/HKUST-1/TiO<sub>2</sub>/ITO, the S1/HKUST-CuO/TiO<sub>2</sub>/ITO electrode demonstrated a wider linear response range ( $1.0 \times 10^{-6}$ – $4.0 \times 10^{-1} \text{ nM}$ ) with a lower detection limit of  $3.73 \times 10^{-7} \text{ nM}$  (S/N = 3). Due to its good specificity and stability, this biosensor exhibited a promising strategy for molecular diagnosis in the bio-analysis field.

Singh *et al.* developed an electrochemical biosensor for the detection of organophosphorus (OP) pesticides based upon AChE-inhibition, operating in the pM concentration range.<sup>236</sup> The synthesized TiO<sub>2</sub>NPs and molybdenum disulfide nanomaterials were deposited on a screen-printed electrode, followed by modification with chitosan and immobilization of AChE on the modified electrode. The AChE modification of this TiO<sub>2</sub>-based electrode provided a selectivity for this biosensor. Also, the chitosan modification resulted in an enhanced stability and biocompatibility of the TiO<sub>2</sub>NPs on the surface of this electrode. The biosensor was successfully tested for the low OP pesticide concentration detection in forensic visceral samples demonstrating a low detection limit of 50 pM. Other recent works on the biosensing applications of modified TiO<sub>2</sub>NPs are summarized in Table 9.

#### 4.5. Antifungal

More than 300 million people worldwide are being threatened by severe fungal infections which have caused 1.6 million deaths every year.<sup>244</sup> To overcome this issue, many nano-based approaches have been developed, and among them, the photocatalytic deactivation of fungi has become a promising strategy for disinfection of aqueous media to have microbial control.<sup>245–248</sup> As a semiconductor material, TiO<sub>2</sub>NPs have been introduced as a great candidate for the development of advanced antifungal agents.

For instance, in 2022, Wang fabricated chitosan/alginate–TiO<sub>2</sub>NP based bilayer films incorporated with different concentrations of cinnamon essential oil (CEO) to study the effect of this bilayer film on improving the postharvest quality of mangoes.<sup>249</sup> In this study, chitosan was used as a packaging material for food preservation due to its biodegradable, antibacterial, and good film-forming properties. The cinnamon essential oil (CEO) is also considered as a natural antioxidant and antibacterial agent and has attracted increasing attention in the field of packaging material. In this study, the film of chitosan/CEO was formed by the interaction of the aldehyde group of CEO with the amino group of the chitosan matrix to improve the hydrophobicity, antibacterial, and antioxidant properties of the chitosan films. To improve the photostability of this film, the modified TiO<sub>2</sub>NPs–alginate was used as anti-ultraviolet packaging materials, in which the alginate contains –COO<sup>−</sup> functional groups which can electrostatically interact with cations of the inner chitosan layer to form a bilayer to



prevent the volatilization of CEO in the inner layer. The modification of TiO<sub>2</sub>NPs with alginate improved the antimicrobial performance of the outer part of this film due to their synergistic advantages of TiO<sub>2</sub>NPs and alginate. This TiO<sub>2</sub>NP-based film demonstrated an improved mechanical and antimicrobial properties for the film which could be a promising candidate as a multifunctional packaging material to maintain the freshness of harvested mangoes.

Siddiqui *et al.* fabricated TiO<sub>2</sub>NPs using 37 strains of cyanobacteria and evaluated their antifungal, antioxidant, antibacterial, and hemolytic activities.<sup>250</sup> *Synechocystis* NCCU-370 was introduced as the best strain for the synthesis of TiO<sub>2</sub>NPs in terms of size (73.39 nm), followed by optimization of the synthesis to obtain smaller nanoparticles (an average grain size of 16 nm). The antifungal activity was studied against *Candida albicans* (MIC = 125 µg mL<sup>-1</sup>), *Candida glabrata* (MIC = 500 µg mL<sup>-1</sup>), and *Candida tropicalis* (MIC = 250 µg mL<sup>-1</sup>), and the modified TiO<sub>2</sub>NPs demonstrated the partial synergistic effect and excellent biocompatibility. The biocompatible nature of these biomodified TiO<sub>2</sub>NPs is an advantage for their potential in biomedical purposes.

Sultan *et al.* fabricated gelatin active packaging films based on nano-sized droplets of coconut oil emulsified by pickering emulsion (PE) and stabilized by chitosan/Arabic gum (CH/AG) nanoparticles, in the presence of TiO<sub>2</sub>NPs.<sup>251</sup> The films showed a significant antifungal activity for all tested microorganisms, such as *Bacillus cereus* and *C. albicans*. The antimicrobial and antioxidant packaging materials are frequently produced by embedding natural antimicrobial and antioxidant additives into the natural polymer matrices providing new functionalities to the film and extend shelf life of packaged food. As a natural biopolymer, gelatin shows excellent biodegradability, biocompatibility, and film-forming ability. The coconut oil is another biocompatible candidate for using the packaging biofilm due to its potential antimicrobial and antioxidant characteristics. Chitosan is also considered as an excellent biocompatible, non-toxic, and biodegradable material, showing some important functions such as antibacterial and antifungal properties. Arabic gum (AG) is the last organic component of this film, having amphiphilic polysaccharides with emulsifying properties. These organic polymeric matrices provided a stabilizing biocompatible medium for the TiO<sub>2</sub>NPs to synergistically enhance the antifungal properties of the individual components of this film.

Mohammad Taghizadeh Kashania *et al.* synthesized TiO<sub>2</sub>NPs modified with *C. arabis* and studied their effect on improving the biological properties of the dichloromethane fraction (DF) of *C. arabis* root smoke (the largest species in the Costaceae plant family).<sup>252</sup> The synthesized DF/TiO<sub>2</sub>NPs (200 mg L<sup>-1</sup>) showed the maximum radical scavenging level up to the IC<sub>50</sub> = 8.31 µg mL<sup>-1</sup>. In this study, the TiO<sub>2</sub>NPs were modified with the biologically active biomolecule, *C. arabis* which is known as a good candidate for the treatment of infectious diseases. The modification of TiO<sub>2</sub>NPs with this biomolecule can provide the synergistic effect of antifungal for this modified system and can decrease the potential toxicity of TiO<sub>2</sub>NPs.

Duan *et al.* prepared a nanocomposite film made by *K-carrageenan* (KC), *Konjac glucomannan* (KGM) and TiO<sub>2</sub>NPs. The TiO<sub>2</sub>NPs improved the mechanical and thermal properties of the KC/KGM films.<sup>253</sup> Specifically, the film containing 7 wt% of TiO<sub>2</sub>NPs showed effective photocatalytic antifungal activity (79%) against *Penicillium viridicatum* after irradiation for 6 h and revealed a protective effect on strawberry storage. The results demonstrated that the nanocomposite films have a broad potential for food preservation and packaging applications. For the food packaging applications, *K-carrageenan* (KC) is a hydrophilic biomolecule, obtained from red seaweed, with gelling and film-forming properties which allow biodegradable packing films to be produced. Also, *Konjac glucomannan* (KGM) is a natural polysaccharide which has been widely used to prepare film materials due to its good film-forming ability. Thus, when TiO<sub>2</sub>NPs are incorporated into these polymer matrices, it will effectively inhibit bacterial growth and food spoilage due to the synergistic effects of these three components to improve the properties of each other. Other studies on the antifungal applications of modified TiO<sub>2</sub>NPs are summarized in Table 10.

#### 4.6. Antiviral

Since 2019, with the emergence of pathogenic human coronavirus pandemic, SARS-CoV-2 (COVID-19) has caused serious issues in many aspects of life such as public health and economy, all around the world. Based on the 2019 World Health Organization prediction, the mortality of infection-related diseases will be similar to that of cancer by 2050.<sup>11,12,261–263</sup> Modified TiO<sub>2</sub>NPs have provided some promising candidates for controlling virus-type infections, supported by recent worthwhile publications in this frontier area of nanomedicine.

Because of the paramount importance of antiviral modified TiO<sub>2</sub>NP systems, recent publications in this field are presented; for instance, in 2022, Elsayed *et al.* studied the condensation of 3-acetylindol, thiophene-2-carbaldehyde and malononitrile in the presence of TiO<sub>2</sub>NPs, yielded 2-amino-6-(1*H*-indol-3-yl)-4-(thiophen-2-yl)-4*H*-pyran-3-carbonitrile derivatives.<sup>264</sup> Then, they were reacted with formic acid, formamide, ethyl chloroacetate, chloroacetyl chloride, thiourea and sodium nitrite to form several three-combination systems which were safe, ecologically friendly, and non-toxic. The synthesized compounds were successfully tested for antiviral activity against Vero cells (HAV) and showed an effective activity. In this research, new indoles were synthesized and used for the TiO<sub>2</sub>NP modification and tested for their antioxidant's outcome. The indole nominees verified their strength as antioxidants, antimicrobial, and anticancer. Specifically, the authors used synthesized contestants containing pyrimidine, pyrazole, pyrane, and pyridine rings. As a crucial nucleobase, pyrimidine derivatives are considered as antioxidant agents in contrast to ROS and reactive nitrogen species (RNS). Similarly, pyridine, pyrazole, and pyrane rings displayed antioxidants properties in their derivatives. The modification of the TiO<sub>2</sub>NP surface with these compounds





Table 10 Recent studies of antifungal applications of the TiO<sub>2</sub>NPs

Nanosystem	Applications	Ref.
TiO <sub>2</sub> NPs were produced by <i>Bacillus sp.</i> bacteria	Significant antifungal activities against the oral <i>C. albicans</i> pathogen	254
Green synthesis of S-doped TiO <sub>2</sub> NPs using <i>Malva parviflora</i> plant extract	Antimicrobial and antioxidant activities under sunlight illumination	255
TiO <sub>2</sub> /Ag nanoparticles	For its activity as an antifungal material for the inhibition of <i>C. albicans</i> in water under visible light irradiation	256
TiO <sub>2</sub> -SiO <sub>2</sub> /chitosan	Enhancement of antifungal capability	257
TiO <sub>2</sub> NPs were synthesized by using <i>trianthema portulacastrum</i> , <i>chenopodium quinoa</i> leaf extracts and sol-gel method	Antifungal activities against wheat rust	258
Cyclodextrin-grafted TiO <sub>2</sub> NPs	As food preservative carriers	259
PVA/TiO <sub>2</sub> -based nanocomposites	Antifungal activity study	260

could provide opportunity to increase the antiviral effect of TiO<sub>2</sub>NPs.

Souza *et al.* developed TiO<sub>2</sub>-based antiviral hydrophobic cellulose cotton or non-woven fabrics for their potential virucidal effect on Murine Coronavirus (MHV-3) and Human Adenovirus (HAdV-5), under indoor light irradiation.<sup>265</sup> In the non-woven fabric, the results demonstrated 90% and 99% reduction of HAdV-5 and MHV-3, respectively, with no reduction of HAdV-5 in cotton fabric. The antiviral activity was assigned to the photocatalytic effects of the modified TiO<sub>2</sub> powders, and the hydrophobic properties of fabrics and high surface of the TiO<sub>2</sub> particles facilitated their interaction with the viruses, especially MHV-3. These results showed the potential ability of these composite materials as highly effective virucidal agents against MHV-3 and HAdV-5 viruses, particularly for applications in healthcare indoor contaminated environments. In fact, the fabrics used in this study acted as a support for TiO<sub>2</sub>NPs to significantly promote the interaction between viruses and TiO<sub>2</sub>NPs. In this regard, cellulose-based fabrics such as cotton and non-woven fabrics have been commonly studied for the application of TiO<sub>2</sub> hydrosols to prepare fabrics with photocatalytic and self-cleaning properties. The flexible, porose, and layered surface structures of cotton contributed to the incorporation of TiO<sub>2</sub>NPs in its structure, providing enhanced antiviral properties.

Regarding SARS-CoV-2 infection, Da Silva *et al.* developed antimicrobial cotton fabrics based on the Ag/TiO<sub>2</sub> nanohybrid and they showed that more than 50% of infectious SARS-CoV-2 survived after direct contact with the nanohybrid under the tested conditions, which indicated that more studies are required on using silver and TiO<sub>2</sub> nanostructures as self-disinfecting agents for the prevention of coronavirus transmission.<sup>266</sup> In this case, the cotton provided a matrix for the immobilization of Ag/TiO<sub>2</sub>NPs, which protected the nanosystem against aggregation.

Wang *et al.* successfully tested the antiviral efficacy of TiO<sub>2</sub>-chitosan (CS) -AgNP filter for viral aerosols and reported the infection risk reduction and long-term antiviral efficacy of this nanosystem.<sup>267</sup> In this study, the TiO<sub>2</sub>-CS-AgNP filter was synthesized for the removal and deactivation of airborne MS2 bacteriophage particles. In the air purification system, their results showed a 93% removal of the airborne MS2 particles, and more than 95% of MS2 can be efficiently deactivated on the

surface of this nanosystem within 20 minutes. The filter could maintain 50% of its original antiviral efficiency after continuous operating for 1 week. The surface modification of TiO<sub>2</sub> with the chitosan polymer provided possibility for the AgNP attachment to the surface of TiO<sub>2</sub>.

Levina *et al.* used a combination of biocompatible TiO<sub>2</sub>NPs and immobilized polylysine-containing oligonucleotides (PL) with native (ODN) and partially modified (ODNm) internucleotide to form a new delivery system for the effective attack of oligonucleotides on the viral genome of highly pathogenic H5N1 influenza A virus (IAV) *in vivo*.<sup>268</sup> The intraperitoneal injection of this TiO<sub>2</sub>-PL-ODN nanocomposite exhibited 65–70% survival of mice, while the intraperitoneal or oral administration of TiO<sub>2</sub>-PL-ODN was more efficient (~80% survival). The nanocomposites showed no toxicity on mice under the tested conditions. Interestingly, the TiO<sub>2</sub>NPs, unbound ODN, and the nanocomposite bearing the random oligonucleotide demonstrated a low protective effect, demonstrating the key role of targeting oligonucleotides in this nanocomposite for the site-specific interaction with complementary RNAs of the target virus. In this antiviral system, the ODN loaded polylysine was non-covalently immobilized onto the TiO<sub>2</sub>NPs, which enhanced the biocompatibility and enabled the ODN delivery *via* the cell membrane. More importantly, this modification of TiO<sub>2</sub>NPs could stabilize and protect ODN against intracellular enzymes, and the carried oligonucleotides were released from the nanocomposites in the cytoplasm or penetrated into the nuclei and bind to the RNA molecules.

León-Gutiérrez *et al.* studied the modification of TiO<sub>2</sub>NPs with secondary metabolites implanted to prepare antiviral TiO<sub>2</sub>NPs (SMNP) and tested them on SARS-CoV-2 infectivity and healthy cells as well. Surprisingly, SMNP showed a considerable reduction of viral infectivity *in vitro* with minimal toxicity to healthy cells when compared to other commercially available antiseptics (glutaraldehyde, chlorine, chlorhexidine, ethanol, and Lysol™), which indicated this SMNP nanosystem as a safe and effective antiviral against SARS-CoV-2.<sup>269</sup> Citrus-derived compounds have shown the clear clinical benefit for viral infections, inducing stimulate immunity. Natural secondary metabolites are considered as antiviral agents due to their inhibitory effect on key metabolic enzymes that influence signaling pathways, cellular function, and gene expression. Conjugation of these therapeutic agents with the TiO<sub>2</sub>NP





surface could provide the synergistic effect for the antiviral ability of the modified TiO<sub>2</sub>NPs.

#### 4.7. Tissue engineering

Tissue engineering is a multidisciplinary field which includes the fabrication of these biocompatible materials suitable for repairs or replacement of abnormal tissues/organs. It is worth mentioning that the scaffolds, used for different applications in tissue engineering, need to be highly compatible with the cellular matrix inside the body and they should not cause cytotoxic, immunogenic, inflammatory, or any other host reaction. Also, they should exhibit suitable mechanical and physical properties suitable for the biological conditions. Despite many advantages of TiO<sub>2</sub>NPs in tissue engineering, one of their restrictions is their agglomeration which diminishes their biological effectiveness. Therefore, there is a need for a polymeric matrix to fix and stabilize these TiO<sub>2</sub>NPs and prevent their leaching out to different parts of the body. In recent years, modified TiO<sub>2</sub>NPs have attracted significant attention for using in different platforms/scaffolds in the tissue engineering field to promote biological and physicochemical processes of cell/tissue culturing.<sup>270,271</sup> In this field, the TiO<sub>2</sub>NPs are often used as a part of the biocompatible polymeric matrix which can fix and stabilize TiO<sub>2</sub>NPs, enhancing the biocompatibility and effectiveness of these nanoparticles. Simultaneously, these incorporated TiO<sub>2</sub>NPs can improve the mechanical and physicochemical properties of the scaffolds.

For bone regeneration scaffolds, in 2022, Karbowniczek *et al.* reported the additions of hydroxyapatite (HA) and TiO<sub>2</sub>NPs on poly(3-hydroxybutyrate-co-3-hydroxyvalerate) (PHBV) based fibers and studied the tensile strength, elongation, and toughness of the fibers after this addition.<sup>14</sup> It should be mentioned that the biodegradable poly(3-hydroxybutyrate-co-3-hydroxyvalerate) (PHBV) is a biopolymer synthesized by bacteria, considered as a good alternative for many non-biodegradable synthetic polymers. For tissue engineering purposes, this biopolymer can be processed *via* electrospinning for the construction of scaffolds. To improve its *in vitro* cell growth and mechanical properties, PHBV can be combined with ceramic particles such as hydroxyapatite (HA) and antibacterial TiO<sub>2</sub>NPs. Regarding the effect of HA on the surface properties of TiO<sub>2</sub>NPs, the authors reported that the presence of HA could decrease the agglomeration of TiO<sub>2</sub>NPs in the PHBV + HA + TiO<sub>2</sub> composite, compared to that in PHBV + TiO<sub>2</sub>, which is very important for increasing the effectiveness of TiO<sub>2</sub>NPs. Also, they observed a dramatic improvement in the mechanical strength of the PHBV fibers containing HA nanoparticles, compared with the fibers alone. The homogenous distribution of HA nanoparticles resulted in a 3-time improved tensile strength and a 16-time higher toughness. The authors showed a strategy for tuning mechanical properties by controlling the size and distribution of ceramic fillers (TiO<sub>2</sub> and HA) in hybrid scaffolds.

As another surface modifier, poly-*ortho*-toluidine (POT) has been used as a conductive polymer to stimulate a multitude of cell functions such as attachment, proliferation, migration, and

differentiation *via* the modulation of transferred electrical stimuli from the external support to cell. So, the modification of TiO<sub>2</sub>NPs with the POT polymer brings several benefits to the TiO<sub>2</sub>NPs, including promoted cell-material interaction, better antibacterial activity, and excellent biocompatibility. In this regard, Balan *et al.* synthesized an organic/inorganic nanocomposite poly-*ortho*-toluidine-TiO<sub>2</sub> to construct the POT + TiO<sub>2</sub>/PCL nanocomposite scaffolds.<sup>272</sup> The surface roughness of this nanocomposite provided a great influence on the viability of different cells. Besides, the *in vitro* antibacterial activities of POT + TiO<sub>2</sub> and POT + TiO<sub>2</sub>/PCL composite scaffolds were tested on *S. aureus* and *E. coli* and the POT + TiO<sub>2</sub>/PCL scaffold demonstrated an improved surface roughness, cell viability and antibacterial activity, indicating economical and effective TiO<sub>2</sub>NP-based nanocomposites for tissue engineering applications.

Sharaf Saeed *et al.* prepared a series of poly(ethylene-co-vinyl alcohol)/TiO<sub>2</sub>NPs (PEVAL/TiO<sub>2</sub>) nanocomposites containing 1, 2, 3, 4 and 5 weight ratios of TiO<sub>2</sub>NPs.<sup>273</sup> The cell culture tests of these nanohybrids were evaluated on human gingival fibroblast cells (HGFs) in accordance with ISO 10993-5 and ISO 10993-12 standards, with studying the cell viability after 1, 4, and 7 days. The results showed a time-dependent improvement in the cell activity for all systems, and the cell survival for all samples was higher than that of the virgin PEVAL on day 7 (*p* < 0.002). The bio-SEM results also demonstrated the successful cell adhesion and growth of HGFs on all types of scaffolds (PEVAL/TiO<sub>2</sub>). In this system, the incorporation of TiO<sub>2</sub>NPs into the PEVAL polymer matrix exhibited a uniform dispersion of these TiO<sub>2</sub> fillers, which are well covered by the copolymer. This could be due to the presence of good affinity between these two components in which the expansion PEVAL macromolecule chain in the solvent promotes the dislocation of the aggregated TiO<sub>2</sub>, leading to their uniform dispersion in the polymer matrix. This homogeneity and stability could positively affect the biocompatibility of TiO<sub>2</sub>NPs for the cell culturing purpose.

Alginate is considered as one of the most promising surface modifiers for TiO<sub>2</sub>NPs in the tissue engineering field, as a marine-based polysaccharide found in brown algae. Compared to synthetic polymers, this biopolymer provides several benefits such as biocompatibility, gel-forming ability at biological pH and temperature, non-toxicity, water solubility, and cost-effectiveness. Alginate-based scaffolds can enhance alkaline phosphatase activity and expressing osteocalcin and mineralization resulting in promoted osteogenesis. In this case, Mallakpour and Naghdi applied a TiO<sub>2</sub>NPs-alginate nanohybrid to fabricate a bone scaffold to take the benefits of both TiO<sub>2</sub>NPs and alginate.<sup>274</sup> In this study, the alginate provided suitable conditions for the biomineralization process, and it can help better dispersion and fixation of TiO<sub>2</sub>NPs and decrease their aggregations. This TiO<sub>2</sub>NP-alginate was incubated in a simulated body fluid at 37 °C for 28 days to evaluate its bioactivity. Cytotoxicity tests were performed on the MG-63 cell line and the scaffold showed no toxicity effects. Besides, this scaffold demonstrated a potent antibacterial effect against the Gram positive strain *S. aureus*, indicating the great properties of this scaffold to be used for bone tissue engineering applications.



As another well-known polymer in tissue engineering, polyvinyl alcohol (PVA) shows great film-forming properties, high tensile strength, biodegradability, emulsifying characteristics, and water solubility. However, for using scaffolds, it requires to blend this polymer with other polymers and inorganic fillers to improve the mechanical and biological properties.<sup>275</sup> Currently, nano-cellulose has been attracting considerable interest due to its strengthening effect, biodegradability, high surface area, non-toxicity, and great mechanical/optical properties. Cellulose can also support cell attachment and facilitate apatite growth. Because of these typical properties, they have been incorporated into nanocomposites and the polymer matrix as reinforcing materials improving the desired properties, which makes it a good choice for biomedical applications.<sup>275</sup> TiO<sub>2</sub>NPs are ideal illustration of inorganic fillers due to their cell adhesion and anti-corrosive properties. Fatima *et al.* prepared a TiO<sub>2</sub>NP-doped ternary nanocomposite film (PVA/NC-TiO<sub>2</sub>) by the fusion of polyvinyl alcohol (PVA), nano-cellulose (NC), and TiO<sub>2</sub>NPs (0.01 wt%), as well as its binary nanocomposite film (PVA/NC).<sup>275</sup> The presence of TiO<sub>2</sub>NPs in the structure of this film significantly improved the thermo-mechanical stability of the nanocomposite film, which can be due to an enhancement of intermolecular interactions in the PVA/NC-TiO<sub>2</sub> film, compared to the PVA/NC binary film. Furthermore, their results showed a higher glass transition temperature and a storage modulus of the PVA/NC-TiO<sub>2</sub> film (9131.26 MPa, 74.3 °C) than those of the PVA/NC film (7588 MPa, 64.3 °C). The ternary PVA/NC-TiO<sub>2</sub> film showed a more uniform surface layer of the Ca-P mineral than the PVA/NC film, upon incubation in simulated buffer saline. The low percentage of TiO<sub>2</sub>NPs improved the strength of this PVA/NC-TiO<sub>2</sub> film, with a cell viability more than 80% and hemolysis less than 1.7%, demonstrating high potential of this nanocomposite to develop better bone templates for bone regeneration applications. The interaction of PVA and NC with the TiO<sub>2</sub>NPs resulted in more homogeneity for the particles in this film, compared to the PVA/NC film. Besides, this surface modification improves the biocompatibility of these TiO<sub>2</sub>NPs.

Nanofiber (NF) scaffolds hold great promise for utilization in bone regeneration purposes and they are interesting stabilizing and modifying matrices for enhancing the efficiency of TiO<sub>2</sub>NPs used in the scaffolds. Among various biomaterials, poly-ε-caprolactone (PCL), an FDA approved biodegradable polyester, has attracted much attention in this field due to its appropriate biocompatibility and mechanical properties.<sup>276</sup> Several works demonstrated that a blend of PCL and gelatin (GEL) can generate a highly biomimetic nanofibrous scaffold with appropriate biodegradability and mechanical stability, and most importantly excellent cytocompatibility. However, PCL/GEL NFs alone are not appropriate for bone regeneration due to the absence of inherent osteoinductive capability. The incorporation of osteoinductive agents or components to these scaffolds can lead to higher mechanical properties and improved biofunctionality of PCL/GEL NFs for bone regeneration. In this regard, nanocomposites based on ceramic nanoparticles such as TiO<sub>2</sub>NPs have recently drawn considerable attention as bone substitute materials and injectable pastes to

fill defects due to their excellent mechanical properties, high chemical stability, and bioactivity.<sup>276</sup> In this regard, Ahmadi *et al.* employed TiO<sub>2</sub>NPs and metformin (MET)-co-embedded composite electrospun poly-ε-caprolactone/gelatin nanofibers (PCL/GEL NFs) to form scaffolds for the improved osteoblastic differentiation of human adipose-derived stem cells (hADSCs).<sup>276</sup> The results showed an improvement of the mechanical properties of this composite due to the presence of TiO<sub>2</sub>NPs, as well as an enhanced adhesion and growth rate of hADSCs on the nTiO<sub>2</sub>/MET-loaded NFs. The nanosurface of TiO<sub>2</sub>NPs and the released metformin could result in a high differentiation capacity toward osteoblasts due to the promoted mineralization content and enhanced expression of osteoblastic markers. This work again demonstrated the high capacity of TiO<sub>2</sub>NP-based scaffolds for bone tissue regeneration and engineering. The incorporation of TiO<sub>2</sub>NPs in the polymer/drug matrix can enhance the cell-differentiating abilities of TiO<sub>2</sub>NPs and prevents their aggregation.

As a soft tissue, skin has potential to repair itself so the key challenge for researchers and clinicians is to find ways to harness this skin regenerative potential to treat cutaneous injuries and diseases. At present, the only gold standard treatment is autologous skin graft for full-thickness skin wounds; however, this treatment also has shortcomings like restricted availability and morbidity of the donor site. Therefore, one of the alternative therapeutic options to treat the skin injuries is tissue-engineered skin (TES) which makes use of natural polymers including proteins which can resolve the autologous donor graft shortcomings and can provide protection against water-electrolyte imbalance and microbial infection as well.<sup>277</sup> Silk fibroin (SF) is a protein (FDA approved), mechanically strong, biocompatible, biodegradable, and permeable material which has been used in a wide range of applications of tissue engineering and wound healing.<sup>277</sup> Similarly, collagen (CG) is biocompatible and biodegradable protein-based natural polymer. These two biocompatible polymers can be applied as the matrix scaffold useful for the incorporation of TiO<sub>2</sub>NPs for the tissue engineering studies. Khalid *et al.* designed silk fibroin/collagen (SF)/(CG) membranes combined with TiO<sub>2</sub>NPs for skin tissue regeneration applications.<sup>277</sup> The membranes exhibited good biocompatibility and antibacterial activity and can be introduced as potential candidates for skin tissue regeneration and wound healing applications.

The natural polymer of chitosan has been used extensively in the field of tissue engineering due to its biocompatibility, biodegradability, non-toxicity and antibacterial properties. Also, bredigite is one of the most well-known silicone biochemicals that has a high potential for the release of silicon ions, which results in the growth of osteoblasts and cellular differentiation. Ghasemi and Ghomi prepared the composite scaffolds of bredigite/TiO<sub>2</sub>, followed by coating with the chitosan polymer to enhance the mechanical, biological, and antibacterial properties of the scaffold.<sup>278</sup> The results showed that the addition of TiO<sub>2</sub> to the scaffold of bredigite resulted in reduced porosity and enhancement of the compressive strength of scaffolds from 0.299 to 0.687 MPa. In addition, the chitosan



coating reduced porosity from 83% to 63% and strongly improved the compressive strength from 0.585 to 2.339 MPa. The scaffolds showed antibacterial effects against *E. coli* (an inhibition zone of 22 mm) and *S. aureus* (an inhibition zone of 29 mm). Besides, these scaffolds exhibited no toxicity on the MG63 bone cells adjacent to the scaffolds. Regarding the modification effect of chitosan, the results showed that the presence of this modifying polymer could enhance the stability, antibacterial, and biocompatibility of the scaffold containing TiO<sub>2</sub>NPs.

Polyurethane is a synthetic, thermoplastic, elastomeric, biodegradable, and biocompatible polymer having increasing applications in tissue engineering.<sup>32</sup> However, the nanofibers made from polyurethane polymers have hydrophobic nature, which makes them undesirable when cultured in the presence of cells and/or implanted *in vivo* using animal models.<sup>33,34</sup> These fibers are efficiently utilized as a bone mineral and modifying the matrix for the TiO<sub>2</sub>NPs and other antibacterial NPs. This stabilizing matrix could enhance the biocompatibility of the used nanoparticles. Ashraf *et al.* fabricated nanofibers containing TiO<sub>2</sub>NPs (as the osteoconductive component) and AgNP (as self-healing) nanostructures.<sup>279</sup> The incubation of the nanofibers in the simulated body fluid at 37 °C triggered mineralization on nanofiber scaffolds and resulted in Ca and P crystals' formation. Also, the scaffolds showed antibacterial activity against *E. coli* (8.3 ± 0.9 mm) than *S. aureus* (1.2 ± 0.1 mm), and the MTT assay on the pre-osteoblasts demonstrated the biocompatibility of both TiO<sub>2</sub>NPs and AgNPs with the bone-like cells. However, at higher contents of AgNPs (*i.e.*, 0.07 M), the scaffold showed cytotoxicity.

Recently, novel hybrid fillers such as TiO<sub>2</sub>NPs/graphene oxide have been constantly emerging to be used in the structure of polymeric scaffolds to enhance the properties of composites. Since TiO<sub>2</sub>NPs are antibacterial components, they have been widely used as nanofillers to enhance the performance of the composite scaffold. In this case, recently, Zhang *et al.* synthesized the reduced graphene oxide/TiO<sub>2</sub>NP (RGO@TiO<sub>2</sub>NPs) nanohybrid as a filler to investigate its synergistic effects on electrospun regenerated silk fibroin (RSF) mats (Fig. 7).<sup>280</sup> The hybrid filler resulted in an increase in the average diameter of RSF fibers and decrease the content of  $\beta$ -sheet conformation. Interestingly, a 220% increase of the strength of the RSF/RGO@TiO<sub>2</sub>NP composite mat was detected. Moreover, the

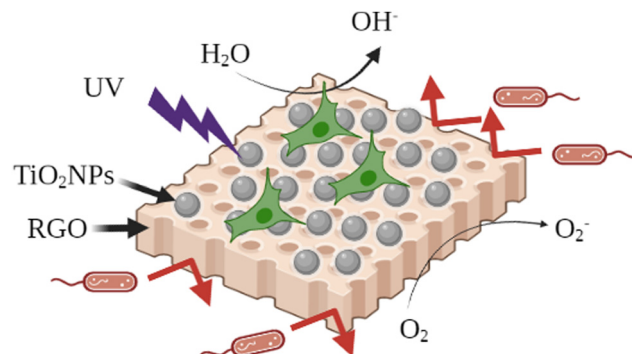


Fig. 7 The graphene oxide/titanium dioxide (RGO@TiO<sub>2</sub>) nanohybrid as a filler to investigate their synergistic effects on electrospun regenerated silk fibroin (RSF) mats. Adapted with permission from ref. 280. Copyright 2021 Elsevier.

growth and expansion of the cells were reported on the composite mat due to the good antibacterial properties of TiO<sub>2</sub>NPs. In this system, the RGO could bring a stabilizing matrix for the TiO<sub>2</sub>NPs, protecting them against agglomeration which could result in well dispersion of TiO<sub>2</sub>NPs in the scaffold and enhanced their antibacterial activity.

For bone tissue engineering, a scaffold with the optimized pore size and interconnected porosity is desirable to establish the tissue response and cell growth. It is essential for cell penetration and migration to effectively vascularize the growth of new tissues to have a maximum porosity (90%) and a suitable pore diameter (minimum 100  $\mu$ m and maximum 450  $\mu$ m). The TiO<sub>2</sub>NPs play a significant role in controlling the pore size and porosity. For bone regeneration, a combination of TiO<sub>2</sub>NPs with bioceramics (such as hydroxyapatite (HA)) has gained attention, due to the chemical similarity of HA to the mineral phase of natural bone and its extreme biocompatibility. HA can gain optimized microstructures for defected bone by combining with biodegradable polymers (including poly(glycolic acid), chitosan, arabinosyl, and guar gum). These biodegradable polymers also act as binders that reduce brittleness of HA. Aslam Khan *et al.* synthesized a TiO<sub>2</sub>NP-based nanocomposite containing nano-hydroxyapatite (HA NPs), acrylic acid (AA)/guar gum (GG), and optimum graphene oxide (GO) to construct porous scaffolds coated with silver sulfadiazine (as a drug).<sup>281</sup> Their results showed that the TiO<sub>2</sub>NPs and optimized

Table 11 Recent publications of TiO<sub>2</sub>NPs for the tissue engineering applications

Nanosystem	Applications	Ref.
Poly(lactate-co-glycolate) (PLGA)/TiO <sub>2</sub> scaffolds	Scaffolds	283
TiO <sub>2</sub> /poly(vinyl alcohol) nanocomposite	Bone tissue engineering	284
Silk fibroin/TiO <sub>2</sub> nanocomposite	Bone tissue engineering	285
Nanostructured chitosan/PLA/HA scaffolds doped with TiO <sub>2</sub> /Au/Pt NPs	Bone tissue engineering	286
TiO <sub>2</sub> -chitosan/sodium alginate blended nanocomposite	Bone tissue engineering	287
Nanotubular TiO <sub>2</sub> with gold nanoparticles		288
Poly(lactic acid)/TiO <sub>2</sub> nanocomposite	Potential ability of PLA/TiO <sub>2</sub> nanocomposites to reduce cutaneous scarring in scaffolds	289
Alginate/chitosan multilayer films coated on IL-4-loaded TiO <sub>2</sub> nanotubes	Alginate/chitosan multilayer films coated on IL-4-loaded TiO <sub>2</sub> nanotubes for modulation of the macrophage phenotype	290



GO improved the physicochemical and microstructural properties of this scaffold and the promising results obtained with mouse pre-osteoblast (MC3T3-E1) cell lines. Also, the organic part of this scaffold provided a stabilizing matrix for the TiO<sub>2</sub>NPs, increasing their effectiveness.<sup>280</sup>

Poly(lactic acid) (PLA) is a well-known biocompatible and biodegradable polymer and it is a promising candidate to be used in the bone tissue engineering as the scaffold. It biodegrades to lactic acid without the aid of any enzymes which is innocuous to the body and avoids inflammatory responses. Modification of TiO<sub>2</sub>NPs with this kind of biodegradable polymer provides a golden opportunity to prepare advanced bone scaffolds; for instance, Mota *et al.* incorporated TiO<sub>2</sub>NPs inside the PLA matrix to prepare a modified nanohybrid for its potential ability in bone tissue engineering.<sup>282</sup> The cell viability tests on L929 fibroblast confirmed the biocompatibility of this TiO<sub>2</sub>NP-PLA nanohybrid and its potential for use in the scaffolds. In this system, PLA could provide a biodegradable matrix for the well dispersion and fixation of TiO<sub>2</sub>NPs against aggregation, enhancing the biocompatibility of the TiO<sub>2</sub>NPs. Also, other recent articles in this field are summarized in Table 11.

## 5. Conclusion and perspectives

This review demonstrates the paramount importance of the surface modification of TiO<sub>2</sub>NPs to improve their physicochemical properties and biocompatibility. In this regard, a broad range of organic and organosilane molecules were presented in this review paper which have been used as surface modifiers, according to the final applications of the modified TiO<sub>2</sub>NPs. The potential biomedical applications of these modified TiO<sub>2</sub>NPs have been studied in different fields, *e.g.*, photodynamic therapy, drug delivery, antibacterial, tissue engineering, anticancer, antifungals, biosensors, and antivirals. Furthermore, the anti-COVID-19 performance of modified TiO<sub>2</sub>NPs has attracted growing attention of multidisciplinary groups to develop this field and improve current therapeutic methods. In these fields, surface modifiers were selected from biocompatible and bioactive materials which can improve the therapeutic effectiveness of the TiO<sub>2</sub>NPs. It is worth mentioning that the clinical trials of the modified TiO<sub>2</sub>NPs require much more research to fulfill all the requirements of clinical agents in terms of physicochemical and biological properties. For example, much more *in vivo* studies should be performed for evaluating the toxicity of modified TiO<sub>2</sub>NPs on mammals. Thus, it is still a frontier research area with worthwhile background knowledge provided by previous research. So, future studies can be more focused on the development of safe, cost-effective, and scalable modified TiO<sub>2</sub>NPs for the clinical fields, specifically antimicrobial agents. We believe that the modified TiO<sub>2</sub>NPs will be an important research topic with great vitality and practical potential in biomedical applications.

## Conflicts of interest

There are no conflicts to declare.

## References

- N. Rodríguez-Barajas, M. L. Anaya-Esparza, Z. Villagrán-de la Mora, A. J. Sánchez-Burgos and A. Pérez-Larios, *Adv. Anticancer Agents Med. Chem.*, 2022, **22**, 2241–2254.
- X. He, H. Deng and H. Hwang, *J. Food Drug Anal.*, 2019, **27**, 1–21.
- L. M. Margarucci, V. Romano Spica, G. Gianfranceschi and F. Valeriani, *Environ. Int.*, 2019, **133**, 105095.
- A. Morlando, M. Chaki Borrás, Y. Rehman, S. Bakand, P. Barker, R. Sluyter and K. Konstantinov, *J. Mater. Chem. B*, 2020, **8**, 4016–4028.
- H. Chang, Q. Wang, X. Meng, X. Chen, Y. Deng, L. Li, Y. Yang, G. Song and H. Jia, *Chem. Res. Toxicol.*, 2022, **35**, 1435–1456.
- C. J. Dedman, A. M. King, J. A. Christie-Oleza and G.-L. Davies, *Environ. Sci.: Nano*, 2021, **8**, 1236–1255.
- S. Sargazi, S. ER, S. Sacide Gelen, A. Rahdar, M. Bilal, R. Arshad, N. Ajalli, M. Farhan Ali Khan and S. Pandey, *J. Drug Delivery Sci. Technol.*, 2022, **75**, 103605.
- R. Javed, N. Ul Ain, A. Gul, M. Arslan Ahmad, W. Guo, Q. Ao and S. Tian, *IET Nanobiotechnol.*, 2022, **16**, 171–189.
- F. Valeriani, L. M. Margarucci and V. Romano Spica, *Int. J. Environ. Res. Public Health*, 2018, **15**, 2675.
- G. Lofrano, F. Ubaldi, L. Albarano, M. Carotenuto, V. Vaiano, F. Valeriani, G. Libralato, G. Gianfranceschi, I. Fratoddi, S. Meric, M. Guida and V. Romano Spica, *Nanomaterials*, 2022, **12**, 2831.
- L. M. Margarucci, V. Romano Spica, C. Protano, G. Gianfranceschi, M. Giuliano, V. Di Onofrio, N. Mucci, F. Valeriani, M. Vitali and F. Romano, *Ann. Ig.*, 2019, **31**, 461–473.
- L. M. Margarucci, G. Gianfranceschi, V. Romano Spica, G. D'Ermo, C. Refi, M. Podico, M. Vitali, F. Romano and F. Valeriani, *Int. J. Environ. Res. Public Health*, 2021, **18**, 8662.
- T. Feng, S. Yan, S. Hou and X. Fan, *Spectrochim. Acta, Part A*, 2022, **280**, 121548.
- J. E. Karbowniczek, D. P. Ura and U. Stachewicz, *Composites, Part B*, 2022, **241**, 110011.
- G. Sanità, B. Carrese and A. Lamberti, *Front. Mol. Biosci.*, 2020, **7**, 587012.
- K. V. Korpany, C. Mottillo, J. Bachelder, S. N. Cross, P. Dong, S. Trudel, T. Frišćić and A. S. Blum, *Chem. Commun.*, 2016, **52**, 3054–3057.
- S. Benkoulou, O. Sublemontier, M. Patanen, C. Nicolas, F. Sirotti, A. Naitabdi, F. Gaie-Levrel, E. Antonsson, D. Aureau, F.-X. Ouf, S.-I. Wada, A. Etcheberry, K. Ueda and C. Miron, *Sci. Rep.*, 2015, **5**, 15088.
- S. Wendt, R. Schaub, J. Matthiesen, E. K. Vestergaard, E. Wahlström, M. D. Rasmussen, P. Thøstrup, L. M. Molina, E. Lægsgaard, I. Stensgaard, B. Hammer and F. Besenbacher, *Surf. Sci.*, 2005, **598**, 226–245.
- M.-I. Baraton and L. Merhari, *J. Eur. Ceram. Soc.*, 2004, **24**, 1399–1404.
- C. E. Nanayakkara, W. A. Larish and V. H. Grassian, *J. Phys. Chem. C*, 2014, **118**, 23011–23021.





- 21 L. T. Zhuravlev, *Colloids Surf., A*, 2000, **173**, 1–38.
- 22 P. Pallavicini, E. Cabrini, A. Casu, G. Dacarro, Y. Antonio Diaz-Fernandez, A. Falqui, C. Milanese and F. Vita, *Dalton Trans.*, 2015, **44**, 21088.
- 23 E. P. Plueddemann, *Nature of Adhesion Through Silane Coupling Agents, Silane Coupling Agents*, Springer US, Boston, MA, 1991, p. 115.
- 24 F. Ahangaran and A. H. Navarchian, *Adv. Colloid Interface Sci.*, 2020, **286**, 102298.
- 25 N. Zhu, H. Ji, P. Yu, J. Niu, M. U. Farooq, M. W. Akram, I. O. Udego, H. Li and X. Niu, *Nanomaterials*, 2018, **8**, 810.
- 26 R. S. Fernandes, I. M. Raimundo and M. F. Pimentel, *Colloids Surf., A*, 2019, **577**, 1–7.
- 27 C. Chen, W. Wu, W. Z. Xu and P. A. Charpentier, *Nanotechnology*, 2017, **28**, 115709.
- 28 N. D. Bansod, B. P. Kapgate, C. Das, A. Das, D. Basu and S. C. Debnath, *J. Sol-Gel Sci. Technol.*, 2016, **80**, 548–559.
- 29 J. Xie, L. F. Mei, L. B. Liao, G. C. Lv, Z. G. Xia and G. X. Du, *Key Eng. Mater.*, 2014, **602–603**, 59–62.
- 30 F. Temerov, J. Haapanen, J. M. Mäkelä and J. J. Saarinen, *Inorganics*, 2021, **9**, 21.
- 31 H. Maskrot, N. Herlin-Boime, Y. Leconte, K. Jursikova, C. Reynaud and J. Vicens, *J. Nanopart. Res.*, 2006, **8**, 351–360.
- 32 G. N. Shao, Y. Kim, S. M. Imran, S. J. Jeon, P. B. Sarawade, A. Hilonga, J.-K. Kim and H. T. Kim, *Microporous Mesoporous Mater.*, 2013, **179**, 111–121.
- 33 Y. Zhang, F. Fang, C. Wang, L. Wang, X. Wang, X. Chu, J. Li, X. Fang, Z. Wei and X. Wang, *Polym. Compos.*, 2014, **35**, 1204–1211.
- 34 S. Mallakpour and M. Madani, *J. Mater. Sci.*, 2014, **49**, 5112–5118.
- 35 S. W. Chong, C. W. Lai, J. C. Juan and B. F. Leo, *Sol. Energy*, 2019, **191**, 663–671.
- 36 H. P. Duong, C.-H. Hung, H. C. Dao, M. D. Le and C.-Y. Chen, *New J. Chem.*, 2018, **42**, 8745–8751.
- 37 D. Meroni, L. Lo Presti, G. Liberto, M. Ceotto, R. G. Acres, K. C. Prince, R. Bellani, G. Soliveri and S. Ardizzone, *J. Phys. Chem. C*, 2017, **121**, 430–440.
- 38 S. Raqema, U. Hashim, N. Azizah, S. Nadzirah, M. K. M. Arshad, A. R. Ruslinda and S. C. B. Gopinath, *AIP Conf. Proc.*, 2017, **1808**, 20007.
- 39 Y.-L. Liu, Y.-H. Su and J.-Y. Lai, *Polymer*, 2004, **45**, 6831–6837.
- 40 Z.-M. Dang, Y.-J. Xia, J.-W. Zha, J.-K. Yuan and J. Bai, *Mater. Lett.*, 2011, **65**, 3430–3432.
- 41 Q. F. Xu, Y. Liu, F.-J. Lin, B. Mondal and A. M. Lyons, *ACS Appl. Mater. Interfaces*, 2013, **5**, 8915–8924.
- 42 M. M. Rahim-Abadi, A. R. Mahdavian, A. Gharieh and H. Salehi-Mobarakeh, *Prog. Org. Coat.*, 2015, **88**, 310–315.
- 43 P. Toh-Ae, B. Junhasavasdikul, N. Lopattananon and K. Sahakaro, *Adv. Mater. Res.*, 2014, **844**, 276–279.
- 44 J. D. Ambrósio, C. V. M. Balarim and G. B. de Carvalho, *Polym. Compos.*, 2016, **37**, 1415–1424.
- 45 M. Sabzi, S. M. Mirabedini, J. Zohuriaan-Mehr and M. Atai, *Prog. Org. Coat.*, 2009, **65**, 222–228.
- 46 T. P. Selvin, J. Kuruvilla and T. Sabu, *Mater. Lett.*, 2004, **58**, 281–289.
- 47 L. Meng, Z. Liu, C. Lan and N. Xu, *Catal. Lett.*, 2022, **152**, 912–920.
- 48 P. A. Zapata, H. Palza, K. Delgado and F. M. Rabagliati, *J. Polym. Sci., Part A: Polym. Chem.*, 2012, **50**, 4055–4062.
- 49 V. G. Nguyen, H. Thai, D. H. Mai, H. T. Tran, D. L. Tran and M. T. Vu, *Composites, Part B*, 2013, **45**, 1192–1198.
- 50 E. Džunuzović, M. Marinović-Cincović, J. Vuković, K. Jeremić and J. M. Nedeljković, *Polym. Compos.*, 2009, **30**, 737–742.
- 51 Y. Qi, B. Xiang, W. Tan and J. Zhang, *Appl. Surf. Sci.*, 2017, **419**, 213–223.
- 52 J. Zhao, M. Milanova, M. M. C. G. Warmoeskerken and V. Dutschk, *Colloids Surf., A*, 2012, **413**, 273–279.
- 53 R. Mokhtari Aghdami, S. R. Mousavi, S. Estaji, R. K. Dermen, H. A. Khonakdar and A. Shakeri, *Polym. Compos.*, 2022, **43**, 4165–4178.
- 54 H. Massoumi, R. Kumar, M. K. Chug, Y. Qian and E. J. Brisbois, *ACS Appl. Bio Mater.*, 2022, **5**, 2285–2295.
- 55 A. Dymerska, B. Zielińska, K. Sielicki, X. Chen and E. Mijowska, *Diamond Relat. Mater.*, 2022, **125**, 109027.
- 56 J. Yoo, H. Jeong, S. K. Park, S. Park and J. S. Lee, *Biosensors*, 2021, **11**, 2012.
- 57 P. Zhang, L. Cao, X. Wang, J. Cui, Z. Lin, S. Ngai, F. Vogel, H. Wang, W. Li, S. Li and Q. Wang, *Ceram. Int.*, 2022, **48**, 1731–1739.
- 58 A. Wanag, A. Sienkiewicz, P. Rokicka-Konieczna, E. Kusiak-Nejman and A. W. Morawski, *J. Environ. Chem. Eng.*, 2020, **8**, 103917.
- 59 S. Mallakpour and A. Barati, *Prog. Org. Coat.*, 2011, **71**, 391–398.
- 60 A. Shakeri, D. Yip, M. Badv, S. M. Imani, M. Sanjari and T. F. Didar, *Materials*, 2018, **11**, 1003.
- 61 R. Klaysri, T. Tubchareon and P. Praserttham, *J. Ind. Eng. Chem.*, 2017, **45**, 229–236.
- 62 G. Lee, J. Lee and C. Kang, *J. Coat. Technol. Res.*, 2019, **16**, 1399–1409.
- 63 M. A. Ashraf, Z. Liu, W.-X. Peng and N. Yoysefi, *Prog. Org. Coat.*, 2019, **136**, 105296.
- 64 N. Tangchantra, J. Kruenate, C. Aumnate and T. Sooksom-song, *Adv. Mater. Res.*, 2010, **93–94**, 300–303.
- 65 C. Yang and C. Yang, *J. Mater. Sci.: Mater. Electron.*, 2014, **25**, 3285–3289.
- 66 C. H. M. Caris, R. P. M. Kuijpers, A. M. van Herk and A. L. German, *Makromol. Chem., Macromol. Symp.*, 1990, **35–36**, 535–548.
- 67 C.-C. Weng and K.-H. Wei, *Chem. Mater.*, 2003, **15**, 2936–2941.
- 68 B. Erdem, E. D. Sudol, V. L. Dimonie and M. S. El-Aasser, *J. Polym. Sci., Part A: Polym. Chem.*, 2000, **38**, 4431–4440.
- 69 M. Z. Rong, M. Q. Zhang, H. B. Wang and H. M. Zeng, *Appl. Surf. Sci.*, 2002, **200**, 76–93.
- 70 M. Yang and Y. Dan, *Colloid Polym. Sci.*, 2005, **284**, 243–250.
- 71 F. Milanese, G. Cappelletti, R. Annunziata, C. L. Bianchi, D. Meroni and S. Ardizzone, *J. Phys. Chem. C*, 2010, **114**, 8287–8293.





- 72 J. Z. B. Xiang and G. Jiang, *Plast., Rubber Compos.*, 2015, **44**, 148–154.
- 73 C. Wang, H. Mao, C. Wang and S. Fu, *Ind. Eng. Chem. Res.*, 2011, **50**, 11930–11934.
- 74 J. Godnjavec, B. Znoj, J. Vince, M. Steinbacher, A. Žnidaršič and P. Venturini, *Mater. Technol.*, 2012, **46**, 19–24.
- 75 M.-A. E. Antoine, R. M. Dalod, L. Henriksen and T. Grande, *Beilstein J. Nanotechnol.*, 2017, **8**, 304–312.
- 76 M. Connolly, D. Hernández-Moreno, E. Conde, A. Garnica, J. M. Navas, F. Torrent, I. Rucandio and M. L. Fernandez-Cruz, *Environ. Sci. Eur.*, 2022, **34**, 1.
- 77 D. Tsotetsi, M. Dhlamini and P. Mbule, *Results Mater.*, 2022, **14**, 100266.
- 78 S. Katebi Koushali, M. Hamadani, A. R. Ghasemi and M. Ashrafi, *J. Nanostruct.*, 2021, **11**, 38–47.
- 79 B. A. Dehkordi, M. R. Nilforoushan, N. Talebian and M. Tayebi, *Mater. Res. Express*, 2021, **8**, 35403.
- 80 H. M. Yadav, N. D. Thorat, M. M. Yallapu, S. A. M. Tofail and J.-S. Kim, *J. Mater. Chem. B*, 2017, **5**, 1461–1470.
- 81 Z. Landolsi, I. Ben Assaker, D. Nunes, E. Fortunato, R. Martins, R. Chtourou and S. Ammar, *J. Mater. Sci.: Mater. Electron.*, 2020, **31**, 20753–20773.
- 82 S. Bai, N. Yang, X. Wang, F. Gong, Z. Dong, Y. Gong, Z. Liu and L. Cheng, *ACS Nano*, 2020, **14**, 15119–15130.
- 83 Y. Birinci, J. H. Niazi, O. Aktay-Çetin and H. Basaga, *Enzyme Microb. Technol.*, 2020, **138**, 109559.
- 84 X. Wang, X. Zhong, L. Bai, J. Xu, F. Gong, Z. Dong, Z. Yang, Z. Zeng, Z. Liu and L. Cheng, *J. Am. Chem. Soc.*, 2020, **142**, 6527–6537.
- 85 H. M. Yadav, N. D. Thorat, M. M. Yallapu, S. A. M. Tofail and J.-S. Kim, *J. Mater. Chem. B*, 2017, **5**, 1461–1470.
- 86 S. Salou, C.-M. Cirtiu, D. Larivière and N. Fleury, *Anal. Bioanal. Chem.*, 2020, **412**, 1469–1481.
- 87 Y. Li, Z. Qin, H. Guo, H. Yang, G. Zhang, S. Ji and T. Zeng, *PLoS One*, 2014, **9**, e114638.
- 88 V. A. Ortega, D. Boyle, J. W. Hodgkinson, D. B. D. Simmons, M. Belosevic, J. L. Stafford and G. G. Goss, *Environ. Sci.: Nano*, 2021, **8**, 1910–1926.
- 89 V. A. Ortega, M. S. Bahniuk, S. Memon, L. D. Unsworth, J. L. Stafford and G. G. Goss, *Biointerphases*, 2020, **15**, 51003.
- 90 H. E. Ali, A. M. Elbarbary, A. M. Abdel-Ghaffar and N. A. Maziad, *J. Appl. Polym. Sci.*, 2022, **139**, 52344.
- 91 Z. He, H. Wu, Z. Shi, Z. Kong, S. Ma, Y. Sun and X. Liu, *ACS Omega*, 2022, **7**, 7084–7095.
- 92 S. Dong, G. Xiao, C. Chen, Z. Yang, C. Chen, Q. Wang and L. Lin, *Prog. Org. Coat.*, 2021, **157**, 106291.
- 93 S. Naghibi, H. R. Madaah Hosseini and M. A. Faghihi Sani, *Ceram. Int.*, 2013, **39**, 8377–8384.
- 94 B. E. Castillo, E. Prokhorov, G. Luna-Bárcenas and Y. Kovalenko, *Polymers*, 2022, **14**, 1686.
- 95 H. Moulahoum, F. Ghorbanizamani, S. Sakarya and S. Timur, *Prog. Org. Coat.*, 2022, **169**, 106923.
- 96 N. Y. Elmehbad, N. A. Mohamed and N. A. Abd El-Ghany, *Int. J. Biol. Macromol.*, 2022, **205**, 719–730.
- 97 M. F. Majnis, O. C. Yee, M. A. Mohd Adnan, M. R. Yusof Hamid, K. Z. Ku Shaari and N. Muhd Julkapli, *Opt. Mater.*, 2022, **124**, 111967.
- 98 O. D. Saliu, M. Mamo, P. Ndungu and J. Ramontja, *J. Energy Storage*, 2022, **49**, 104155.
- 99 F. L. Gomes de Menezes, R. H. de Lima Leite, F. K. Gomes dos Santos, A. I. Aria and E. M. M. Aroucha, *Colloids Surf., A*, 2021, **630**, 127661.
- 100 M. Ren, H. Horn and F. H. Frimmel, *Water Res.*, 2017, **123**, 678–686.
- 101 F. Loosli, L. Vitorazi, J.-F. Berret and S. Stoll, *Water Res.*, 2015, **80**, 139–148.
- 102 M. N. Alomary and M. A. Ansari, *Chemistry*, 2021, **27**, 5817–5829.
- 103 G. Sarigul, I. Chamorro-Mena, N. Linares, J. García-Martínez and E. Serrano, *Adv. Sustainable Syst.*, 2021, **5**, 2100076.
- 104 S. Dessai, M. Ayyanar, S. Amalraj, P. Khanal, S. Vijayakumar, N. Gurav, N. Rarokar, M. Kalaskar, S. Nadaf and S. Gurav, *Mater. Lett.*, 2022, **311**, 131639.
- 105 S. Gulla, V. C. Reddy, P. B. Araveti, D. Lomada, A. Srivastava, M. C. Reddy and K. R. Reddy, *J. Mol. Struct.*, 2022, **1249**, 131556.
- 106 S. Iqbal, M. Fakhar-e-Alam, K. S. Alimgeer, M. Atif, A. Hanif, N. Yaqub, W. A. Farooq, S. Ahmad, Y.-M. Chu, M. Suleman Rana, A. Fatehmulla and H. Ahmad, *Saudi J. Biol. Sci.*, 2021, **28**, 1226–1232.
- 107 H.-X. Wang, X.-X. Li and L. Tang, *Appl. Phys. A: Mater. Sci. Process.*, 2020, **126**, 448.
- 108 A. Razzaz, S. Ghorban, L. Hosayni, M. Irani and M. Aliabadi, *J. Taiwan Inst. Chem. Eng.*, 2016, **58**, 333–343.
- 109 A. Babaei-Ghazvini, B. Acharya and D. R. Korber, *Polymers*, 2021, **13**, 2790.
- 110 V. K. Bui, D. Park and Y.-C. Lee, *Polymers*, 2017, **9**, 21.
- 111 R. Gobi, P. Ravichandiran, R. S. Babu and D. J. Yoo, *Polymers*, 2021, **13**, 1962.
- 112 X. Wang, Z. Li, Y. Wu, H. Guo, X. Zhang, Y. Yang, H. Mu and J. Duan, *ACS Appl. Mater. Interfaces*, 2021, **13**, 10902–10915.
- 113 R. Khan and M. Dhayal, *Electrochem. Commun.*, 2008, **10**, 492–495.
- 114 S. A. Matboo, S. Nazari, A. Niapour, M. V. Niri, E. Asgari and S. A. Mokhtari, *Water Sci. Technol.*, 2022, **85**, 605–616.
- 115 A. Maleki, B. Hayati, F. Najafi, F. Gharibi and S. W. Joo, *J. Mol. Liq.*, 2016, **224**, 95–104.
- 116 Z. Zhang, Y. Wang, T. Li, P. Ma, X. Zhang, B. Xia, M. Chen, M. Du and W. Dong, *Ind. Eng. Chem. Res.*, 2021, **60**, 3999–4008.
- 117 Z. Qiaorun, S. Honghong, L. Yao, J. Bing, X. Xiao, D. Julian McClements, C. Chongjiang and Y. Biao, *Food Res. Int.*, 2022, **159**, 111574.
- 118 A. Tajdari, A. Babaei, A. Goudarzi and R. Partovi, *J. Plast. Film Sheeting*, 2020, **36**, 285–311.
- 119 F. Loosli, P. Le Coustumer and S. Stoll, *Sci. Total Environ.*, 2015, **535**, 28–34.
- 120 S. Li, G. Chen, S. Qiang, Z. Yin, Z. Zhang and Y. Chen, *Int. J. Food Microbiol.*, 2020, **331**, 108763.
- 121 A. Deghiche, N. Haddaoui, A. Zerriouh, S. E. Fenni, D. Cavallo, A. Erto and Y. Benguerba, *J. Environ. Chem. Eng.*, 2021, **9**, 106541.



- 122 J. Zhang, M. Zheng, Y. Zhou, L. Yang, Y. Zhang, Z. Wu, G. Liu and J. Zheng, *Membranes*, 2022, **12**, 386.
- 123 J.-H. Li, Y.-Y. Xu, L.-P. Zhu, J.-H. Wang and C.-H. Du, *J. Membr. Sci.*, 2009, **326**, 659–666.
- 124 K. Liu, Z. Cai, X. Chi, B. Kang, S. Fu, X. Luo, Z.-W. Lin, H. Ai, J. Gao and H. Lin, *Nano Lett.*, 2022, **22**, 3219–3227.
- 125 J. L. Peper, N. E. Gentry, B. Boudy and J. M. Mayer, *Inorg. Chem.*, 2022, **61**, 767–777.
- 126 Y.-Z. Lü, S.-N. Zhang, Y.-F. Du, M.-T. Chen and C.-R. Li, *J. Inorg. Mater.*, 2013, **28**, 594–598.
- 127 Y. Lv, C. Li, Q. Sun, M. Huang, C. Li and B. Qi, *Nanoscale Res. Lett.*, 2016, **11**, 515.
- 128 M. S. Hanafy, W. M. Desoky, E. M. Hussein, N. H. El-Shaer, M. Gomaa, A. A. Gamal, M. A. Esawy and O. W. Guirguis, *J. Biomed. Mater. Res., Part A*, 2021, **109**, 232–247.
- 129 L. Goñi-Ciaurritz and I. Vélaz, *Int. J. Biol. Macromol.*, 2022, **216**, 347–360.
- 130 T. Ukmar, A. Godec, U. Maver, O. Planinšek, M. Bele, J. Jamnik and M. Gaberšček, *J. Mater. Chem.*, 2009, **19**, 8176–8183.
- 131 C. Ronchi, D. Selli, W. Pipornpong and C. Di Valentin, *J. Phys. Chem. C*, 2019, **123**, 7682–7695.
- 132 M. Qi, C. Li, Z. Song and L. Wang, *Drug Delivery*, 2021, **28**, 1785–1794.
- 133 R. Mohan, J. Drbohlavova and J. Hubalek, *Nanoscale Res. Lett.*, 2013, **8**, 503.
- 134 R. Binaymotlagh, L. Chronopoulou, F. Hajareh Haghighi, I. Fratoddi and C. Palocci, *Materials*, 2022, **15**, 5871.
- 135 R. Binaymotlagh, A. Del Giudice, S. Mignardi, F. Amato, A. G. Marrani, F. Savori, I. Cavallo, E. G. Di Domenico, C. Palocci and L. Chronopoulou, *Gels*, 2022, **8**, 700.
- 136 X. Yang, Y. Wang, W. Qi, R. Xing, X. Yang, Q. Xing, R. Su and Z. He, *J. Mater. Chem. B*, 2019, **7**, 2981–2988.
- 137 E. Makhado, B. R. Motshabi, D. Allouss, K. E. Ramohlola, K. D. Modibane, M. J. Hato, R. M. Jugade, F. Shaik and S. Pandey, *Chemosphere*, 2022, **306**, 135524.
- 138 S. Zhao, C. Hou, L. Shao, W. An and W. Cui, *Appl. Surf. Sci.*, 2022, **590**, 153088.
- 139 R. R. Mansurov, V. S. Zverev and A. P. Safronov, *J. Catal.*, 2022, **406**, 9–18.
- 140 A. Ulu, E. Birhanlı, S. Köytepe and B. Ateş, *Int. J. Biol. Macromol.*, 2020, **163**, 529–540.
- 141 Y. Yue, X. Wang, Q. Wu, J. Han and J. Jiang, *J. Colloid Interface Sci.*, 2020, **564**, 99–112.
- 142 R. F. Bonan, M. F. Mota, R. M. da Costa Farias, S. D. da Silva, P. R. F. Bonan, L. Diesel, R. R. Menezes and D. E. da Cruz Perez, *Mater. Sci. Eng., C*, 2019, **104**, 109876.
- 143 S. Shiva Samhitha, G. Raghavendra, C. Quezada and P. Hima Bindu, *Mater. Today: Proc.*, 2022, **54**, 765–770.
- 144 N. Lagopati, K. Evangelou, P. Falaras, E.-P. C. Tsilibary, P. V. S. Vasileiou, S. Havaki, A. Angelopoulou, E. A. Pavlatou and V. G. Gorgoulis, *Pharmacol. Ther.*, 2021, **222**, 107795.
- 145 S. Çeşmeli and C. Biray Avci, *J. Drug Targeting*, 2019, **27**, 762–766.
- 146 Z. Youssef, V. Jouan-Hureau, L. Colombeau, P. Arnoux, A. Moussaron, F. Baros, J. Toufaily, T. Hamieh, T. Roques-Carmes and C. Frochot, *Photodiagn. Photodyn. Ther.*, 2018, **22**, 115–126.
- 147 Z. Youssef, P. Arnoux, L. Colombeau, J. Toufaily, T. Hamieh, C. Frochot and T. Roques-Carmes, *J. Photochem. Photobiol., A*, 2018, **356**, 177–192.
- 148 P. Huang, C. Xu, J. Lin, C. Wang, X. Wang, C. Zhang, X. Zhou, S. Guo and D. Cui, *Theranostics*, 2011, **1**, 240–250.
- 149 X. Liang, Y. Xie, J. Wu, J. Wang, M. Petković, M. Stepić, J. Zhao, J. Ma and L. Mi, *J. Photochem. Photobiol., B*, 2021, **215**, 112122.
- 150 B. Salama, C.-J. Chang, K. Kanehira, E.-S. El-Sherbini, G. El-Sayed, M. El-Adl and A. Taniguchi, *Molecules*, 2020, **25**, 4467.
- 151 S. Gai, G. Yang, P. Yang, F. He, J. Lin, D. Jin and B. Xing, *Nano Today*, 2018, **19**, 146–187.
- 152 M. A. Behnam, F. Emami, Z. Sobhani and A. R. Dehghanian, *Iran. J. Basic Med. Sci.*, 2018, **21**, 1133–1139.
- 153 Y. Gao, L. Zhang, Y. Liu, S. Sun, Z. Yin, L. Zhang, A. Li, G. Lu, A. Wu and L. Zeng, *Nanoscale*, 2020, **12**, 1801–1810.
- 154 T. Dai, W. He, S. Tu, J. Han, B. Yuan, C. Yao, W. Ren and A. Wu, *Bioact. Mater.*, 2022, **17**, 18–28.
- 155 Y. Zhang, X. Zhang, H. Yang, L. Yu, Y. Xu, A. Sharma, P. Yin, X. Li, J. S. Kim and Y. Sun, *Chem. Soc. Rev.*, 2021, **50**, 11227–11248.
- 156 R. L. Siegel, K. D. Miller, H. E. Fuchs and A. Jemal, *Cancer J. Clin.*, 2021, **71**, 7–33.
- 157 A. Vincent, J. Herman, R. Schulick, R. H. Hruban and M. Goggins, *Lancet*, 2011, **378**, 607–620.
- 158 A. Zinger, L. Koren, O. Adir, M. Poley, M. Alyan, Z. Yaari, N. Noor, N. Krinsky, A. Simon and H. Gibori, *ACS Nano*, 2019, **13**, 11008–11021.
- 159 K. P. Olive, M. A. Jacobetz, C. J. Davidson, A. Gopinathan, D. McIntyre, D. Honess, B. Madhu, M. A. Goldgraben, M. E. Caldwell and D. Allard, *Science*, 2009, **324**, 1457–1461.
- 160 A. Neesse, P. Michl, K. K. Frese, C. Feig, N. Cook, M. A. Jacobetz, M. P. Lolkema, M. Buchholz, K. P. Olive and T. M. Gress, *Gut*, 2011, **60**, 861–868.
- 161 J. Luo, J. Cao, G. Ma, X. Wang, Y. Sun, C. Zhang, Z. Shi, Y. Zeng, T. Zhang and P. Huang, *ACS Appl. Mater. Interfaces*, 2022, **14**, 40535–40545.
- 162 X. Wei, Z. Feng, J. Huang, X. Xiang, F. Du, C. He, M. Zhou, L. Ma, C. Cheng and L. Qiu, *ACS Appl. Mater. Interfaces*, 2021, **13**, 32810–32822.
- 163 X. Lin, R. Huang, Y. Huang, K. Wang, H. Li, Y. Bao, C. Wu, Y. Zhang, X. Tian and X. Wang, *Int. J. Nanomed.*, 2021, **16**, 1889–1899.
- 164 G. P. Lee, A. Willis, S. Pernal, A. Phakatkar, T. Shokuhfar, V. Blot and H. H. Engelhard, *Nanomedicine*, 2021, **16**, 523–534.
- 165 E. Yousefi, S. Javadpour, M. Ansari and H. Eslami, *Mater. Technol.*, 2021, **36**, 521–528.
- 166 A. Pariente, E. Peled, I. Zlotver and A. Sosnik, *Mater. Today Chem.*, 2021, **22**, 100613.
- 167 P. Magesan, K. I. Dhanalekshmi, J. Prabha, M. J. Umashathy, X. Zhang, N. Punitha, K. Kadambary and



- K. Sangeetha, *Photodiagn. Photodyn. Ther.*, 2022, **40**, 103064.
- 168 J.-Y. Zhou, W.-J. Wang, C.-Y. Zhang, Y.-Y. Ling, X.-J. Hong, Q. Su, W.-G. Li, Z.-W. Mao, B. Cheng, C.-P. Tan and T. Wu, *Biomaterials*, 2022, **289**, 121757.
- 169 E. Donadoni, P. Siani, G. Frigerio and C. Di Valentin, *Nanoscale*, 2022, **14**, 12099–12116.
- 170 L. Fang, H. Huang, J. D. Quirk, J. Zheng, D. Shen, B. Manion, M. Mixdorf, P. Karmakar, G. P. Sudlow, R. Tang and S. Achilefu, *Curr. Anal. Chem.*, 2022, **18**, 826–835.
- 171 Y. Hou, A. Mushtaq, Z. Tang, E. Dempsey, Y. Wu, Y. Lu, C. Tian, J. Farheen, X. Kong and M. Z. Iqbal, *J. Sci.: Adv. Mater. Devices*, 2022, **7**, 100417.
- 172 X. Wen, N. Liu, J. Ren, X. Jiao, J. Lv, M. H. Akhtar, H. Qi, J. Zhu, C. Yu and Y. Li, *New J. Chem.*, 2022, **46**, 6966–6970.
- 173 P. Ramachandran, B.-K. Khor, C. Y. Lee, R.-A. Doong, C. E. Oon, N. T. K. Thanh and H. L. Lee, *Biomedicines*, 2022, **10**, 421.
- 174 E. Tutun, V. Tekin, V. Yasakci, Ö. Aras and P. Ünak, *Appl. Organomet. Chem.*, 2021, **35**, e6435.
- 175 A. Mushtaq, Y. Hou, C. Tian, T. Deng, C. Xu, Z. Sun, X. Kong and M. Zubair Iqbal, *Mater. Res. Bull.*, 2021, **144**, 111481.
- 176 J. Li, S. Dai, R. Qin, C. Shi, J. Ming, X. Zeng, X. Wen, R. Zhuang, X. Chen, Z. Guo and X. Zhang, *ACS Appl. Mater. Interfaces*, 2021, **13**, 54727–54738.
- 177 M. Matijević, J. Žakula, L. Korićanac, M. Radoičić, X. Liang, L. Mi, J. F. Tričković, A. V. Šobot, M. N. Stanković, Đ. Nakarada, M. Mojović, M. Petković, M. Stepić and M. D. Nešić, *Photochem. Photobiol. Sci.*, 2021, **20**, 1087–1098.
- 178 J. Cao, Y. Sun, C. Zhang, X. Wang, Y. Zeng, T. Zhang and P. Huang, *Acta Biomater.*, 2021, **129**, 269–279.
- 179 Z. Shi, X. Meng, K. Zhang, S. Tang, C. Zhang, Z. Yang, H. Dong and X. Zhang, *ACS Mater. Lett.*, 2021, **3**, 781–789.
- 180 Q. Tang, H.-L. Zhang, Y. Wang, J. Liu and S.-P. Yang, *J. Mater. Chem. B*, 2021, **9**, 4241–4248.
- 181 Q. Pan, M. Li, M. Xiao, Y. He, G. Sun, T. Xue, Y. Luo, L. Chen, B. Ai and J. Xiong, *J. Nanomater.*, 2021, **2021**, 4125350.
- 182 A. Mansoor, Z. Khurshid, M. T. Khan, E. Mansoor, F. A. Butt, A. Jamal and P. J. Palma, *Nanomaterials*, 2022, **12**, 3670.
- 183 J. Han, E.-K. Jang, M.-R. Ki, R. G. Son, S. Kim, Y. Choe, S. P. Pack and S. Chung, *J. Ind. Eng. Chem.*, 2022, **112**, 258–270.
- 184 J. Cano-Mejia, R. A. Burga, E. E. Sweeney, J. P. Fisher, C. M. Bollard, A. D. Sandler, C. R. Y. Cruz and R. Fernandes, *Nanomedicine*, 2017, **13**, 771–781.
- 185 L. Chen, F. Pastorino, P. Berry, J. Bonner, C. Kirk, K. M. Wood, H. D. Thomas, Y. Zhao, A. Daga and G. J. Veal, *Int. J. Cancer*, 2019, **144**, 3146–3159.
- 186 S. G. DuBois, Y. P. Mosse, E. Fox, R. A. Kudgus, J. M. Reid, R. McGovern, S. Groshen, R. Bagatell, J. M. Maris and C. J. Twist, *Clin. Cancer Res.*, 2018, **24**, 6142–6149.
- 187 T. Lopez, J. Sotelo, J. Navarrete and J. A. Ascencio, *Opt. Mater.*, 2006, **29**, 88–94.
- 188 F. Grande and P. Tucci, *Mini-Rev. Med. Chem.*, 2016, **16**, 762–769.
- 189 M. Tian, X. Chen, Z. Gu, H. Li, L. Ma, X. Qi, H. Tan and C. You, *Carbohydr. Polym.*, 2016, **144**, 522–530.
- 190 J. Zhao, L. Yao, S. Nie and Y. Xu, *Int. J. Biol. Macromol.*, 2021, **167**, 921–933.
- 191 S. Klein, T. Luchs, A. Leng, L. V. R. Distel, W. Neuhuber and A. Hirsch, *Bioengineering*, 2020, **7**, 1–22.
- 192 K. Zheng, R. Chen, Y. Sun, Z. Tan, Y. Liu, X. Cheng, J. Leng, Z. Guo and P. Xu, *Thorac. Cancer*, 2020, **11**, 1476–1486.
- 193 S. Kim, S. Im, E.-Y. Park, J. Lee, C. Kim, T.-I. Kim and W. J. Kim, *Nanomedicine*, 2020, **24**, 102110.
- 194 T. Yu, L. Tong, Y. Ao, G. Zhang, Y. Liu and H. Zhang, *Drug Delivery*, 2020, **27**, 855–863.
- 195 W. Chen, J. Wang, L. Cheng, W. Du, J. Wang, W. Pan, S. Qiu, L. Song, X. Ma and Y. Hu, *ACS Appl. Bio Mater.*, 2021, **4**, 1483–1492.
- 196 Y. He, J. Wan, Y. Yang, P. Yuan, C. Yang, Z. Wang and L. Zhang, *Adv. Healthcare Mater.*, 2019, **8**, 1801254.
- 197 S. Bhullar, N. Goyal and S. Gupta, *Sci. Rep.*, 2022, **12**, 4600.
- 198 M. I. Torres-Ramos, M. F. Martín-Marquez, M. D. C. Leal-Moya, S. Ghotekar, J. A. Sánchez-Burgos and A. Pérez-Larios, *Int. J. Mol. Sci.*, 2022, **23**, 10755.
- 199 A. Chahardoli, F. Qalekhani, Y. Shokoohinia and A. Fattahi, *J. Mol. Liq.*, 2022, **361**, 119674.
- 200 N. Karki, H. Tiwari, M. Matiyani, R. Bal, M. Pal and N. G. Sahoo, *J. Vinyl Addit. Technol.*, 2022, **28**, 474–486.
- 201 A.-M. Negrescu, V. Mitran, W. Draghicescu, S. Popescu, C. Pirvu, I. Ionascu, T. Soare, S. Uzun, S. M. Croitoru and A. Cimpean, *J. Funct. Biomater.*, 2022, **13**, 43.
- 202 X. Zeng, W. Yang, F. X. Song, H. X. Wang and Y. Li, *J. Drug Delivery Sci. Technol.*, 2022, **68**, 103120.
- 203 M. Motiei Pour, M. R. Moghbeli, B. Larijani and H. Akbari Javar, *Chem. Pap.*, 2022, **76**, 439–451.
- 204 Y. Feng, L. Liu, J. Zhang, H. Aslan and M. Dong, *J. Mater. Chem. B*, 2017, **5**, 8631–8652.
- 205 E. J. Diana and T. V. Mathew, *Colloids Surf., B*, 2022, **220**, 112949.
- 206 P. Maheswari, S. Harish, M. Navaneethan, C. Muthamizchelvan, S. Ponnusamy and Y. Hayakawa, *Mater. Sci. Eng., C*, 2020, **108**, 110457.
- 207 A. M. Mathew, V. I. Chukwuike, K. Venkatesan, S. Raveendran, R. C. Barik and D. K. Pattanayak, *Surf. Interfaces*, 2022, **33**, 102275.
- 208 A. Sathiyaseelan, K. Saravanakumar, K. V. Naveen, K.-S. Han, X. Zhang, M. S. Jeong and M.-H. Wang, *Environ. Res.*, 2022, **212**, 113237.
- 209 A. O. Özdemir, B. Caglar, O. Çubuk, F. Coldur, M. Kuzucu, E. K. Guner, B. Doğan, S. Caglar and K. V. Özdoğur, *Mater. Chem. Phys.*, 2022, **287**, 126342.
- 210 S. Metanawin and T. Metanawin, *Polym. Int.*, 2022, **71**, 777–789.
- 211 T. Singh, D. B. Pal, A. H. Almalki, Y. S. Althobaiti, M. F. Alkhanani, S. Haque, S. Sharma and N. Srivastava, *Mater. Lett.*, 2022, **316**, 132012.
- 212 S. Mallakpour and N. Mohammadi, *Carbohydr. Polym.*, 2022, **285**, 119226.



- 213 A. M. Youssef, M. E. Abd El-Aziz and S. M. M. Morsi, *Polym. Bull.*, 2022, **79**, 1–15.
- 214 Y. F. Makableh, N. F. Momani, T. Athamneh, R. Al-Abed and I. Alshorman, *Polym. Bull.*, 2022, **79**, 1–13.
- 215 P. Maheswari, S. Ponnusamy, S. Harish, C. Muthamizhchelvan and Y. Hayakawa, *Mater. Sci. Semicond. Process.*, 2020, **105**, 104724.
- 216 P. Maheswari, S. Ponnusamy, S. Harish, M. R. Ganesh and Y. Hayakawa, *Arabian J. Chem.*, 2020, **13**, 3484–3497.
- 217 P. Maheswari, S. Ponnusamy, S. Harish, C. Muthamizhchelvan, M. R. Ganesh and Y. Hayakawa, *Appl. Surf. Sci.*, 2019, **494**, 989–999.
- 218 S. Li, J. Zeng, D. Yin, P. Liao, S. Ding, P. Mao and Y. Liu, *Mater. Res. Express*, 2021, **8**, 85012.
- 219 A. M. Alakrach, A. A. Al-Rashdi, T. Alqadi, M. A. Al Saadi, S. S. Ting, O. S. Dahham and N. N. Zulkepli, *Mater. Sci. Forum*, 2021, **1021**, 270–279.
- 220 X. Wang, X. Li, X. Yang, K. Lei and L. Wang, *Colloids Surf., B*, 2021, **197**, 111410.
- 221 V. Soltaninejad and A. Maleki, *J. Photochem. Photobiol., A*, 2021, **404**, 112906.
- 222 T. Li, Y. Xiao, D. Guo, L. Shen, R. Li, Y. Jiao, Y. Xu and H. Lin, *J. Colloid Interface Sci.*, 2020, **572**, 114–121.
- 223 R. K. Manoharan, S. Ayyaru and Y.-H. Ahn, *New J. Chem.*, 2020, **44**, 807–816.
- 224 Y. Gao, X. Wang, X. Li and H. Dai, *New J. Chem.*, 2020, **44**, 20751–20758.
- 225 N. M. Ngoepe, M. M. Mathipa and N. C. Hintsho-Mbita, *Optik*, 2020, **224**, 165728.
- 226 S. Janfaza, M. Banan Nojavani, M. Nikkhah, T. Alizadeh, A. Esfandiar and M. R. Ganjali, *Microchim. Acta*, 2019, **186**, 137.
- 227 B. Mahyad, S. Janfaza and E. S. Hosseini, *Adv. Colloid Interface Sci.*, 2015, **225**, 194–202.
- 228 M.-C. Estevez, M. A. Otte, B. Sepulveda and L. M. Lechuga, *Anal. Chim. Acta*, 2014, **806**, 55–73.
- 229 Y. Xu, J. Lin, X. Wu, X. Xu, D. Zhang, Y. Xie, T. Pan, Y. He, A. Wu and G. Shao, *J. Mater. Chem. B*, 2022, **10**, 3808–3816.
- 230 Q. Y. Siew, S. Y. Tham, H.-S. Loh, P. S. Khiew, W. S. Chiu and M. T. T. Tan, *J. Mater. Chem. B*, 2018, **6**, 1195–1206.
- 231 S. Tao, Y. Guo, S. Wang, F. Xu, X. Zhou and Q. Guo, *Anal. Methods*, 2022, **14**, 2396–2404.
- 232 S. P. Hong, N. F. Mohd-Naim, N. A. Keasberry and M. U. Ahmed, *Electroanalysis*, 2022, **34**, 684–691.
- 233 S. Shi, Q. Nie, S. Jiang, S. Wu, B. Tang and M. Zhao, *Acta Opt. Sin.*, 2022, **42**, 0106001.
- 234 V. Rajeshwari, C. Vedhi and J. Fernando, *Mater. Today: Proc.*, 2022, **68**, 287–293.
- 235 D. Zheng, M. Chen, J. Peng, J. Chen, T. Chen, Y. Chen, L. Huang and W. Gao, *Microchim. Acta*, 2021, **188**, 328.
- 236 A. P. Singh, S. Balayan, S. Gupta, U. Jain, R. K. Sarin and N. Chauhan, *Process Biochem.*, 2021, **108**, 185–193.
- 237 J. Zhang, H. Hu and L. Yang, *Microchem. J.*, 2021, **168**, 106435.
- 238 M. Nycz, K. Arkusz and D. G. Pijanowska, *Materials*, 2021, **14**, 3767.
- 239 B. Baykal, G. Kadikoylu, H. Senturk, Y. O. Donar, A. Sinağ and A. Erdem, *J. Electroanal. Chem.*, 2021, **892**, 115262.
- 240 N. Gao, B. Fan, L. Li, X. Sun, X. Wang, H. Ma, Q. Wei and H. Ju, *ACS Appl. Bio Mater.*, 2021, **4**, 4479–4485.
- 241 J. Guo, G. Fang, S. Wang and J. Wang, *Food Chem.*, 2021, **344**, 128656.
- 242 R. H. Sakban, S. M. Abdulmohsin and M. D. Noori, *J. Phys. Conf. Ser.*, 2021, **1818**, 12038.
- 243 M. K. Choinśka, I. Šestáková, V. Hrdlička, J. Skopalová, J. Langmaier, V. Maier and T. Navrátil, *Biosensors*, 2022, **12**, 26.
- 244 J. Geddes-McAlister and R. S. Shapiro, *Ann. N. Y. Acad. Sci.*, 2019, **1435**, 57–78.
- 245 J. You, Y. Guo, R. Guo and X. Liu, *Chem. Eng. J.*, 2019, **373**, 624–641.
- 246 X. Zhao, G. Zhang and Z. Zhang, *Environ. Int.*, 2020, **136**, 105453; Y. Rilda, D. Dwiyantri, S. Syukri, A. Agustien and H. Pard, *J. Dispers. Sci. Technol.*, 2021, **42**, 784–790.
- 247 X. He, P. Wu, S. Wang, A. Wang, C. Wang and P. Ding, *J. Clean. Prod.*, 2021, **289**, 125755.
- 248 P. A. K. Reddy, P. V. L. Reddy, E. Kwon, K.-H. Kim, T. Akter and S. Kalagara, *Environ. Int.*, 2016, **91**, 94–103.
- 249 T. Wang, Z. Yang, C. Zhang, X. Zhai, X. Zhang, X. Huang, Z. Li, X. Zhang, X. Zou and J. Shi, *Int. J. Biol. Macromol.*, 2022, **222**, 2843–2854.
- 250 T. Siddiqui, N. J. Khan, N. Asif, I. Ahamad, D. Yasin and T. Fatma, *Environ. Sci. Pollut. Res.*, 2022, **29**, 39052–39066.
- 251 M. Sultan, H. Elsayed, A. E. F. Abdelhakim and G. Taha, *J. Appl. Polym. Sci.*, 2022, **139**, 51442.
- 252 L. Mohammad Taghizadeh Kashani, Shiva Masoudi and M. M. Ahmadian-Attari, *Inorg. Nano-Metal Chem.*, 2022, **52**, 297–307.
- 253 N. Duan, Q. Li, X. Meng, Z. Wang and S. Wu, *Food Chem.*, 2021, **364**, 130441.
- 254 H. Moradpoor, M. Safaei, A. Golshah, H. R. Mozaffari, R. Sharifi, M. M. Imani and M. S. Mobarakeh, *Inorg. Chem. Commun.*, 2021, **130**, 108748.
- 255 E. T. Helmy, E. M. Abouellef, U. A. Soliman and J. H. Pan, *Chemosphere*, 2021, **271**, 129524.
- 256 N. Rahmat, E. T. Wahyuni and A. Suratman, *Indones. J. Chem.*, 2021, **21**, 14–23.
- 257 H. P. Yetria Rilda, Dita Dwiyantri, Syukri Syukri and Anthoni Agustien, *J. Dispers. Sci. Technol.*, 2021, **42**, 784–790.
- 258 M. A. Irshad, R. Nawaz, M. Z. U. Rehman, M. Imran, J. Ahmad, S. Ahmad, A. Inam, A. Razzaq, M. Rizwan and S. Ali, *Chemosphere*, 2020, **258**, 127352.
- 259 L. Goñi-Ciauriz, M. Senosiain-Nicolay and I. Vélaz, *Int. J. Mol. Sci.*, 2021, **22**, 2257.
- 260 R. Chougale, D. Kasai, S. Nayak, S. Masti, A. Nasalapure and A. V. Raghu, *Green Mater.*, 2020, **8**, 40–48.
- 261 S. Krishnan, A. Dusane, R. Morajkar, A. Venkat and A. A. Vernekar, *J. Mater. Chem. B*, 2021, **9**, 5967–5981.
- 262 M. A. Sadique, S. Yadav, P. Ranjan, S. Verma, S. T. Salammal, M. A. Khan, A. Kaushik and R. Khan, *J. Mater. Chem. B*, 2021, **9**, 4620–4642.





- 263 H. Liu, W. Zhong, X. Zhang, D. Lin and J. Wu, *J. Mater. Chem. B*, 2021, **9**, 7878–7908.
- 264 D. A. Elsayed, M. G. Assy, S. M. Mousa, G. T. El-Bassyouni, S. M. Mouneir and W. S. Shehab, *Bioorg. Chem.*, 2022, **124**, 105805.
- 265 D. C. S. Souza, S. M. Amorim, R. D. Cadamuro, G. Fongaro, R. A. Peralta, R. M. Peralta, G. L. Puma and R. F. P. M. Moreira, *Carbohydr. Polym. Technol. Appl.*, 2022, **3**, 100182.
- 266 D. J. da Silva, A. G. Souza, G. S. Ferreira, A. Duran, A. D. Cabral, F. L. A. Fonseca, R. F. Bueno and D. S. Rosa, *ACS Appl. Nano Mater.*, 2021, **4**, 12949–12956.
- 267 I.-J. Wang, Y.-C. Chen, C. Su, M.-H. Tsai, W.-T. Shen, C.-H. Bai and K.-P. Yu, *J. Aerosol Med. Pulm. Drug Delivery*, 2021, **34**, 293–302.
- 268 A. Levina, M. Repkova, N. Shikina, Z. Ismagilov, M. Kupryushkin, A. Pavlova, N. Mazurkova, D. Pyshnyi and V. Zarytova, *Eur. J. Pharm. Biopharm.*, 2021, **162**, 92–98.
- 269 G. León-Gutiérrez, C. Cabello-Gutiérrez, M. H. Martínez-Gómez, P. Azuara, B. Madden, J. Shalkow and A. Mejía, *J. Nano Res.*, 2021, **70**, 137–145.
- 270 L. Zhang, H. Forgham, A. Shen, J. Wang, J. Zhu, X. Huang, S.-Y. Tang, C. Xu, T. P. Davis and R. Qiao, *J. Mater. Chem. B*, 2022, **10**, 7473–7490.
- 271 Z.-Y. Chen, S. Gao, Y.-W. Zhang, R.-B. Zhou and F. Zhou, *J. Mater. Chem. B*, 2021, **9**, 2594–2612.
- 272 R. Balan and V. Gayathri, *Polym. Bull.*, 2022, **79**, 4269–4286.
- 273 W. S. Saeed, D. H. Alotaibi, A.-B. Al-Odayni, A. S. Haidyrah, A. A. Al-Owais, R. Khan, M. A. De Vera, A. Alrahlah and T. Aouak, *Int. J. Mol. Sci.*, 2022, **23**, 3449.
- 274 S. Mallakpour and M. Naghdi, *Ceram. Int.*, 2022, **48**, 2045–2057.
- 275 T. Fatima, R. Jolly, M. R. Wani, G. G. H. A. Shadab and M. Shakir, *Results Mater.*, 2021, **12**, 100240.
- 276 S. Ahmadi, Y. Pilehvar, N. Zarghami and A. Abri, *J. Drug Delivery Sci. Technol.*, 2021, **66**, 102798.
- 277 H. Khalid, H. Iqbal, R. Zeeshan, M. Nasir, F. Sharif, M. Akram, M. Irfan, F. A. Khan, A. A. Chaudhry and A. F. Khan, *Polym. Bull.*, 2021, **78**, 7199–7218.
- 278 S. Ghasemi and H. Ghomi, *J. Biomater. Appl.*, 2021, **36**, 406–418.
- 279 R. Ashraf, T. Maqbool, M. A. Beigh, A. H. Jadhav, H. S. Sofi and F. A. Sheikh, *J. Appl. Polym. Sci.*, 2021, **138**, 50594.
- 280 C. Zhang, X. Wang, A. Liu, C. Pan, H. Ding and W. Ye, *Mater. Lett.*, 2021, **291**, 129563.
- 281 M. U. Aslam Khan, W. S. Al-Arjan, M. S. Binkadem, H. Mehboob, A. Haider, M. A. Raza, S. I. Abd Razak, A. Hasan and R. Amin, *Nanomaterials*, 2021, **11**, 1319.
- 282 R. C. de Azevedo Gonçalves Mota, L. R. de Menezes and E. O. da Silva, *J. Mater. Res.*, 2021, **36**, 406–419.
- 283 S. S. Pelaseyed, H. R. Madaah Hosseini and A. Samadikuchak-saraei, *J. Biomed. Mater. Res., Part A*, 2020, **108**, 1390–1407.
- 284 N. A. Pattanashetti, C. Hiremath, S. R. Naik, G. B. Heggannavar and M. Y. Kariduraganavar, *New J. Chem.*, 2020, **44**, 2111–2121.
- 285 N. Johari, H. R. Madaah Hosseini and A. Samadikuchak-saraei, *Iran. Polym. J.*, 2020, **29**, 219–224.
- 286 J. Radwan-Pragłowska, Ł. Janus, M. Piątkowski, D. Bogdał and D. Matysek, *Polymers*, 2020, **12**, 792.
- 287 B. K. Shanmugam, S. Rangaraj, K. Subramani, S. Srinivasan, W. K. Aicher and R. Venkatachalam, *Mater. Sci. Eng., C*, 2020, **110**, 110710.
- 288 X. Zheng, J. Sun, W. Li, B. Dong, Y. Song, W. Xu, Y. Zhou and L. Wang, *J. Electroanal. Chem.*, 2020, **871**, 114362.
- 289 M. Kaseem, K. Hamad and Z. U. Rehman, *Materials*, 2019, **12**, 3659.
- 290 X. Yin, Y. Li, C. Yang, J. Weng, J. Wang, J. Zhou and B. Feng, *Int. J. Biol. Macromol.*, 2019, **132**, 495–505.

